

## TOPICAL REVIEW

# Spatial localization in nuclear magnetic resonance spectroscopy

**Stephen F Keevil**

Department of Medical Physics, Guy's and St Thomas' NHS Foundation Trust, Guy's Hospital, London, SE1 9RT, UK

and

Division of Imaging Sciences, King's College London, Guy's Campus, London, SE1 9RT, UK

E-mail: [stephen.keevil@kcl.ac.uk](mailto:stephen.keevil@kcl.ac.uk)

Received 6 December 2005, in final form 15 May 2006

Published 26 July 2006

Online at [stacks.iop.org/PMB/51/R579](http://stacks.iop.org/PMB/51/R579)

## Abstract

The ability to select a discrete region within the body for signal acquisition is a fundamental requirement of *in vivo* NMR spectroscopy. Ideally, it should be possible to tailor the selected volume to coincide exactly with the lesion or tissue of interest, without loss of signal from within this volume or contamination with extraneous signals. Many techniques have been developed over the past 25 years employing a combination of RF coil properties, static magnetic field gradients and pulse sequence design in an attempt to meet these goals. This review presents a comprehensive survey of these techniques, their various advantages and disadvantages, and implications for clinical applications. Particular emphasis is placed on the reliability of the techniques in terms of signal loss, contamination and the effect of nuclear relaxation and *J*-coupling. The survey includes techniques based on RF coil and pulse design alone, those using static magnetic field gradients, and magnetic resonance spectroscopic imaging. Although there is an emphasis on techniques currently in widespread use (PRESS, STEAM, ISIS and MRSI), the review also includes earlier techniques, in order to provide historical context, and techniques that are promising for future use in clinical and biomedical applications.

*This review is dedicated to the memory of Anne Keevil, the author's mother, who died during its composition.*

(Some figures in this article are in colour only in the electronic version)

## Contents

1. Introduction	580
2. Principles of NMR spectroscopy	581
2.1. The NMR phenomenon	581
2.2. Nuclear relaxation	583

2.3. Chemical shift and spectroscopy	584
2.4. The spin echo and pulse sequences	585
2.5. $T_1$ - and $T_2$ -weighting	585
2.6. $J$ -coupling	586
2.7. Static field gradients, spatial localization and encoding	587
3. Overview of spatially localized NMR spectroscopy	588
4. Surface coil techniques	589
4.1. Surface coil localization	589
4.2. Surface coils with depth pulses and composite pulses	591
4.3. Rotating frame spectroscopy and Fourier series windowing	592
4.4. $B_1$ 'sensitive volume' techniques	594
5. Static field gradient techniques	594
5.1. Field focusing, topical magnetic resonance and gradient modulation	594
5.2. One-dimensional static field gradient localization with surface coils—DRESS	594
5.3. Introduction to three-dimensional static field gradient localization	595
5.4. Volume selection by elimination of magnetization outside the VOI	597
5.5. Volume selection using spin echoes and stimulated echoes	601
5.6. Volume selection by post-acquisition signal combination—ISIS	608
5.7. Volume selection using multi-dimensional designer pulses and high-order gradients	611
6. Magnetic resonance spectroscopic imaging	613
6.1. Introduction to MRSI	613
6.2. Fourier techniques	614
6.3. Projection reconstruction techniques	616
6.4. Rapid MRSI	616
6.5. Hadamard techniques	620
6.6. Volume selection by phase encoding	621
7. Conclusions	622
Acknowledgments	623
References	624

## 1. Introduction

In view of the impressive and growing capabilities of magnetic resonance imaging (MRI), it is easy to overlook the fact that nuclear magnetic resonance (NMR) is in origin a spectroscopic technique capable of providing much richer information about biological systems than simply the spatial distribution of water. Biological applications of NMR considerably predate the development of MRI, which is perhaps properly regarded as a special case of NMR spectroscopy in which frequency differences arise from the imposition of magnetic field gradients rather than from purely endogenous physicochemical factors. In the years following its discovery (Bloch *et al* 1946, Purcell *et al* 1946), NMR was soon applied to the analysis of biological materials and systems. Indeed, Felix Bloch himself may be regarded as the first biological NMR researcher, since he is reputed to have inserted his own finger into his apparatus at Stanford and detected an NMR signal. Not to be outdone, Purcell and Ramsey subsequently placed their heads into their own apparatus at Yale (Andrew 2000). More conventional experiments followed (e.g., Shaw and Palmer (1951), Shaw *et al* (1952), Odeblad *et al* (1956)), and in time intact cells (Moon and Richards 1973) and tissues (Hoult *et al* 1974) were examined spectroscopically. In parallel with these

developments, the advent of spatial encoding using magnetic field gradients (Lauterbur 1973, Mansfield and Grannell 1973) opened the way for MRI and modern forms of localized spectroscopy.

Early spectroscopic studies of intact tissues largely focused not on the hydrogen nucleus that dominates MR imaging and spectroscopy today, but on the phosphorus-31 nucleus. Hydrogen (or proton) spectroscopy of animals was attempted as early as 1968 (Jackson and Langham 1968), but was limited by the problem of suppressing the water signal so that much smaller signals due to proton-containing metabolites could be observed. Phosphorus-31 NMR, technically easier although less sensitive, is rich in information: the concentrations of phosphorus-containing compounds in living tissues were found to be sufficient for non-invasive pH measurement and the study of cellular energy metabolism (Radda *et al* 1983). Although a number of other biologically important nuclei have subsequently been studied, issues of sensitivity, together with the convenience of performing proton spectroscopy using instrumentation designed primarily for proton MRI, mean that proton studies constitute a large majority of spectroscopic examinations performed today, now that adequate water suppression can be achieved on a routine basis.

Acquisition of NMR spectra from the body of an intact animal was accomplished in 1980 (Ackerman *et al* 1980). Study of intact animal and human subjects requires some means of restricting the region of the body from which signal is collected, so that a specific organ or tissue can be analysed. In these early studies, localization was achieved simply by using a small radiofrequency coil placed close to the surface of the animal—known, prosaically enough, as a surface coil. Today more elaborate localization methods have greatly expanded the potential clinical and biomedical applications of NMR, or magnetic resonance spectroscopy (MRS) as it is known in this context. The ability to localize a region of signal acquisition within a patient's body in a reliable manner, and to obtain predictable signal sensitivity within that region, has been of key importance in the development of MRS, and is becoming increasingly important as the use of quantitative MRS becomes more widespread.

This review presents a survey of techniques for spatial localization in MRS, focusing primarily on methods developed for *in vivo* proton and phosphorus-31 spectroscopy of human subjects. Many such techniques have been proposed over the past 25 years, and the review aims to be comprehensive in order to put the development of better-known techniques into context and to provide a complete record in a field in which the success and commercial exploitation of a few methods has now largely consigned the remainder to history. However, techniques in widespread use today (primarily PRESS and STEAM for proton MRS and ISIS for phosphorus) are given particular attention. The review does not address other issues of importance in clinical MRS, such as water and lipid suppression—except where there is an element of spatial selectivity such as in the outer volume suppression techniques used to eliminate lipid contamination in MRSI.

## 2. Principles of NMR spectroscopy

### 2.1. The NMR phenomenon

It is not possible to do justice to the physics and biochemistry of *in vivo* MRS in a review of this nature, but a brief overview is given to introduce concepts to be used later. For a more comprehensive account the reader is referred to de Graaf (1998).

NMR has its origin in the nuclear spin quantum number,  $I$ , and the resulting magnetic dipole moment,  $\mu$ . In the presence of a static magnetic field,  $\mathbf{B}_0$ , each moment is oriented with

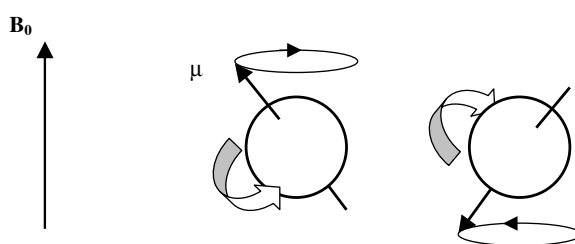


**Figure 1.** A nucleus with  $I = \frac{1}{2}$  spins on its axis (broad arrows), generating a magnetic moment,  $\mu$ . The nucleus adopts either of two possible orientations in an applied static magnetic field,  $\mathbf{B}_0$ , and precesses about the direction of the field (black arrows).

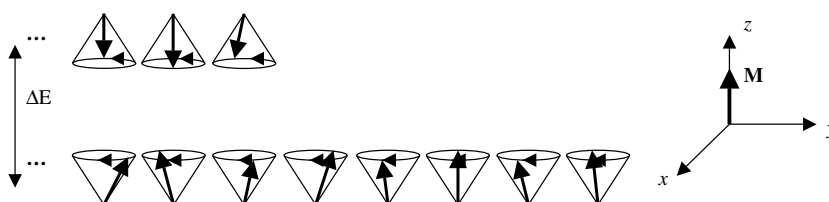


**Figure 2.** Origin of the bulk magnetization vector in a macroscopic sample. Excess magnetic moments aligned in the positive  $z$ -direction sum to give  $\mathbf{M}$ , while the random  $x$  and  $y$  components cancel. The population difference has been greatly exaggerated in this diagram—the ellipses represent approximately one million nuclei in each energy level.

**Table 1.** Gyromagnetic ratios of some nuclei commonly encountered in biomedical NMR.

Isotope	$\gamma$ (MHz T <sup>-1</sup> )
<sup>1</sup> H	42.58
<sup>13</sup> C	10.71
<sup>19</sup> F	40.08
<sup>31</sup> P	17.25

a component either parallel or antiparallel to the field (denoted by the  $z$ -axis) and experiences a torque causing it to precess about this axis at the Larmor frequency:

$$\omega_0 = \gamma B_0 \quad (1)$$

where the gyromagnetic ratio,  $\gamma$ , is characteristic of a given nuclear species (figure 1, table 1). Because the two orientations represent different energy levels, and hence have slightly different populations, the sample as a whole acquires a bulk magnetization,  $\mathbf{M}$ , which lies along the  $z$ -axis and is the sum of the  $z$ -components of the magnetic moments of all the nuclei in the sample. Because of the precession of the magnetic moments there is no net magnetization in the  $xy$  (or transverse) plane (figure 2).

Nuclear magnetic resonance is fundamentally a quantum mechanical phenomenon. However, it is usually possible to adopt an entirely classical model in which NMR is described in terms of interactions between  $\mathbf{M}$  and two applied magnetic fields—the static field along the  $z$ -axis,  $\mathbf{B}_0$ , and a radiofrequency field,  $\mathbf{B}_1$ , rotating with frequency  $\omega_{\text{RF}}$  (tens to hundreds of megahertz) applied in the  $xy$ -plane. If  $\omega_{\text{RF}} \approx \omega_0$ , then  $\mathbf{M}$  will experience a further torque and nutate towards the  $xy$ -plane, generating transverse magnetization,  $M_{xy}$ . Nutation ceases when

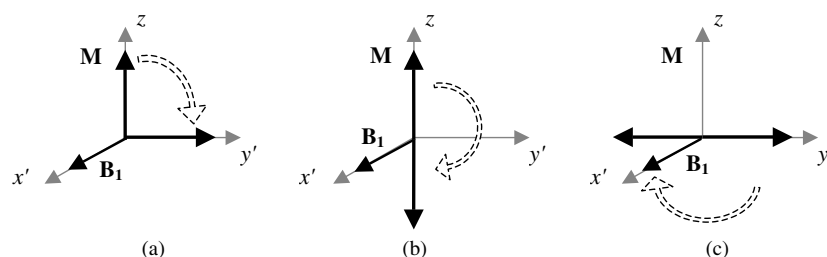


**Figure 3.** Special cases of RF pulse: (a) 90° pulse, (b) 180° inversion pulse, (c) 180° refocusing pulse.

$\mathbf{B}_1$  is removed, so by altering the intensity ( $B_1$ ) or duration ( $t_\theta$ ) of  $\mathbf{B}_1$  it is possible to tip  $\mathbf{M}$  through an arbitrary angle  $\theta$  (often known as the flip angle) where

$$\theta = \gamma B_1 t_\theta. \quad (2)$$

For the  $\mathbf{B}_1$  field strengths used in MRS (of the order of microtesla),  $t_\theta$  is typically a few milliseconds or less. This brief application of  $\mathbf{B}_1$  is generally referred to as an ‘RF pulse’—although strictly speaking it is not a pulse of RF electromagnetic radiation but rather a near-field phenomenon involving a magnetic field alone (Chen and Hoult 1989).

During an RF pulse,  $\mathbf{M}$  precesses about both  $\mathbf{B}_0$  and  $\mathbf{B}_1$ . Appreciation of this complicated situation can be simplified by working in a frame of reference with axes  $x'$ ,  $y'$  and  $z$ , rotating at a frequency  $\omega_{\text{RF}}$  relative to the transverse plane in the laboratory frame. In this rotating frame, if  $\omega_{\text{RF}} = \omega_0$ , the effect of  $\mathbf{B}_0$  is eliminated and the effect of an RF pulse may be considered purely in terms of nutation of  $\mathbf{M}$  about a static field,  $\mathbf{B}_1$  (figure 3). An important special case, known as a 90° pulse, nutates  $\mathbf{M}$  entirely into the transverse plane. Similarly, a 180° pulse inverts  $\mathbf{M}$  (an inversion pulse) or, if applied after a 90° pulse, rotates  $\mathbf{M}$  through 180° about an axis in the transverse plane (a refocusing pulse—see section 2.4).

Following nutation, precession of  $M_{xy}$  about  $\mathbf{B}_0$  can be detected by means of the current induced in a tuned antenna (known as an RF coil) placed close to the sample—a so-called free induction decay (FID) signal. Coils are used both to apply RF pulses to the sample and to detect the resulting NMR signal.

In MRS it is often desirable to nutate magnetization through exactly 90° or 180° over a region of tissue despite use of an RF coil with an inhomogeneous field. In such cases, adiabatic pulses can be used. These are a special class of pulse that produce a nutation angle that is independent of  $B_1$ . Adiabatic pulses involve simultaneous modulation of the amplitude and frequency of the RF field in such a way that  $\mathbf{B}_1$  rotates from the  $z$ -axis into the transverse plane (adiabatic half passage, AHP) or the  $-z$  direction (adiabatic full passage, AFP). If rotation of  $\mathbf{B}_1$  is slow relative to the Larmor frequency, the magnetization vector becomes ‘locked’ to the direction of  $\mathbf{B}_1$  and is nutated through the required angle. Maintenance of this adiabaticity condition throughout the pulse requires careful selection of the amplitude and frequency modulation schemes, and the amplitude of  $\mathbf{B}_1$  must exceed a threshold value (Silver *et al* 1984, 1985, Baum *et al* 1985, Bendall and Pegg 1986, Ugurbil *et al* 1987). Conversely, if rotation of  $B_1$  is too slow there can be loss of magnetization due to  $T_2$  relaxation (Norris *et al* 1991).

## 2.2. Nuclear relaxation

Following excitation, the spin system returns to its original configuration via a variety of relaxation mechanisms, categorized phenomenologically as those causing loss of energy from

the spin system and those leading to exchange of energy between spins—known as spin–lattice and spin–spin relaxation, with relaxation times  $T_1$  and  $T_2$ , respectively.  $T_1$  relaxation results in exponential recovery of  $z$ -magnetization,  $M_z$ , while  $T_2$  processes cause exponential decay of transverse magnetization,  $M_{xy}$ .

$$M_z(t) = M(1 - e^{-t/T_1}) \quad (3)$$

$$M_x(t)_y = M e^{-t/T_2}. \quad (4)$$

The relaxation times exhibited by a nucleus depend on the chemical group of which it forms a part and the physicochemical environment of the tissue in which it is located.

In practice, it is found that  $M_{xy}$  decays with a relaxation time  $T_2^*$ , shorter than  $T_2$ , because inhomogeneities in the static magnetic field lead to dispersion of the transverse magnetization. This dephasing can be reversed using the spin echo technique (see section 2.4).

### 2.3. Chemical shift and spectroscopy

It is clear from equation (1) that the resonance frequency of a nucleus is determined by the strength of the applied static magnetic field. However, in most cases electron clouds associated with the molecular environment of the nucleus partially shield it from  $\mathbf{B}_0$ , so that the effective field is reduced, and the resonance frequency is given by

$$\omega_0 = \gamma B_0(1 - \sigma) \quad (5)$$

where  $\sigma$  is a shielding term dependent on the chemical group and overall molecular structure in which the nucleus is located. This ‘chemical shift’, of the order of millionths of the static field strength, is the basis of NMR spectroscopy, since it allows detection and quantification of nuclei in different chemical groups based on their slightly different NMR frequencies. Chemical shift is usually expressed as the difference between the resonance frequencies of nuclei in a chemical group of interest and in an agreed standard, expressed in terms of parts per million (ppm).

An FID consists of several exponentially decaying sinusoids with different frequencies, each corresponding to nuclei with a different chemical shift. Fourier transformation results in a spectrum composed of discrete Lorentzian peaks, the intensities of which reflect the quantities of nuclei in each chemical environment (figure 4). Because the chemical shift between resonances is small, as high a  $\mathbf{B}_0$  as possible is required to maximize frequency resolution. Clinical MRS is generally carried out at a static field strength of 1.5 T (tesla) or increasingly at 3 T.

Although spectral peaks do not necessarily correspond to specific chemical compounds, the number of NMR-visible compounds in the body is small enough that in many cases peaks may be assumed to originate from a single compound either entirely (e.g. the phosphocreatine peak in  $^{31}\text{P}$  MRS) or predominantly (e.g. the peak due to methyl protons in *N*-acetyl aspartate in  $^1\text{H}$  MRS). In other cases a peak with contributions from a number of compounds nevertheless imparts valuable information because of the nature and role of the compounds involved (e.g. the peak due to methyl protons in choline-containing compounds in  $^1\text{H}$  MRS). Compounds that contain the nucleus of interest in more than one chemical group give rise to multiple peaks in the spectrum; this occurs frequently in proton MRS, since many compounds contain hydrogen atoms in several different chemical groups (e.g. the peaks due to methyl and methine protons in lactate in  $^1\text{H}$  MRS), but also in the case of ATP in  $^{31}\text{P}$  spectra.

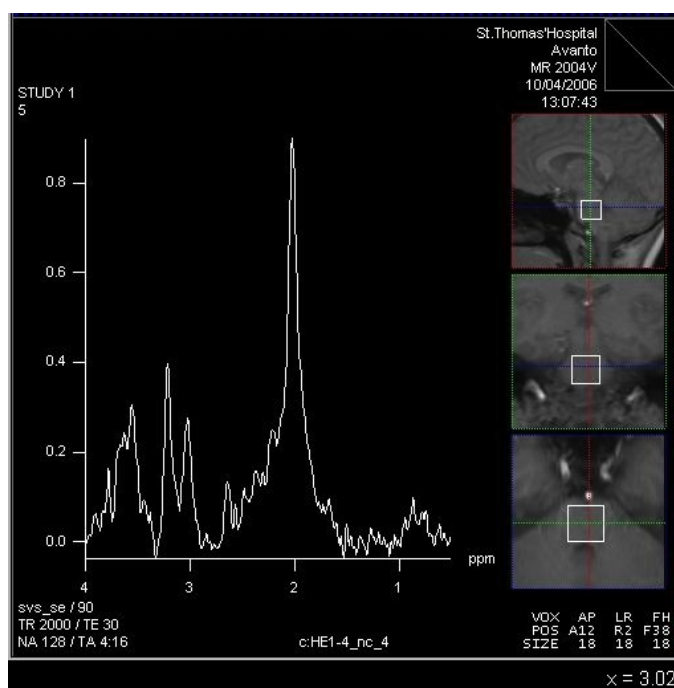


**Figure 4.** *In vivo*  $^1\text{H}$  NMR spectrum collected from the pons in a healthy volunteer using PRESS with  $T_E = 30$  ms and a VOI size of  $18 \times 18 \times 18$  mm (see section 5.5.2). The main resonances of interest are due to *N*-acetyl compounds (primarily *N*-acetylaspartate) (2.02 ppm), creatine and phosphocreatine (3.03 ppm) and choline compounds (3.22 ppm).

#### 2.4. The spin echo and pulse sequences

Dispersal of transverse magnetization due to static field inhomogeneity (see section 2.2) can be eliminated using the spin echo technique (Hahn 1950), in which a  $180^\circ$  pulse is applied at a time  $\tau$  after the  $90^\circ$  pulse. This pulse ‘flips’ precessing magnetization through  $180^\circ$  about an axis in the  $xy$ -plane, so that spins return to coherence at a time  $T_E = 2\tau$ , known as the echo time (figure 5). The spin echo is a simple example of a ‘pulse sequence’—application of a series of RF pulses prior to signal acquisition. An infinite variety of pulse sequences may be envisaged, giving the investigator considerable control over the extent to which the collected signal reflects different physical properties of the sample. This flexibility lies at the heart of the power of both MRI and MRS as analytical and clinical techniques.

#### 2.5. $T_1$ - and $T_2$ -weighting

Use of a spin echo reverses the effects of field inhomogeneity, but not true  $T_2$  decay. Thus in a signal collected at echo time  $T_E$ , the intensity of each resonance peak will be reduced by a factor

$$S(T_E) = S(t = 0) e^{-T_E/T_2}. \quad (6)$$

Furthermore, an NMR experiment is typically repeated at an interval  $T_R$  (the repetition time). Unless  $T_R \gg T_1$ , recovery of  $M_z$  between consecutive excitations will be incomplete, resulting in a reduction in subsequent signal intensities by a factor

$$S(T_R) = S(t = 0)(1 - e^{-T_R/T_1}). \quad (7)$$

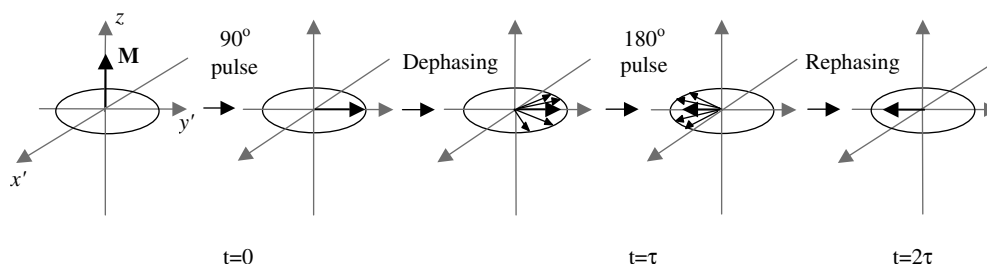


**Figure 5.** The spin-echo mechanism, depicted in the rotating frame. Following nutation into the transverse plane by a  $90^\circ$  RF pulse, elements of magnetization (known as ‘isochromats’) experiencing local magnetic fields of different strengths precess at different frequencies and hence dephase, leading to decay of the net magnetization vector  $\mathbf{M}$ . A  $180^\circ$  pulse applied at time  $\tau$  ‘flips’ isochromats so that they rephase on the opposite side of the transverse plane at time  $2\tau$ .

Because  $T_1$  and  $T_2$  differ for nuclei in different environments, the extent of signal  $T_1$  and  $T_2$  weighting in a spectrum will vary from peak to peak.

### 2.6. *J*-coupling

Another factor that complicates the evolution of transverse magnetization is *J*-coupling, otherwise known as spin–spin coupling. This phenomenon arises from interactions between magnetic nuclei situated in the same molecule. For a system consisting of two interacting spins, A and X, the local magnetic field of spin X is dependent on the orientation of spin A relative to  $\mathbf{B}_0$ . Since A spins in their two possible orientations (if  $I = \frac{1}{2}$ ) are present in approximately equal numbers, the resonance peak due to X spins will be split into two equal-sized components with slightly different frequencies (a doublet). Similarly, the resonance peak due to A spins will also be split. If more magnetic nuclei are present, a triplet or higher order multiplet may arise, depending on the structure of the molecule and the nature of the coupled spins. The frequency differences between multiplet components in each case are given by a coupling constant, *J*, which is typically 1–15 Hz for coupling between protons and up to 100 Hz or so if other nuclei are involved. The impact of coupling depends on the magnitude of *J* relative to the chemical shift,  $\delta$ , between the nuclei. The behaviour of spins in the strong coupling regime ( $J \approx \delta$ ) is much more complicated than that of weakly coupled spins ( $J \ll \delta$ ), and requires quantum-mechanical treatment. In the notation used to describe coupled spin systems, strength of coupling may be inferred from the alphabetical proximity of the letters used to designate the spins—e.g. AX is a weakly coupled two-spin system and AB a strongly coupled one. The same principles extend to systems with more than two spins, such as AX<sub>3</sub> (e.g. lactate) and AMNPQ (e.g. glutamate).

When *J*-coupled magnetization is nutated into the transverse plane, the resonance frequency differences between the components of the multiplet lead to dephasing. If different nuclear species are involved (known as heteronuclear coupling), this dephasing is not refocused in a spin echo sequence. Therefore the phase difference between different elements of magnetization, and the resultant phase of the peak as a whole, will evolve with  $T_E$ . A concrete example of great interest in *in vivo* proton MRS is lactate: the resonance due to methyl protons in the lactate molecule (X in the AX<sub>3</sub> system) forms a doublet because of interactions with the methine proton (A). This doublet evolves in a characteristic manner as a function of  $T_E$ : it is inverted in phase relative to the rest of the spectrum at  $T_E = 135$  ms and fully in phase at  $T_E = 270$  ms. This phenomenon aids in identification of lactate in a spectrum, which can

otherwise be ambiguous due to the similar resonance frequencies of lipids, but complicates quantification.

The evolution of  $J$ -coupled magnetization during more elaborate echo-based sequences can be very complicated, and is relevant to the performance of some localization techniques. This behaviour is discussed in section 5.5, but for detailed coverage the reader is referred to more general texts (e.g., de Graaf (1998)) and to references given in that section.

### 2.7. Static field gradients, spatial localization and encoding

In MRI and MRS, extensive use is made of magnetic field gradients. This term usually refers to temporary imposition of an additional static magnetic field, which lies parallel to  $\mathbf{B}_0$  but varies linearly in strength with position along the  $x$ -,  $y$ - or  $z$ -axis (or some direction oblique to these axes). It follows from equation (1) that this results in linear variation in the Larmor frequency, so that in the case of a gradient along the  $x$ -axis we have

$$\omega(x) = \gamma(B_0 + G_x x), \quad (8)$$

where  $G_x$  is the gradient strength (often expressed in  $\text{mT m}^{-1}$ ). Thus if a gradient field is switched on while there is magnetization in the transverse plane, the precessional frequency of this magnetization will vary linearly along the gradient direction. When the gradient is switched off magnetization throughout the sample once again precesses at the common Larmor frequency (equation (1)), but the period of differential precession results in a difference in phase that persists unless removed by application of a gradient in the opposite sense.

The pattern of gradient switching in MRS varies widely, from solitary gradients kept on for periods of several milliseconds or longer to oscillating gradients driven at hundreds of kilohertz. The principal applications are as follows. Numerous examples of each will be encountered in this review.

**2.7.1. Spoiling of magnetization.** Application of an intense gradient will result in complete phase dispersal, and hence elimination, of transverse magnetization. This can be used to ‘spoil’ unwanted magnetization that might otherwise result in spurious signals or artefacts.

**2.7.2. Refocusing of magnetization.** It is often desirable to delay acquisition of a NMR signal to allow time for other pulse sequence elements to be applied. The spin echo is one approach to this. Another is to dephase magnetization intentionally using a gradient and then apply a gradient in the opposite sense to rephase it into a ‘gradient echo’ when required (frequently spin and gradient echoes are used together, and careful pulse sequence timing is needed to ensure that the two echo conditions coincide in time). A similar approach is used if gradients employed for other purposes during a pulse sequence incidentally result in dephasing of magnetization, which must be reversed for signal collection. The condition that must be satisfied for complete rephasing along, for example, the  $x$ -axis is

$$\int G_x x \, dt = 0, \quad (9)$$

so that reversal of the effects of all the gradients in a pulse sequence can be achieved in a very short period of time if the refocusing gradients are sufficiently intense. Conversely, it is important in sequence design to guard against inadvertent rephasing of unwanted magnetization due to the cumulative effect of gradients.

**2.7.3. Slice selection.** If a gradient is applied at the same time as an RF pulse, and the pulse contains a narrow band of frequencies, a defined slice of  $z$ -magnetization can be selectively

nutated into the transverse plane, while that elsewhere in the sample ideally remains unaffected. The concept may be extended to selective inversion or selective refocusing using a  $180^\circ$  pulse.

It is desirable to select a slice with a rectangular profile across the slice, falling sharply to no excitation outside. In practice this is unachievable. Barring instrumental imperfections, the profile of the excited slice is similar to the frequency profile of the RF pulse, which is simply the Fourier transform of the pulse shape in the time domain. A rectangular slice profile therefore requires application of a sinc-shaped RF pulse, which is of infinite duration. Clearly compromises must be made. It is common to use truncated sinc pulses that are then apodized with a Gaussian (or hamming) function for slice selection, although numerically optimized pulses are increasingly widespread. Pulse design is an important aspect of localized spectroscopy, since imperfect slice profiles can lead to loss of signal and contamination with extraneous signal. In the case of a  $180^\circ$  pulse, profile imperfections often lead to generation of unwanted transverse magnetization towards the edges of the slice, and this is commonly eliminated using spoiler gradients.

The bandwidth of the RF pulse and the strength of the gradient are chosen to give the required slice thickness, but are often subject to other constraints. In MRS, the bandwidth must be sufficient to excite magnetization uniformly across the whole chemical shift range of the spectrum, or there may be significant off-resonance effects leading to distortion at the extremes of the spectrum. Particular problems arise when it is necessary to apply a nonselective RF pulse in the presence of a gradient, since the bandwidth required for uniform performance across the sample may necessitate very intense pulses that raise safety concerns in clinical applications.

*2.7.4. Spatial encoding.* In MRI, gradients are used to encode spatial information into the collected signal so that an image can be generated. This is done using frequency encoding and phase encoding. In the former technique, a gradient is applied during signal acquisition and the signal is Fourier transformed to yield a projection through the sample along the gradient direction. In phase encoding, a gradient is applied for a short time after excitation, imparting phase to transverse magnetization as a function of position along the gradient direction, which persists into the collected signal. Repetition a number of times with different gradient amplitudes yields a set of signals with phase development mimicking that which would occur in the presence of a constant gradient, and again Fourier transformation can be used to yield a projection. In MRI frequency and phase encoding are used together for two-dimensional localization. In MRS, phase encoding, and in some cases frequency encoding, are encountered in spectroscopic imaging (see section 6) and related techniques.

Data acquisition using frequency and phase encoding is best appreciated using the ‘*k*-space’ formalism, which readily generalizes to other data acquisition strategies and provides a powerful tool for their design and comparison. *k*-space is a space with axes  $k_x$ ,  $k_y$  (and in the case of three-dimensional imaging  $k_z$ ) where, for example,

$$k_x(t) = \gamma \int_0^t G_x(t') dt'. \quad (10)$$

The variable *k* represents spatial frequency. The signal collected in *k*-space is the two-dimensional Fourier transform of the desired image, and many features of the image are best understood by reference to the trajectory of data acquisition in *k*-space.

### 3. Overview of spatially localized NMR spectroscopy

The collection of NMR spectra from restricted regions within the body of a patient is an important prerequisite for clinical MRS. In general, spatial localization is achieved by

a combination of RF coil properties and specially designed pulse sequences. The ideal localization technique would allow collection of a spectrum from an organ or lesion of arbitrary shape and position without loss of signal from within this region or contamination with signal from outside. In practice, control over the shape of the region of signal collection (referred to here as the volume of interest or VOI) is limited, and it rarely corresponds exactly to the structure the investigator wishes to study (the tissue of interest). Even in the case of anatomically ideal localization, signal loss and contamination due to the properties of the localization technique itself limit the extent to which the spectrum collected is truly representative of the tissue of interest. Often, performance depends upon the degree of  $T_1$  and  $T_2$  relaxation during the pulse sequence. Phosphorus-31 nuclei tend to have longer  $T_1$ s and shorter  $T_2$ s than protons, so the two nuclei may require quite different localization strategies. Furthermore, the desire for good spatial resolution means that the volume of interest often constitutes a small proportion of the volume of the subject's body within the sensitive region of the coil (referred to loosely as the 'sample' in this review). In such cases there may be significant contamination even if suppression of extraneous signals is excellent, especially if compounds containing the nucleus of interest are present in higher concentrations outside the VOI than within it.

Another factor affecting the choice of localization strategy is the feasibility of incorporating additional pulse sequence elements. This is particularly important in proton spectroscopy, which is impossible without good water suppression because the concentration of water in tissues is typically higher than the concentrations of metabolites of interest by four orders of magnitude. More generally, it may be desirable to be able to combine localization with spectral editing—i.e. manipulating  $J$ -coupling to simplify spectra or to elucidate coupling patterns and hence molecular structure.

Numerous localization techniques have been described in the literature over the past 25 years—although relatively few have achieved widespread use or been implemented commercially. These techniques may be crudely divided into three broad classes, each discussed in turn below. Techniques based primarily on the properties of RF coils and pulses (section 4) dominated the early years of localized MRS, but are now of largely historical interest. They are typically characterized by relatively poor localization quality. The development of volume selection methods using static field gradients (section 5) has led to domination of single voxel localized spectroscopy by techniques that localize signal acquisition to a cuboidal region that is at best only approximately coincident with the tissue of interest. Within this category, the echo-based techniques, PRESS and STEAM (see section 5.5) have come to dominate proton spectroscopy, while ISIS (see section 5.6) is the method of choice for phosphorus studies. These three techniques are the only ones to have achieved widespread and lasting commercial implementation. Finally, MR spectroscopic imaging (section 6) combines methodology drawn from MRI and MRS to facilitate the mapping out of spectra and of metabolite levels over a slice or volume, and holds out the promise of conformal spectroscopy.

## 4. Surface coil techniques

### 4.1. Surface coil localization

In the first *in vivo* NMR experiments, Ackerman *et al* (1980) collected localized spectra from rats simply by placing a small tuned coil on the surface of the animal and relying on the  $B_1$  field profile of the coil for localization. Such 'surface coils' have subsequently found many applications in imaging and spectroscopy. The elementary surface coil study is a

‘pulse-acquire’ experiment, in which excitation of the spin system is followed by immediate collection of an FID. In the simplest case, excitation is achieved using a coil large enough to ensure uniform (ideally  $90^\circ$ ) nutation of magnetization throughout the sample. Signal is collected using a smaller surface coil. By the principle of reciprocity, the detection sensitivity at a distance  $z$  along the axis of a circular coil of  $n$  turns and radius  $a$  carrying a current  $I$  is proportional to the magnitude of  $\mathbf{B}_1$  per unit current at that position where, in free space (Bleaney and Bleaney 1976),

$$B_1 = \frac{\mu_0 n I a^2}{(a^2 + z^2)^{3/2}}. \quad (11)$$

The elaborate off-axis field structure (Haase *et al* 1984) will not be discussed here.

It is common to assume that surface coil acquisition is localized to an approximately hemispherical region, but sensitivity is neither uniform within this region nor negligible outside. Metabolites near the coil windings contribute disproportionately to the spectrum, while high concentrations of metabolites can make a large contribution even if they are some distance from the coil.

Complications arise if a small coil is used to transmit as well as to receive RF pulses, but this can be used to advantage. Because of the nonuniform  $\mathbf{B}_1$  field, the nutation angle in this situation is a function of position relative to the coil. Neglecting  $T_1$  and  $T_2$  weighting and off-resonance effects, from equation (2) the signal collected following such a pulse is

$$S \propto B_1 \sin \theta = B_1 \sin(\gamma B_1 t_\theta) \quad (12)$$

where  $B_1$  and  $\theta$  are functions of position. On axis,  $B_1$  is given by equation (11). Peaks and troughs of sensitivity occur at positions relative to the coil that can be varied by changing  $B_1$  or  $t_\theta$ . The depth from which adequate signal can be obtained is limited by the fall-off of  $\mathbf{B}_1$ . Furthermore, if the repetition time is short, the region of greatest sensitivity no longer corresponds to  $\theta = 90^\circ$ , and varies from one metabolite to another depending on  $T_1$  (Evelhoch *et al* 1984).

The send-and-receive surface coil is a crude but easily implemented technique that can achieve a measure of depth selection, since  $t_\theta$  can be chosen to give maximum signal from a particular depth. Unfortunately, the pulse length required to produce a  $90^\circ$  pulse at the chosen depth frequently results in additional signal maxima near the coil where the flux is strong and nutation angles of  $(2n + 1)90^\circ$  occur. This can be partially alleviated by offsetting the coil from the tissue surface. Alternatively, signal from the surface can be eliminated using magnetic field gradients (Crowley and Ackerman 1985, Jehenson and Bloch 1991) or even a sheet of ferromagnetic particles (Hennig *et al* 1987, Engelstad *et al* 1990). In FROGS (fast rotating gradient spectroscopy) (Sauter *et al* 1987), signal from this region is eliminated by spatially selective saturation: RF pulses and static field gradients are used together to tip the spins in a selected slice towards the  $xy$ -plane and the resulting magnetization is dephased using a further gradient. This process is repeated many times with different gradient directions and amplitudes and RF pulse amplitudes until no net magnetization remains in the high flux region. Although no longer in use as such, FROGS may be regarded as the forerunner of techniques such as PROPRES (see section 5.4.3) and outer volume suppression techniques (OVS) used today in conjunction with spectroscopic imaging (see section 6.2).

In summary, surface coil based techniques are simple to implement, requiring no elaborate pulse programming, and have good sensitivity. However, these advantages are offset by poor definition of the selected region and high contamination.

#### 4.2. Surface coils with depth pulses and composite pulses

Depth pulse techniques aim to improve depth selection by suppressing signal from regions in which the nutation angle differs from  $90^\circ$ . The concept was introduced by Bendall and Gordon (1983), and a comprehensive theoretical framework has been presented by Bendall and Pegg (1985a). A depth pulse sequence may include many elements, but in the simplest example an RF pulse is applied along the  $x'$ -axis in the rotating frame, nutating spins through a range of angles,  $\theta$ , as a function of distance from the coil. This is followed by a further pulse of twice the duration, yielding a spin echo. Four echoes are collected in separate experiments using such ' $2\theta$ ' pulses, each incremented by  $90^\circ$  in phase (i.e. applied along the axes  $x'$ ,  $y'$ ,  $-x'$  and  $-y'$  in turn). It can be shown that the signal produced by summing these echoes is

$$S \propto B_1 \sin^3 \theta. \quad (13)$$

Using notation based on Bendall and Pegg (1985a), this sequence is written ' $\theta[x']; 2\theta[\pm x', \pm y'];$  acquire'. The second set of brackets shows the phase cycling scheme applied to the  $2\theta$  pulse, designed to eliminate transverse magnetization in regions in which  $\theta \neq 90^\circ$ . (Phase cycling is frequently used in this way in localized MRS, and we shall see many examples in this review.)

Improved suppression of signal from regions in which  $\theta \neq 90^\circ$  may be achieved by adding further  $2\theta[\pm x', \pm y]$  pulses after the  $\theta$  pulse and/or pulses of the form  $2\theta[\pm x']$  before it, while signals from high flux regions near the coil can be minimized by preceding the sequence with 'fractional' pulses of the form  $\theta/(2n + 1)[\pm x']$  so that magnetization in the region where  $\theta = (2n + 1)90^\circ$  is nutated into the transverse plane and eliminated by phase cycling. In each case, dependence of signal intensity on  $\theta$  is manipulated to improve localization, while phase cycling eliminates signal due to unwanted transverse magnetization. The more extensive phase cycling schemes provide fairly good localization to the region in which  $\theta = 90^\circ$ , and the position of this region within the sample is quite flexible. However, these sequences require summation of an increasing number of signals, and are therefore of prohibitive duration as well as being troublesome to implement (Bendall and Gordon 1983, Bendall and Pegg 1985a). Also, the region of localization is not simple in shape, particularly when a single transmit and receive coil is used. This problem can be minimized by using multiple concentric surface coils (Bendall 1983, Bendall and Pegg 1984, 1985b, Bendall *et al* 1984). Alternate RF pulses are transmitted on different coils, and localization is restricted to the region of overlap between their  $\mathbf{B}_1$  fields, but care is needed to minimize phase distortion in the spectra due to the differing field distributions of the coils (Blackledge *et al* 1987). Further problems of depth pulses include determination of the  $90^\circ$  pulse length in the desired position (Pan *et al* 1989) and degraded localization performance when  $T_R \approx T_1$  (Michael and Schleich 1991). Bendall (1984) has described a variant in which localization is improved by applying static field gradients and depth pulses together. This suffers from many of the same drawbacks as conventional depth pulse methods.

A somewhat similar class of techniques employs 'composite pulses'—clusters of RF pulses designed to emulate the effect of a single pulse but with special features such as reduced sensitivity to  $\mathbf{B}_1$  inhomogeneity (e.g., Levitt (1982)). The essence of the simplest such technique (NarOWBand for Localization of Excitation, or NOBLE) (Tycko and Pines 1984) is to subtract the signal obtained using an excitation pulse following application of a  $\mathbf{B}_1$ -selective inversion pulse from that obtained using an excitation pulse alone to yield the signal from the inverted region. Phase cycling or spoiling can be used to eliminate any transverse magnetization inadvertently generated outside this region. The subtraction scheme is a forerunner of that in widespread use today in ISIS (see section 5.6), although  $\mathbf{B}_1$  rather than static field gradients are used, and has similar disadvantages in terms of dynamic range.

An elaborate ‘single-shot’ composite pulse scheme, which may be written  $(4\theta[x'], \text{spoil})_m, (2\theta[x'], \text{spoil})_n, \theta[x']$ , acquire’ was suggested by Thulborn and Ackerman (1983). Each of the  $4\theta$  and  $2\theta$  elements leaves magnetization in the  $\theta = 90^\circ$  region along the  $z$ - or  $-z$ -axis while magnetization elsewhere acquires a transverse component, which is destroyed by spoiler gradients. These elements are repeated  $m$  and  $n$  times respectively until all extraneous magnetization is eliminated. Unfortunately, magnetization in  $\theta = (2n + 1)90^\circ$  regions is also preserved. Cleaner selection is achieved using a frequency selective pulse train in the presence of a linear  $\mathbf{B}_1$  gradient (Canet *et al* 1988).

Composite pulses and depth pulses were combined by Shaka *et al* (1985) and Shaka and Freeman (1985a, 1985b, 1985c), who suggest replacing the RF pulses in depth pulse schemes with  $\mathbf{B}_1$  sensitive composite pulses, allowing considerable reduction in phase cycle complexity. The penalty is greater signal loss from within the region of interest. A scheme presented by Karczmar *et al* (1986) uses composite pulses and spoiler gradients to eliminate high flux signals while preserving signal from the  $\theta = 90^\circ$  region. The sequence can be implemented in ‘single-shot’ mode, but phase cycling improves its performance.

Because of their drawbacks and complexity, none of these techniques have been widely implemented for clinical use, but depth pulses remain valuable in other areas such as cardiac MRS in animal models (e.g., Himmelreich and Dobson (2000)) and  $^{13}\text{C}$  spectroscopy.

#### 4.3. Rotating frame spectroscopy and Fourier series windowing

Early in the development of MRI, Hoult (1979) proposed an imaging strategy using constant linear  $\mathbf{B}_1$  gradients applied to an otherwise homogeneous  $\mathbf{B}_1$  field by clever RF coil design. If such a gradient lies along the  $x$ -axis, application of an RF pulse with  $\mathbf{B}_1$  along the  $x'$ -axis in the rotating frame causes  $z$  magnetization to nutate towards  $y'$  through an angle that varies linearly with distance from the coil along  $x$ . This spatial information can be incorporated into an FID by applying a  $90^\circ$  detection pulse with  $\mathbf{B}_1$  along  $y'$  to tip the prepared magnetization into the  $xy$ -plane. The phase of the resultant transverse magnetization varies linearly along  $x$ . Repetition with nutation pulses of increasing duration, with signal collection after each repetition, yields a data set in which position along the  $x$ -axis is encoded much as in conventional MRI phase encoding. The sequence may be written  $n\theta[x'], 90^\circ[y']$ , acquire’. In the spectroscopic application, two-dimensional Fourier transformation of these data yields a set of spectra resolved in one spatial dimension (Cox and Styles 1980). Rotating frame spectroscopy is demanding in terms of instrumentation, because it requires a surface coil that can provide linear variation of  $\mathbf{B}_1$ . This was achieved by Cox and Styles (1980) using an asymmetric saddle coil and by Styles *et al* (1985), who used a large transmit coil with a small detect coil on the axis.

In the absence of switched static field gradients, eddy current artefacts and spatial chemical shift offset (see section 5.2) are absent, and certain safety issues do not arise. However, because a surface coil is used, curved regions are selected rather than well-defined volumes, and this worsens if a single transmit and receive coil is used (Garwood *et al* 1986). The coil used by Cox and Styles (1980) was capable of generating linear  $\mathbf{B}_1$  gradients along two orthogonal axes, but with coils more suited to clinical work the technique is limited to one-dimensional localization. Another difficulty is that good spatial resolution requires RF pulses of considerable duration or amplitude, leading to problems with spatial distortion or excessive power deposition, respectively. Problems in common with depth pulse schemes (section 4.2) include spatially dependent phase distortion if separate transmit and receive coils are used (Garwood *et al* 1987) and degraded localization if  $T_R \approx T_1$  (Blackledge *et al* 1987). The latter can be overcome by using composite pulses to eliminate residual magnetization

prior to each repetition of the sequence, at the cost of further phase distortion (Garwood *et al* 1987). In an approach described by Metz *et al* (1994), a train of RF pulses is applied rapidly during the FID, with one data point collected after each pulse. This dramatically reduces power deposition and improves time efficiency, but is limited to collection of a single spectral peak at a time.

Phase and off-resonance distortion in rotating frame spectroscopy can be reduced by modulating the amplitude of the longitudinal magnetization rather than the phase of the transverse (Garwood *et al* 1987). The new sequence can be written as ' $n2\theta[\pm x']; \theta[x']$ '. The  $2\theta$  pulse is incremented on each repetition, providing longitudinal modulation, and the  $\theta$  pulse is used for detection. Phase cycling eliminates transverse magnetization generated by the  $2\theta$  pulse. In the absence of phase distortion, extension to multiple coils to improve localization is easier. A further modification uses adiabatic half passage (AHP) pulses in place of the  $\theta$  pulses to produce uniform  $90^\circ$  nutation over a wide range of  $\mathbf{B}_1$  field strength (Robitaille *et al* 1989).

Amplitude-modulated rotating frame spectroscopy is inefficient, since magnetization at a given depth nutates through an angle far from  $90^\circ$  in most repetitions of the sequence. This is avoided in Fourier series windowing (FSW) (Garwood *et al* 1985, Pekar *et al* 1985), using the fact that detection of signal from a specific depth is favoured if the pulse lengths used in each of the repetitions satisfy the following equation:

$$t_\theta = (2n + 1)t_{90} \quad (14)$$

where  $t_{90}$  is the pulse length for  $90^\circ$  nutation at the required depth (Blackledge *et al* 1987). The localization window can be optimized and extraneous excitation reduced by weighting the FIDs by the Fourier coefficients,  $C_n$ , of the desired window. Selection of a slice with a rectangular profile therefore requires  $C_n$  to vary as a sinc function with  $n$ ; since a smoother spatial window requires fewer Fourier coefficients and hence fewer repetitions, there is a trade-off between localization quality and simplicity and speed of acquisition (Hodgkinson and Hore 1995). The weighted FIDs are summed directly, without the need for Fourier transformation in the spatial dimension. It is possible to manipulate  $C_n$  in order to window about angles other than  $90^\circ$  or about more than one angle in the same experiment (Garwood *et al* 1986). Techniques to correct for cross-contamination in these multi-voxel approaches have been implemented by Abduljalil *et al* (1996). FSW has proved particularly valuable for cardiac MRS in animal models, as many of the references in this section demonstrate.

Integration of FSW with selection of a two-dimensional column using ISIS (see section 5.6) eliminates off-axis regions in which the  $\mathbf{B}_1$  isocontours are distorted, while dephasing by the ISIS gradients removes the need for phase cycling. This approach has been pursued with both transverse FSW (Segebarth *et al* 1987 (IDESS), Hendrich *et al* 1991, 1994a (RAPP-ISIS) and longitudinal FSW (Robitaille *et al* (1989) (FLAX-ISIS)). RAPP-ISIS replaces the  $90^\circ$  detection pulse with an adiabatic pulse with improved off-resonance behaviour as an alternative to longitudinal modulation, which involves significant signal loss. Both FLAX- and RAPP-ISIS can be used in FSW or multi-voxel modes, but suffer penalties in terms of signal to noise and experimental complexity. Liu and Zhang (1999) proposed improvements to address some of these issues and correct for voxel volume variation and coil sensitivity.

Although some of the rotating frame techniques did achieve commercial implementation, they have generally been superseded by static field gradient techniques that offer better localization quality and can be utilized with a wider range of coils. This is particularly so now that MRSI is widely available for multi-voxel acquisition.

#### 4.4. $\mathbf{B}_1$ 'sensitive volume' techniques

An unusual method devised by Friedrich and Freeman (1988) uses two circular coils on a common axis, set apart by their common radius and driven in opposition. The net  $\mathbf{B}_1$  field of this 'straddle coil' cancels in a region which can be moved by adjusting the currents in the coils. An elaborate series of pulses eliminates magnetization outside this null region, and remaining magnetization is detected using one or both of the coils.

### 5. Static field gradient techniques

#### 5.1. Field focusing, topical magnetic resonance and gradient modulation

Crude localization is achieved if  $\mathbf{B}_0$  is made uniform in a small region and inhomogeneous elsewhere. RF pulses will then elicit a well-defined signal from the homogeneous region only; transverse magnetization generated elsewhere is rapidly dephased due to the inhomogeneous field. The inhomogeneity may be a permanent feature of the magnet (Damadian *et al* 1976), or due to addition of nonlinear static field gradients to an otherwise uniform magnet (Gordon *et al* 1980). The latter approach, topical magnetic resonance (TMR), was popular before the advent of more sophisticated selection schemes (Gordon *et al* 1982). Romer *et al* (1989) and Engelstad *et al* (1990) adopted an unusual method in which inhomogeneity is generated *in vivo* by injection of a suspension of superparamagnetic particles. The observed signal originates only from tissues that do not take up the particles.

Field focusing results in poor localization. The selected region is ill-defined and complex in shape, and the inhomogeneous  $\mathbf{B}_0$  field increases spectral line widths significantly. Furthermore, the position of the sensitive region is usually fixed, so that the subject must be moved to localize in different parts of the body. This last drawback, but not the others, is overcome using modulated gradients. Slowly varying magnetic field gradients applied during a spectroscopy experiment dephase signal outside a chosen region in which the gradients are kept at zero at all times. This null region, which may be a 'point' (Scott *et al* 1982) or a 'line' (Bottomley 1982), can be moved within the magnet.

These crude methods were soon superseded, but pointed the way for more sophisticated schemes using linear static field gradients.

#### 5.2. One-dimensional static field gradient localization with surface coils—DRESS

Most of the methods to be discussed in the remainder of section 5 are designed primarily for three-dimensional localization (volume selection) within a volume coil (i.e. an RF coil enclosing the whole of the trunk or head) generating a reasonably homogeneous  $\mathbf{B}_1$  field. Some can also be applied in a one-dimensional mode for use with a surface coil. Firstly, however, an intrinsically one-dimensional technique will be considered in which the localizing properties of a surface coil are combined with a magnetic field gradient for slice selection. This will serve to illustrate principles and problems common to all localization methods using magnetic field gradients and selective excitation.

In Depth REsolved Surface-coil Spectroscopy (DRESS) (Bottomley *et al* 1984), a static field gradient is applied perpendicular to the plane of the coil, and a selective RF pulse applied to excite a slice of spins parallel to the coil. Ideally the profile of this slice should be rectangular, but in practice this is not achievable with a finite RF pulse (see section 2.7.3), and in DRESS the profile is further degraded because of the inhomogeneous  $\mathbf{B}_1$  field. The lateral extent of the slice is limited by the transaxial  $\mathbf{B}_1$  profile of the coil. The gradient is switched off and signal is detected as an FID or as a spin echo (the latter approach being unsuitable

for short  $T_2$  species such as  $^{31}\text{P}$  nuclei). In the notation to be used in this review for such sequences, DRESS is represented by

$$\frac{G_i}{\theta(x)} - t_d - Acq \quad (15)$$

where  $G_i$  is a gradient applied along the  $i$  direction ( $x$ ,  $y$  or  $z$ , or some oblique axis),  $t_d$  is a delay to allow for decay of eddy currents, and the use of parentheses rather than square brackets indicates a ‘soft’ (i.e. frequency selective) pulse. The material beneath the ‘/—\’ symbol indicates pulses applied in the presence of the gradient. Ideally,  $\theta$  should be  $90^\circ$  within the slice of interest (subject to slice profile limitations). Extension to multislice acquisition (SLIT DRESS) is straightforward (Bottomley *et al* 1985).

One major problem with DRESS is common to all static field gradient methods using selective excitation. RF radiation of frequency  $\omega$  applied in the presence of a gradient of strength  $G_x$  will excite spins whose combination of chemical shift  $\delta$  (ppm) and displacement  $x$  along the slice select direction satisfies the following expression:

$$\omega = \gamma(B_0 + xG_x + 10^{-6}\delta \cdot B_0). \quad (16)$$

It follows that when a narrowband pulse is applied, the position of the excited slice varies with  $\delta$ , and hence different metabolites are detected from slices that are slightly offset from one another in depth. The error is reduced by using a high gradient strength, so that the gradient term in equation (16) dominates. The required high bandwidth pulse also ensures uniform excitation across the frequency range of the spectrum, but the higher power deposition may be a problem in clinical use.

DRESS requires a large surface coil for more uniform excitation over the slice of interest. A smaller concentric coil can be used for sensitive detection. The method is, of course, unsuitable for studying tissues located far from the coil.

DRESS was formerly a popular technique, implemented on some clinical MR systems, but has now been largely supplanted by volume selection techniques that offer better-defined localization in three dimensions.

### 5.3. Introduction to three-dimensional static field gradient localization

The common feature of the techniques discussed in sections 5.4 to 5.6 is use of narrowband RF pulses and static field gradients to localize on a volume of interest (VOI). This volume is typically, but not invariably, cuboidal. In most cases, selection is achieved by applying slice selective pulse clusters to prepare spins along each of three orthogonal axes in turn. The VOI is formed at the intersection of the prepared slices (figure 6). One or two-dimensional localization can often be effected by using fewer clusters.

These techniques now dominate single-voxel localized MRS. The dimensions and location of the VOI are very flexible, being determined by the gradient strengths and the frequency content of the RF pulses. In commercial implementations, the user is able to select a VOI graphically from an MR image, manipulating its dimensions and location to coincide as closely as possible with an anatomical region or tissue of interest—although of course a cuboid is a poor approximation to the shape of most anatomical structures, and for reasons of sensitivity the minimum volume of the VOI is limited to about  $1 \text{ cm}^3$  for proton and  $30 \text{ cm}^3$  for phosphorus MRS. However, the ease with which the VOI can be prescribed does tend to reinforce the expectation that the spectrum subsequently collected will originate entirely from the indicated volume. Although the quality of localization to the VOI is generally good relative to the techniques discussed thus far, this confidence is not always well founded.

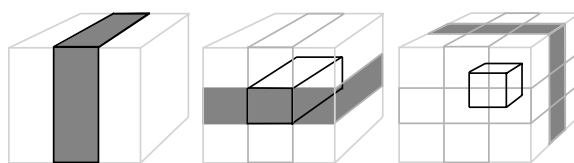


**Figure 6.** Principle of volume selection using static magnetic field gradients. Clusters of RF and gradient pulses are applied to prepare magnetization along each of three orthogonal axes in turn. Each cluster defines a slice of magnetization. Magnetization in the column formed by the intersection of the first two slices is affected by two clusters, and magnetization in the cuboid formed by the intersection of all three slices is affected by three clusters. This differential preparation of magnetization in different parts of the sample is used to localize signal acquisition to the central cuboid. The net effect on magnetization outside the cuboid depends on the details and relative timings of the pulse clusters.

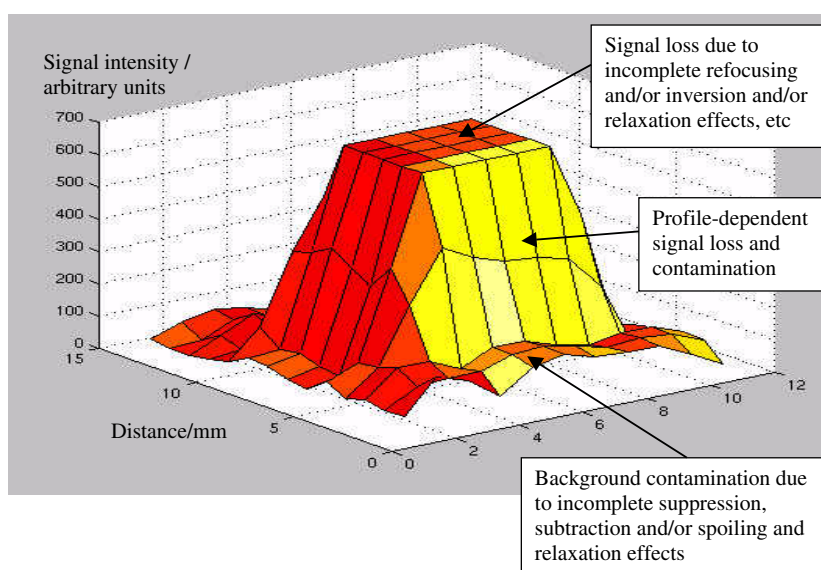


**Figure 7.** Typical VOI profile, in this case for a PRESS VOI of nominal side length 50 mm.

Several factors can compromise volume selection performance, and in considering these, it is useful to define the parameters *selection efficiency* ( $E_{\text{sel}}$ ), a measure of the efficiency with which signal is collected from within the tissue of interest (ideally 100%), and *contamination* ( $K$ ), a measure of the proportion of the acquired signal that actually originates from outside the intended tissue of interest (ideally 0%) (Keevil *et al* 1990, Bovée *et al* 1995).

$E_{\text{sel}}$  and  $K$  are both affected by the sensitivity profile of the VOI, which depends in turn on the quality of the slice profiles generated by the individual pulses (see section 2.7.3), together with other hardware and sequence imperfections and relaxation effects. The profile typically consists of a maximum sensitivity plateau at the centre of the VOI falling gradually to zero sensitivity at some distance outside the nominal VOI (see figure 7). On commercial MR systems, the definition of the VOI size relative to this profile is a matter for the system manufacturer. It is not unknown for the same manufacturer to alter the VOI definition, and hence the extent to which the imperfect profile contributes to loss of  $E_{\text{sel}}$  and to  $K$ , between different software releases (Keevil *et al* 1995, Ljungberg *et al* 1998).

In addition to profile effects,  $K$  is affected by the extent to which signal from outside the VOI is eliminated (figure 7). Magnetization throughout the three intersecting orthogonal slices at least will be affected by the RF pulses, and in many cases the entire sample may be affected. Depending on pulse sequence details, and in some cases on hardware factors, this may result in generation of contaminating signal from outside the VOI (and also affects the potential for multi-volume acquisition). This form of contamination is often addressed by adding outer volume suppression (OVS) techniques to the pulse sequence.

Contamination may therefore be broadly subdivided into ‘profile contamination’ arising from the edges of the VOI and ‘background contamination’ due to imperfect signal suppression outside the VOI. The relative extent of the two types of contamination has profound implications for the utility of a localization technique: high profile contamination may not matter if a small VOI is located well within a homogeneous lesion of interest, but in the same situation the performance of a technique prone to background contamination might be very poor because of the small size of the VOI relative to the rest of the sample. In neither case is the extent of contamination generally evident from inspection of the acquired spectrum, and with this in mind techniques have been developed to assess localization performance (Keevil *et al* 1990, 1992, Bovée *et al* 1995, Leach *et al* 1995, Starck *et al* 1995).

It is often found that  $T_1$  relaxation of material outside the VOI causes background contamination unless the pulse sequence is applied rapidly (relative to  $T_1$ ) to reduce the possibility of recovery of this extraneous magnetization. Conversely, repetition of the sequence should occur at intervals long compared to  $T_1$  if avoidance of  $T_1$ -weighting within the VOI is desirable. Techniques in which spins within the VOI spend a significant period in the transverse plane are unsuitable for species with short  $T_2$ s, such as phosphorus metabolites, but can be useful for proton spectroscopy as  $T_2$ -weighting aids water suppression. Depending on hardware performance, a short delay between spin preparation and signal acquisition is often required for decay of eddy currents induced by gradient switching, and in some sequences this delay can generate  $T_1$  or  $T_2$  related distortion. Sensitivity to  $\mathbf{B}_0$ ,  $\mathbf{B}_1$  and gradient imperfections also varies between sequences. For a given technique, performance can vary between MR systems of different design, age and upgrade level and even between nominally identical systems installed at different sites (Keevil *et al* 1995).

Spatial offset due to chemical shift has been discussed above in the context of DRESS. In the case of cuboidal volume selection using selective excitation, this offset occurs along all three axes. With modern gradient systems the offset is a matter of a few millimetres on each axis at most in  $^1\text{H}$  and  $^{31}\text{P}$  MRS, which can still be significant. The problem is greater for nuclei with a wide chemical shift range, such as carbon-13, and alternative methods (such as depth pulses, see section 4.2) are required with such nuclei.

#### 5.4. Volume selection by elimination of magnetization outside the VOI

The techniques described here use a combination of RF and gradient pulses to eliminate magnetization lying outside the VOI while preserving that inside (figure 8(a)). In this, they may be regarded as a development of the topical magnetic resonance techniques discussed in section 5.1. Most of the sequences consist of identical clusters applied along three orthogonal axes, following the general pattern:

$$(\text{pulse cluster with } G_i)_{i=x,y,z} - t_d - 90^\circ[x'] - Acq \quad (17)$$

where  $G_i$  is a gradient along axis  $i$ , which cycles through  $x$ ,  $y$  and  $z$  (or more generally through any three mutually orthogonal directions to produce a cuboid that is oblique to the Cartesian axes of the MR system).

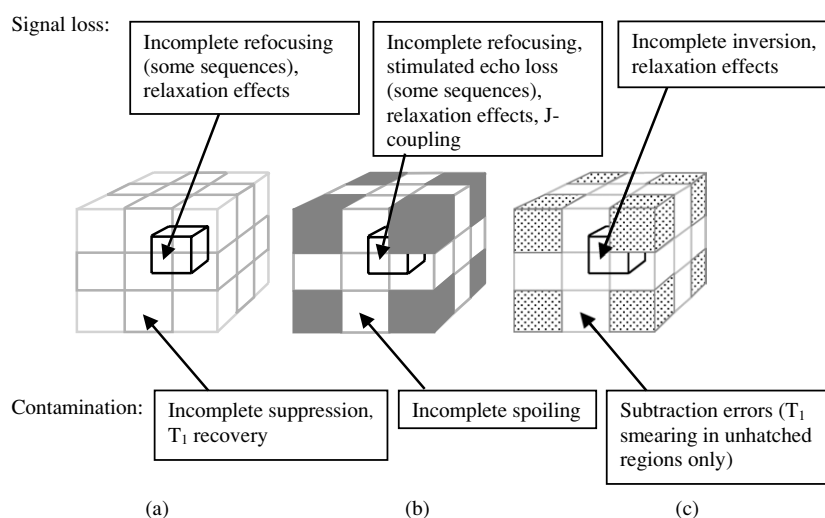


**Figure 8.** Signal loss and background contamination characteristics of static field gradient volume selection techniques based on (a) elimination of extraneous magnetization (section 5.4), (b) volume-selected echoes (STEAM and PRESS—section 5.5), and (c) post-acquisition signal combination (ISIS—section 5.6). In each case, the box edged in black indicates the nominal VOI, boxes edged in grey regions from which background contamination may originate, and grey filled boxes regions that do not contribute to background contamination. Profile signal loss and contamination effects are neglected.

These techniques are all susceptible to spatial chemical shift offset and to contamination due to  $T_1$  recovery of the extraneous magnetization. In many cases, high power RF pulses are needed to ensure that extraneous magnetization is fully suppressed across the entire sample, and this may render such sequences unsuitable for clinical use. Combination with water suppression is possible, but multi-voxel acquisition is not feasible since magnetization outside the single VOI is suppressed. Some of these methods have been used for outer volume suppression (OVS) in combination with other localization techniques (see, e.g., section 6.2).

**5.4.1. Volume selective excitation.** True volume selection was pioneered by Aue *et al* (1984). The volume selective excitation (VSE) pulse cluster consists of a hard  $90^\circ$  pulse between two soft  $45^\circ$  pulses, all applied with a gradient. Magnetization in a slice defined by the  $45^\circ$  pulses is nutated through a total of  $180^\circ$  (i.e. inverted); that elsewhere is placed in the  $xy$ -plane and dephased by the gradient. Repetition of the pulse cluster with the gradient along three orthogonal directions in turn localizes  $-z$  magnetization to a cuboid at the intersection of the three slices, and this is detected using a  $90^\circ$  pulse.

In notation based on that of Doddrell *et al* (1986a, 1986b, 1986c, 1987), the VSE pulse cluster may be written as

$$\frac{G_i}{/45^\circ(x')90^\circ[x']45^\circ(x')\backslash} \quad (18)$$

where  $G_i$  is the static field gradient, and the direction of the  $\mathbf{B}_1$  vector in the rotating frame is shown in parentheses for soft (narrowband, frequency selective) and in brackets for hard (broadband, nonselective) pulses. The VSE sequence is obtained by substituting this cluster into the generic pulse sequence in equation (17), giving

$$\frac{G_i}{(/45^\circ(x')90^\circ[x']45^\circ(x')\backslash)_{i=x,y,z} - t_d - 90^\circ[x'] - Acq.} \quad (19)$$

VSE has all the features common to the methods described in this section. In addition, there is a small degree of signal loss within the VOI as  $-z$  magnetization undergoes  $T_1$  relaxation during the eddy current delay. The sequence is unsuitable for routine clinical use, since high power is required to achieve sufficient bandwidth in the presence of a gradient (although phase cycling provides a less effective alternative). Also, it requires accurate nutation angles for localization—implementation with a surface coil entails phase cycling of the final  $90^\circ$  pulse and an add/subtract scheme to remove extraneous signal (Müller *et al* 1985a, 1985b).

**5.4.2. ‘Excite-refocus-return’ sequences.** These techniques make use of clusters consisting of three pulses: (i) a  $90^\circ$  pulse to generate transverse magnetization, (ii) a  $180^\circ$  pulse to refocus it into a spin echo, and (iii) a  $90^\circ$  pulse of the opposite phase applied at the echo time to return magnetization to the  $z$ -axis. One of the three pulses is made selective, so that only magnetization within a chosen slice experiences all three steps. Magnetization outside this slice is eliminated by the gradients or by phase cycling. Volume selection is achieved by applying the cluster along three orthogonal axes in turn, as indicated in equation (17). Since,  $+z$  magnetization is generated by each pulse cluster, there is no  $T_1$ -weighting of the selected signal. However, use of a spin echo means that there will be a degree of  $T_2$ -weighting.

Three sequences of this type have been described in the literature: in SPARS (SPATIally Resolved Spectroscopy) (Luyten *et al* 1986) (equation (20)), the ‘return’ pulse is selective; in SPACE (SPAtial And Chemical shift selective Excitation) (Doddrell *et al* 1986a) (equation (21)), it is the ‘excite’ pulse; and in SPALL (Symmetric Pulses for Accurate LocaliZation) (von Kienlin *et al* 1988) (equation (22)) the ‘refocusing’ pulse.

$$G_i \quad 90^\circ[x'] \wedge 180^\circ[y'] / 90^\circ[-x'] \quad (20)$$

$$G_i \quad / 90^\circ(x') 180^\circ[\pm x', \pm y'] 90^\circ[\pm x'] \quad (21)$$

$$G_i \quad / 90^\circ[x'] 180^\circ(\pm x', \pm y') 90^\circ[-x'] \quad (22)$$

The additional gradient pulse (‘ $\wedge$ ’) shown in the SPARS cluster is required to balance the later slice select gradient. SPARS was implemented for proton spectroscopy on some commercial MR systems for a time. However, the extent of gradient switching was found to lead to irreversible dephasing and poor quality spectra and the sequence has fallen out of use, despite various proposed improvements (Narayana *et al* 1988a, 1988b, Jackson *et al* 1988, Luyten *et al* 1986, Haxo *et al* 1989, Emsley and Bodenhausen 1990). SPACE and SPALL feature reduced gradient switching, but clinical use is limited by power deposition problems as the broadband  $180^\circ$  pulse is applied with a gradient. Again, various improvements have been suggested (Galloway *et al* 1987a, Emsley and Bodenhausen 1990, Marshman *et al* 1992). SPACE has been shown empirically to have superior performance to VSE, SPARS and DIGGER (see section 5.4.3) (Galloway *et al* 1987a).

**5.4.3. Volume selection without disturbance of the VOI.** These techniques aim to eliminate magnetization outside the VOI without affecting that inside. The signal is therefore largely free of  $T_1$ - and  $T_2$ -weighting, but contamination due to  $T_1$  relaxation outside the VOI remains a possibility, so add/subtract schemes are often used to eliminate extraneous signal.

Doddrell *et al* (1986b) proposed such an approach (discrete isolation from gradient governed elimination of resonances, or DIGGER) using the cluster

$$\frac{G_i}{\sqrt{\{\text{SSC}\} - t_a - \{\text{SSC}\}}} \quad (23)$$

where  $\{\text{SSC}\}$  are 'sin-sinc' pulses of the form

$$\{\text{SSC}\} = \frac{i \sin \pi \beta_1 t \sin \pi \beta_2 t}{\pi t} \quad (24)$$

which have a notched frequency profile and, applied with a gradient, saturate magnetization outside a defined slice. Application of the pulse twice improves slice definition.

Three-dimensional localization leaves a cuboid of unaffected magnetization to be read by the final  $90^\circ$  pulse. Incomplete saturation of magnetization at the edges of the sample due to power deposition limitations may necessitate phase cycling and an add/subtract scheme (Galloway *et al* 1987b).

It is difficult to implement DIGGER with conventional RF hardware. Alternatively, trains of frequency-shifted soft  $90^\circ$  pulses may be used in place of the  $\{\text{SSC}\}$  pulses (Doddrell *et al* 1986c, Haase 1986, Granot *et al* 1990). Better suppression of extraneous magnetisation can be achieved by combining DIGGER and SPACE pulse clusters (Doddrell *et al* 1987) or using SWIFT (stored waveform inverse Fourier transform) pulses as in the SMILE (SWIFT method for *in vivo* localized excitation) technique (Chew *et al* 1987).

Choi *et al* (2000) have described a sequence known as SIRENE (Single-shot Inversion REcovery based Non-Echo) for  $^{13}\text{C}$  MRS using a surface coil. The sequence begins with a pair of slice-selective adiabatic inversion pulses applied with gradients to invert bands of magnetization each side of the desired VOI along the direction of greatest  $\mathbf{B}_1$  inhomogeneity. After a delay chosen to null the inverted magnetization, this is followed by pairs of high-bandwidth adiabatic excitation pulses and gradients applied along each of the three orthogonal axes and followed by spoiler gradients. The net effect is to eliminate magnetization in bands each side of the desired VOI along all three axes. Remaining magnetization within the VOI is read out using an AHP pulse. Chemical shift offset was minimized using the high gradient amplitude possible with a small-bore NMR system. Despite the use of  $T_1$ -dependent inversion nulling, good performance was reported over a range of  $T_1$  values *in vivo*. The authors note that implementation using a volume coil would involve higher RF power deposition and necessitate suppression of larger extraneous signals—limitations that make the technique unsuitable for clinical implementation.

The ROISTER (Region Of Interest Selection by ouTER volume saturation) technique (de Crespigny *et al* 1989) is atypical in that the selected volume is cylindrical rather than cuboidal, and the pulse sequence consequently takes an unusual form. Selection is achieved using numerically-optimized, noise-modulated RF pulses tailored so that magnetization within a slice is unaffected while that outside is randomized (Ordidge 1987). Rather than applying the technique along orthogonal axes, the  $x$  and  $y$  gradients are varied sinusoidally and cosinusoidally, respectively, while the pulses are applied repeatedly, so that the selection direction describes a circle. This is followed by read-out of unaffected magnetization using a  $90^\circ$  pulse. Rotation improves suppression of extraneous signal, which might otherwise be poor with random noise pulses. An additional advantage is the ability to select cylinders of any cross-section by appropriate gradient modulation.

Projection presaturation (PROPRE) (Singh *et al* 1990a) is somewhat similar to ROISTER, saturating magnetization outside a cylindrical region defined using a series of tailored, small angle pulses with a notched frequency response and a rotating gradient. A soft  $90^\circ$  pulse used for read-out defines the length of the cylinder. The use of small angle pulses facilitates

pulse design using simple Fourier methods, which can result in sharper VOI definition than numerical techniques.  $T_1$  contamination is limited because localization is fast, and can be further decreased by adding an inversion pulse and suitable delay time after the PROPRE pulse train to null extraneous signal. Extension to multiple volumes of more complex shape has been described by Singh *et al* (1990b), and other modifications by Singh and Brody (1993). A two-dimensional version designed for outer volume presaturation in combination with other localization techniques has been described by Shungu and Glickson (1993). The localization quality achieved using PROPRE techniques is sensitive to  $\mathbf{B}_1$  inhomogeneity, and improved performance has been achieved by replacing the conventional pulses with adiabatic pulses in a variant known as BISTRO ( $B_1$ -InSensitive TRain to Obliterate signal) (Luo *et al* 2001).

*5.4.4. Other outer volume saturation methods.* The LOSY (LOck pulse Selective spectroscopY) sequence (Rommel and Kimmich 1989a, 1989b) is an unusual technique employing a pulse cluster consisting of a selective spin-locking pulse {SL} sandwiched between two nonselective  $90^\circ$  pulses of opposite sign, all applied with a gradient.

$$G_i \frac{1}{\sqrt{90^\circ[x']\{SL\}(y')90^\circ[-x']}} \quad (25)$$

The  $\mathbf{B}_1$  vector of the {SL} pulse is incremented in phase by  $90^\circ$  relative to the other pulses, so that it lies in the same direction as the transverse magnetization. In this situation magnetization within a selected slice is 'locked' to  $\mathbf{B}_1$  and decays slowly with a relaxation time known as the rotating frame spin-lattice relaxation time,  $T_{1\rho}$ . Magnetization outside this slice is dephased by the gradient. The preserved magnetization is returned to the positive  $z$ -direction at the end of the cluster, and the cluster is substituted into equation (17) to produce the complete LOSY sequence. LOSY employs simple pulses, relatively immune to hardware deficiencies, but in practice VOI definition is poor. A familiar drawback is the high RF power needed for broadband pulses in the presence of a gradient. The resulting spectrum is  $T_{1\rho}$ -weighted, which is an unusual feature.

Slotboom *et al* (1991) developed a technique known as SADLOVE (Single-shot ADiabatic Localized Volume Excitation), using  $\mathbf{B}_1$ -insensitive adiabatic pulses and therefore particularly well suited for use with a surface coil. In SADLOVE, an adiabatic  $90^\circ$  pulse, generating transverse magnetization throughout the sample, is followed by three slice selective adiabatic  $360^\circ$  pulses, each consisting of two hyperbolic secant pulses (Silver *et al* 1984, 1985), applied in the presence of gradients along each orthogonal axis in turn so as to define a cuboidal VOI. Transverse magnetization outside the VOI is dephased by the gradients, but that inside is returned to its original alignment in the transverse plane by each of the  $360^\circ$  pulses, and hence forms an FID. In later work, the authors show that the behaviour of the sequence in the presence of  $J$ -coupling is superior to that of PRESS (see section 5.5). More recently a very similar sequence, Localization by Adiabatic SElective Refocusing (LASER), has been presented by Garwood and de la Barre (2001). Kinchesh and Ordidge (2005) have proposed the use of FOCI pulses rather than hyperbolic secant pulses in LASER to give sharper VOI profiles, reduced chemical shift offset and hence greater suitability for high-field applications.

## 5.5. Volume selection using spin echoes and stimulated echoes

*5.5.1. Introduction to volume selective echo methods.* The techniques described here achieve volume selection by applying frequency-selective RF pulses and gradients along

three orthogonal axes in such a way that magnetization within a cuboidal VOI is refocused into a spin echo or a related type of signal, described below, known as a stimulated echo (figure 8(b)). Refocusing pulses are an element of some of the slice selective pulse clusters discussed in section 5.4, but the present class of techniques is distinguished by the fact that signal is generated from the VOI directly: no additional  $90^\circ$  read pulse is needed. The spin echo and stimulated echo versions of the sequence, usually known as PRESS and STEAM, respectively, are discussed in sections 5.5.2 and 5.5.3. The performance of the two classes of technique are discussed and compared in section 5.5.5. A method known as VOSY (Volume Selective spectroscopyY), illustrating most of the features of both within a somewhat more general framework that provides some useful insights, has been presented by Kimmich and co-workers (Kimmich and Hoepfel 1987, Kimmich *et al* 1987).

Generically, a volume-selective echo sequence consists of three frequency-selective pulses, each applied in the presence of a gradient along a different orthogonal axis. The general sequence may be written as

$$\frac{G_i}{/90^\circ(x')\backslash} - t_a - \frac{G_j}{/\alpha_2(x')\backslash} - t_b - \frac{G_k}{/\alpha_3(x')\backslash} - t_f - Acq \quad (26)$$

where  $\alpha_2$  and  $\alpha_3$  are usually both  $90^\circ$  or both  $180^\circ$ ,  $G_{i,j,k}$  are the gradients along axes  $i, j$  and  $k$ . In this review the intervals between pulses are designated  $t_a$  and  $t_b$ , and  $t_f$  is an echo refocusing time dependent upon  $t_a, t_b$  and whether a spin echo or a stimulated echo is to be collected. Each of the component pulses affects a slice of magnetization, and because these affected slices are mutually orthogonal only magnetization in a cuboidal VOI at the intersection of the three slices experiences all three pulses. FIDs and echoes generated from other parts of the sample by the pulse train are dephased by subsequent gradients, with additional spoiler gradients and phase cycling used as necessary.

**5.5.2. Volume selected spin echoes—PRESS.** This technique was introduced by Ordidge *et al* (1985) and, as PRESS (Point RESolved Spectroscopy), by Bottomley (1984, 1987). The pulse sequence can be written as

$$\frac{G_i}{/90^\circ(x')\backslash} - t_a - \frac{G_j}{/180^\circ(x')\backslash} - t_b - \frac{G_k}{/180^\circ(x')\backslash} - t_f - Acq \quad (27)$$

and is shown in figure 9. Transverse magnetization generated by the  $90^\circ$  pulse is refocused by the first  $180^\circ$  pulse and again by the second. Only magnetization within the desired VOI experiences all three pulses and contributes to the acquired spin echo. If the  $180^\circ$  pulses are placed symmetrically under the slice selection gradients the echo forms without the need for additional rephasing gradients. However, pairs of spoiler gradients around the refocusing pulses are needed to eliminate transverse magnetization inadvertently generated due to pulse imperfections.

Signal acquired with PRESS is  $T_2$ -weighted according to the factor  $\exp(-T_E/T_2)$ . Frequently, the sequence design is highly asymmetric, so that  $t_a \ll t_b$  and weighting is determined primarily by the interval between the two refocusing pulses. Neglecting pulse angle errors, the only source of  $T_1$ -weighting is incomplete recovery of  $z$ -magnetization if  $T_R < 5T_1$ .

**5.5.3. Volume selected stimulated echoes—STEAM.** This technique was developed by Granot (1986) as VEST (Volume Excitation using STimulated echoes) and by Frahm *et al* (1987) as

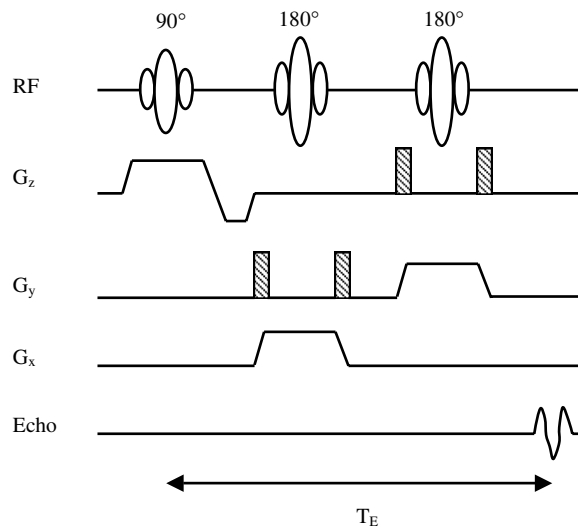


**Figure 9.** Typical PRESS pulse sequence. Spoiler gradients are hatched; the remaining gradients are used for slice selection.

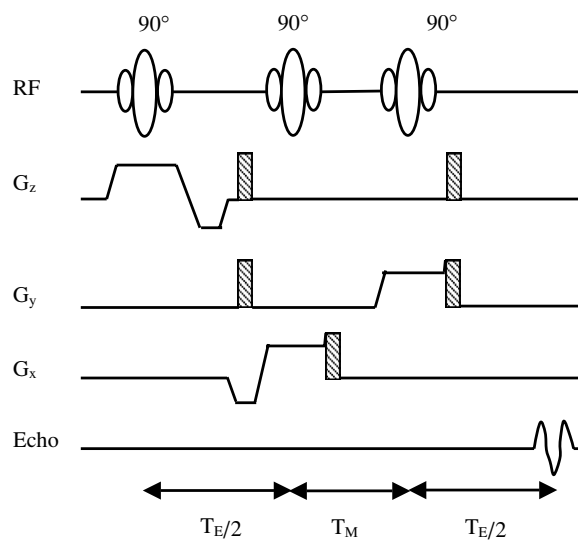


**Figure 10.** Typical STEAM pulse sequence, showing one of a variety of possible spoiler gradient schemes. Spoiler gradients are hatched; the remaining gradients are used for slice selection.

STEAM (STimulated Echo Acquisition Mode) spectroscopy, and is usually known by the latter term. The sequence can be written as

$$\frac{G_i}{\sqrt{90^\circ(x')}} - t_a - \frac{G_j}{\sqrt{90^\circ(x')}} - T_M - \frac{G_k}{\sqrt{90^\circ(x')}} - t_f - Acq \tag{28}$$

where  $T_M$  is known as the ‘mixing time’. Additional spoiler and rephasing gradients are needed to select the desired echo—one possible scheme is shown in figure 10.

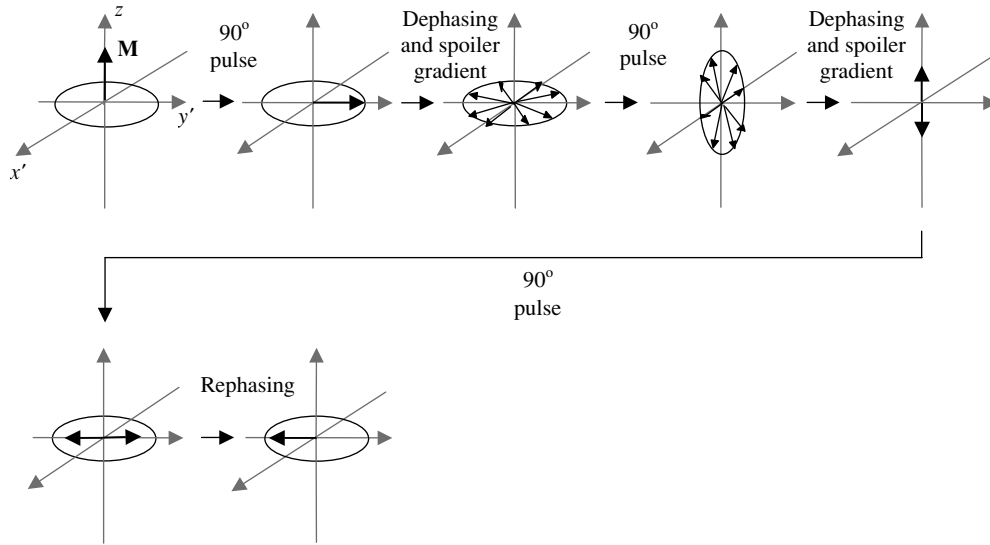


**Figure 11.** The stimulated echo mechanism, depicted in the rotating frame. Following nutation into the transverse plane by a  $90^\circ$  RF pulse, elements of magnetization (known as ‘isochromats’) are intentionally dephased using a spoiler gradient, as well as undergoing dephasing due to local field inhomogeneity. A second  $90^\circ$  pulse tips the resulting plane of isotropically distributed spins into the  $x'$   $z$ -plane, and a further spoiler gradient eliminates the transverse component of each isochromat, leaving only positive and negative  $z$ -magnetization. A final  $90^\circ$  pulse tips this magnetization back into the transverse plane, where it rephases to form an echo.

The origin of the stimulated echo signal is illustrated in figure 11, and can be understood as follows. The initial  $90^\circ$  pulse is followed by a spoiler gradient, so that excited magnetization is distributed isotropically in the  $xy$ -plane before the second  $90^\circ(x')$  pulse is applied. The  $y'$  component of each magnetization isochromat in the column formed by the intersection of the two orthogonal selected slices will be rotated to the  $z$ -axis by this second pulse. The  $z$ -magnetization generated in this way is ‘stored’ along the  $z$ -axis until application of the final pulse, while remaining transverse magnetization is dephased by a further spoiler gradient. Because of the isotropic spin distribution, this process results in loss of 50% of the potential signal (although Zhu and Smith (1999) have shown that it is possible to refocus the lost magnetization as an ‘anti-echo’). Application of the third  $90^\circ(x')$  pulse returns stored magnetization within a cuboidal VOI at the intersection of all three selected slices to the transverse plane and refocuses it as a ‘stimulated echo’.

Loss of 50% of the available signal is partially compensated for by reduced dependence on  $T_2$ , a consequence of storing magnetization along the  $z$ -axis during  $T_M$ , and the potential for shorter  $T_E$ . However, the  $T_M$  interval also introduces a  $T_1$ -weighting factor of  $\exp(-T_M/T_1)$ . Emsley and Bodenhausen (1990) eliminated the  $T_E$  and  $T_M$  intervals altogether by using a soft  $270^\circ$  self-refocusing pulse in place of the train of  $90^\circ$  pulses, although elaborate phase cycling was needed to suppress the resulting FID.

**5.5.4. Hybrid techniques.** The full three-dimensional sequence for the VOISINER (Volume Of Interest by Selective INversion, Excitation and Refocusing) method (Briand and Hall 1988) is as follows:

$$90^\circ[x']/90^\circ(x') \setminus - t_d - /90^\circ(x') \setminus /90^\circ(x') \setminus - T_E/2 - Acq \quad (29)$$

The first cluster inverts magnetization within a slice along the direction of  $G_i$  and dephases that elsewhere, while the rest of the sequence produces a conventional selected spin echo from a VOI within the slice. In later work, Briand and Hall (1991) demonstrated that replacing the first element with the SPACE or SPARS pulse cluster (see section 5.4.2) gives improved selectivity, while the original VOISINER inversion module or the VSE cluster (see section 5.4.1) result in poor slice definition. Phase cycling can be used to eliminate contaminating signal due to imperfect spoiling of magnetization outside the desired VOI during the first element or  $T_1$  recovery of this magnetization before application of the second element.

*5.5.5. Performance of echo-based techniques.* Echo-based localization sequences have a number of advantages and now dominate proton MRS, although there is debate as to the relative merits of spin and stimulated echo acquisition. A useful comparison has been presented by Moonen *et al* (1989), and the main issues are summarized below.

Unlike many techniques, these sequences do not require application of hard pulses in the presence of magnetic field gradients, resulting in lower-power deposition and reduced likelihood of undesirable off-resonance effects. The RF pulses affect only magnetization within the three intersecting slices, so there is reduced potential for background contamination. Contaminating signal can arise from regions of the sample that experience two or more slice selective pulses, but is eliminated by effective spoiling. There is no risk of contamination due to incomplete saturation or  $T_1$  recovery of extraneous magnetization. Taken together, these factors make for excellent localization quality relative to most of the techniques discussed in this review. It also follows that immediately consecutive acquisition from several VOIs is possible so long as the VOIs have no slices in common, although in the case of multi-voxel stimulated echo acquisition, it is necessary to alter the gradient scheme to eliminate additional stimulated echoes originating from outside the desired VOIs (Theberge *et al* 2005). Use of oblique rather than orthogonal gradients can facilitate selection of any desired second volume (Ernst and Hennig 1991b). Conversely, multiple volumes lying along a line defined by the first two RF pulses may be interrogated by replacing the final pulse with a train of frequency-shifted pulses, and STEAM modifications to allow simultaneous two-volume acquisition have been proposed by Hafner *et al* (1990). Combination of echo-based methods with sophisticated NMR techniques is possible, including spectral editing (Kimmich *et al* 1989).

Problems in common with other selective excitation techniques include spatial offset due to chemical shift, and  $T_1$ -weighting of magnetization within the VOI in the event of rapid repetition.  $T_2$ -weighting of the acquired signal is intrinsic to echo-based techniques, and they have therefore traditionally been considered unsuitable for phosphorus spectroscopy, although this is becoming less of a problem as hardware improvements lead to shorter  $T_E$ . In the case of stimulated echo methods there is additional 50% signal loss as described above.

The quality of VOI selection in either sequence relies on the slice profiles excited by the three RF pulses. PRESS is generally regarded as poorer in this regard, since clean slice-selective refocusing is difficult to achieve. High levels of profile contamination when simple truncated sinc pulses are used has been modelled numerically (Moonen *et al* 1989) and observed experimentally (Burtscher *et al* 1999). Truncating pulses further in an attempt to reduce  $T_E$  can have significant impact on contamination (Keevil *et al* 1995). Since STEAM uses only  $90^\circ$  pulses, VOI definition is generally better, with less profile contamination (Keevil *et al* 1995, Yongbi *et al* 1995, Burtscher *et al* 1999) and, since the pulses can be made shorter without serious profile degradation, shorter  $T_E$ . However, modern implementations of PRESS often use optimized pulses (e.g., Mao *et al* (1988)), bringing slice profiles up to the quality of

those obtained in STEAM (Ryner *et al* 1998). Geppert *et al* (2003) report good selection with  $T_E$  as short as 6 ms for animal studies using optimized asymmetric RF pulses.

Since profile, rather than background, contamination dominates in both PRESS and STEAM, one way of minimizing overall contamination is to select a small VOI entirely within the tissue of interest. This is a counterintuitive strategy: generally the largest possible VOI is used to maximize SNR. However, SNR can always be improved by acquiring more signals, while poor contamination is a more fundamental problem. In phantom experiments with a PRESS VOI exactly coincident with the tissue of interest, contamination of between 5–11% (Yongbi *et al* 1995) and 33–35% (Keevil and Newbold 2001) has been reported using sequences with different VOI profiles. With a small PRESS VOI nested within a larger tissue of interest, contamination has been shown to fall to below 2% (Keevil and Newbold 2001). Performance has been found to be essentially independent of  $T_R$ , and also of  $T_E$  except when short echo times are used (Longo and Vidimari 1994, Burtscher *et al* 1999, Keevil and Newbold 2001). Contamination in STEAM is also largely independent of  $T_E$  except at very short echo times, when lower contamination is observed (Burtscher *et al* 1999).

Appreciable background contamination and artefacts can arise in PRESS and STEAM sequences if spoiling of unwanted signals is incomplete. Zhang and van Hecke (1990) demonstrated the importance of complete dephasing of transverse magnetization between the first and second RF pulses in STEAM to avoid chemical shift modulation of both the amplitude and the phase of the acquired signal. They derived conditions for satisfying this requirement in terms of spoiler gradient amplitudes, VOI size and  $T_E$ . For PRESS, Moonen *et al* (1992) derived expressions for the degree of suppression of unwanted signals in terms of spoiler gradient amplitude and duration and VOI size. Keevil and Newbold (2001) showed experimentally that in an asymmetric PRESS sequence performance is highly dependent on the characteristics of the spoiler gradients around the second refocusing pulse. Patient motion and magnetic field gradients generated by susceptibility mismatches within the subject's body also contribute to dephasing and rephasing of magnetization, and Moonen *et al* (1992) and Ernst and Chang (1996) have discussed the consequent influence of slice selection order on spectroscopic artefacts. For human brain MRS, the last RF pulse should select a transverse plane to minimize these effects.

Attempts have been made to minimize echo times for both sequences. Zhong and Ernst (2004) obtained  $T_E = 5$  ms with PRESS on phantoms and 8–10 ms on human subjects by altering the spoiler gradient scheme, requiring additional phase cycling to suppress unwanted signals. By using PROPRE (see section 5.4.3) for slice selection, followed by a  $90^\circ$  excitation pulse and a single  $180^\circ$  refocusing pulse to elicit a volume-selected echo, Shungu and Glickson (1993) also achieved very short  $T_E$  in PRESS. With short RF pulses and high gradient amplitude, an echo time of 5 ms has been achieved for STEAM on a clinical MR system with actively shielded gradients (Seeger *et al* 1998). STEAM generally works rather poorly with a transmit and receive surface coil, but echo times as short as 6.8 ms have been reported with such a coil if the VOI is small and sufficiently sophisticated water suppression is available (Mlynárik *et al* 2000). Shungu and Glickson (1993) proposed replacing one or more of the  $90^\circ$  selective pulses in STEAM with shorter hard pulses, allowing  $T_E$  as short as 3 ms in Hard Observe Transmission STEAM (HOTSTEAM). On small-bore systems with higher gradient performance,  $T_E$  of 1 ms has been reported (Tkáč *et al* 1999). Few of these authors report the impact of their innovations on localization quality.

Echo-based sequences are potentially sensitive to signal loss due to motion during the sequence, which impairs refocusing. Blood flow can be addressed using gradient rephasing techniques similar to those employed for the same purpose in MRI (Gyngell *et al* 1988). STEAM is particularly sensitive to movement, including diffusion, during  $T_M$ . Physiological

motion has been shown to lead to signal loss of up to 40% at long  $T_M$ , which can be recovered to some extent by retrospective cardiac gating (Felblinger *et al* 1998) (or, more simply, by shortening  $T_M$ ). PRESS, by contrast, is relatively insensitive to physiological motion (Katz-Brull and Lenkinski 2004). Dephasing due to more severe patient motion has been addressed by navigator gating in both PRESS (Thiel *et al* 2002) and STEAM (Tyszka and Silverman 1996, 1998).

$J$ -coupling effects during PRESS have been discussed by several authors and are considered in more detail than that is possible here by de Graaf (1998). A useful paper avoiding elaborate mathematical treatment is that of Ernst and Hennig (1991a). These authors focused primarily on the weakly-coupled AX spin system. For PRESS, they found that the effect of  $J$ -coupling amounts simply to modulation of signal intensity as a function of  $T_E$ , as discussed in section 2.6. However, in a more comprehensive model it is necessary to take account of chemical shift offset (see section 5.2), the non-ideal profiles of selective pulses and coupling effects during the RF pulses themselves (Slotboom *et al* 1994, Thompson and Allen 1999, Maudsley *et al* 2005). The impact of chemical shift offset is particularly important. Because the position of the VOI differs for the different spins within the coupled system, there are regions in which all the coupled spins experience the effect of a given component of the pulse sequence and other regions in which only some or one of the spin species does so. The signal acquired must be considered as the sum of signals from a series of 'subvoxels' with different  $J$ -coupling behaviour. This point has been discussed extensively for generic AX<sub>*n*</sub> systems by Yablonskiy *et al* (1998), and Marshall and Wild (1997) have considered the impact on the lactate (AX<sub>3</sub>) lineshape in PRESS-acquired proton spectra. In the case of strong coupling, behaviour is significantly more complicated and the properties of the 180° pulse are particularly critical (Thompson and Allen 1999). Trabesinger *et al* (2005) have studied the behaviour of the AB system during PRESS in the context of citrate (observed in *in vivo* MRS of the prostate), proposing guidelines for optimal detection.

For stimulated echo acquisition, such as STEAM, the effects of  $J$ -modulation, even in the case of weak coupling and ideal pulses, are much more complicated than in PRESS (Ernst and Hennig 1991a). This is because of the development of multiple quantum coherences (beyond the scope of this review) during  $T_M$ . The resulting signal is a superposition of a number of components, each with different dependence on flip angles and pulse timings. There is marked signal oscillation as a function of  $T_M$ , although Wilman and Allen (1993) have shown that this can be eliminated by inserting an inversion pulse during this interval. As with PRESS, realistic selective pulses and the presence of spatial chemical shift offset can further complicate the evolution of magnetization (Thompson and Allen 2001). Wilman and Allen (1993) and Thompson and Allen (2001) have studied the AX<sub>3</sub> spin system, providing useful insight on observation of lactate in proton MRS. The situation is again different in more strongly coupled spin systems: the AB system (citrate) has been modelled and investigated experimentally by Straubinger *et al* (1995) and a variety of weak and strong coupling schemes including AMNPQ (glutamate) by Thompson and Allen (2001). Despite the more complicated behaviour, STEAM is generally favoured over PRESS for detection of  $J$ -coupled nuclei because of the potential for short  $T_E$  acquisition, making the technique especially suited for detection of species where  $J$ -coupling leads to signal loss at longer  $T_E$ , such as glutamate and glutamine in the brain.

Because signal behaviour in either sequence varies with  $J$ -coupling scheme, it is impossible to quantify signal from a molecule of unknown coupling at long  $T_E$ , especially if signals from several metabolites with different coupling schemes overlies each other in the spectrum (Kim *et al* 2005). Conversely, analysis of  $J$ -coupling behaviour as a function of  $T_E$  can help us to verify peak assignment.

**Table 2.** ISIS experimental cycle as described by Ordidge *et al* (1986).

Experiment	$G_x$	$G_y$	$G_z$	$\pm$
1	Off	Off	Off	+
2	On	Off	Off	-
3	Off	On	Off	-
4	Off	Off	On	+
5	On	Off	On	-
6	Off	On	On	+
7	On	On	Off	+
8	On	On	On	-

### 5.6. Volume selection by post-acquisition signal combination—ISIS

Image-selected *in vivo* spectroscopy (ISIS) (Ordidge *et al* 1986) is best introduced in its one-dimensional form. In this technique, slice selection is performed by subtracting the signal obtained using the following sequence:

$$\frac{G_i}{180^\circ(x')} \setminus - t_d - 90^\circ[x'] - Acq \quad (30)$$

From that obtained following a hard  $90^\circ[x']$  pulse alone. In the first sequence, magnetization in a slice defined by the gradient and  $180^\circ$  pulse is selectively inverted, and following the  $90^\circ$  pulse this magnetization is  $180^\circ$  out of phase relative to magnetization elsewhere in the sample, and also relative to magnetization generated throughout the sample in the second experiment. Thus subtraction leads to cancellation of signal from outside the slice while that within the slice adds.

ISIS can also be implemented in two- and three-dimensional modes, the latter being the most common technique for volume selection in  $^{31}\text{P}$  MRS (figure 8(c)). The number of component experiments required for  $n$ -dimensional selection is  $2^n$ , so volume selection requires eight acquisitions. Each experiment includes a different combination of slice selective inversion pulses, as shown in table 2, and in each case a hard  $90^\circ$  pulse is used for signal acquisition. The spatial distribution of magnetization with positive and negative phase varies between experiments depending on the pattern of inversion pulses applied. Localization is achieved by appropriate addition and subtraction of the eight acquired signals: the final column of the table shows the original add/subtract scheme of Ordidge *et al* (1986). This should result in cancellation of signal outside a cuboidal volume defined by the intersection of the three selected slices. Within the VOI, the signal obtained is ideally eight times that achieved with a single unlocalized acquisition. A component of the 3D ISIS cycle is shown in figure 12.

The ISIS signal is  $T_1$ -weighted, unless  $T_R \gg T_1$ , and additional weighting arises in some of the component experiments as magnetization within the VOI that has been inverted recovers during the eddy current delay  $t_d$ . Since an FID is acquired there is no  $T_2$ -weighting, contributing to the status of ISIS as the method of choice for clinical phosphorus spectroscopy and also for experimental work with other nuclei characterized by short  $T_2$ , such as nitrogen-15 (Kanamori and Ross 1999). Another advantage is avoidance of hard pulses applied with magnetic field gradients, allowing lower power deposition without incurring unwanted off-resonance effects.

ISIS is usually implemented with adiabatic inversion pulses—specifically Silver–Hoult hyperbolic secant pulses (Silver *et al* 1984, 1985, Segebarth *et al* 1989)—to improve the quality and uniformity of inversion. This has the added benefits of improving the VOI profile and alleviating signal loss within the VOI due to imperfect inversion (Ordidge *et al* 1986),

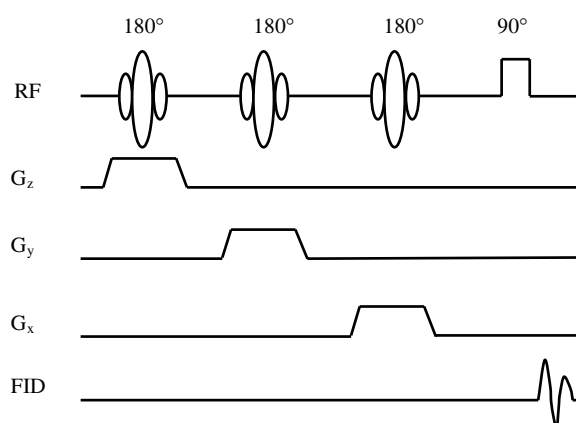


**Figure 12.** ISIS component pulse sequence (experiment 8 in table 1). Other component experiments omit one, two or all three of the inversion pulses.

although with short  $T_2$  species present it can be difficult to satisfy the adiabaticity condition without signal loss and increased profile contamination due to  $T_2$  relaxation (Lawry *et al* 1989).

ISIS requires accurate subtraction of signals originating from the whole sample to yield a localized signal that is usually at least an order of magnitude smaller. This makes the technique prone to dynamic range problems, and any variation in signal intensity between component experiments can result in quite serious subtraction errors and background contamination. This variation may arise from hardware instability or patient motion, and in two- and three-dimensional ISIS there is another important mechanism. In parts of the sample where the detection pulse angle differs from  $90^\circ$  (due to  $\mathbf{B}_1$  inhomogeneity or imperfect optimization), some residual  $z$ -magnetization will remain at the end of each component experiment. If  $z$ -magnetization is allowed to recover fully before the next experiment, this is of no concern. However, under more usual conditions of partial saturation, the size of  $M_z$  at the beginning of any experiment within the ISIS cycle (other than the first) will depend on the residual  $M_z$  at the end of the previous experiment. Outside the three orthogonal slices that define the VOI, repetitive application of identical detection pulses leads to a steady state. However, because magnetization within the selected slices does not experience the same pattern of pulses in each element of the ISIS cycle, a steady state is not reached in at least some locations. Under these circumstances, the signal acquired in each of the experiments will differ in size, and subtraction will not lead to complete cancellation.

This process, termed ' $T_1$  smearing' (Lawry *et al* 1989), is an important source of background contamination in ISIS. It has been modelled by Lawry *et al* (1989) and observed directly as an increase in background signal by Ljungberg *et al* (1995, 1998).  $T_1$  smearing is heavily dependent on  $T_R/T_1$ , and has also been shown to be dependent on the order in which the eight components of the ISIS cycle are performed (Burger *et al* 1992, Matson *et al* 1993). The order originally proposed by Ordidge *et al* (1986) is one of only 48 of the 40 320 possible permutations of the ISIS sequence that are optimal in this respect. These favoured permutations establish a steady state throughout as much of the sample as possible, leaving only a relatively small region within one of the selected slices as a potential source of  $T_1$  smearing (Burger *et al* 1992). Unfortunately, not all subsequent commercial implementations of ISIS adhere to this order. For example, Luyten *et al* (1989) adopted a scheme involving alternation between acquisitions that are to be added and subtracted, later shown by Matson

*et al* (1993) to generate the highest contamination of any alternative included in their study. Ordidge *et al* (1986) proposed separate signal averaging of each of the eight component experiments, allowing development of a steady state throughout the object in each case, with a lengthy delay between the different sets of acquisitions. Although effective at eliminating  $T_1$  smearing, this approach has the potential to increase contamination overall because of sensitivity to patient movement. Ljungberg *et al* (2000) showed, by computer simulation, that by appropriate combination of four complete ISIS cycles, each optimal in terms of  $T_1$  smearing, it is possible essentially to eliminate  $T_1$  smearing over a wide range of detection pulse angles.

Under fully relaxed conditions, in the case of a VOI of nominal dimensions  $50 \times 50 \times 50$  mm coextensive with the anatomical region of interest in a phantom modelling the human head, contamination with  $^{31}\text{P}$  ISIS on different MR systems has been measured as 10–15% (Keevil and Newbold 2001), 14–19% (Keevil *et al* 1992) and approximately 20% (Ljungberg *et al* 1995). Across a range of systems from the same manufacturer, figures of 14–22% have been reported (Keevil *et al* 1995). In the clinically realistic regime  $T_R \approx T_1$ ,  $K$  has been shown to increase modestly (to around 20%) on one commercial MR system (Keevil *et al* 1992) and dramatically (to over 50%) on another (Keevil and Newbold 2001). Because background contamination is dominant in ISIS, selection of a small VOI nested entirely within a tissue of interest is counterproductive as a means of reducing contamination. Applying the definition adopted in this review, contamination of 70% (Keevil and Newbold 2001) and 60% (Ljungberg *et al* 2002) has been measured with such a VOI by different groups using the same non-optimal sequence order for  $^{31}\text{P}$  MRS. Better results are obtained using a larger VOI, even if it extends beyond the edges of the tissue of interest.

Contamination in ISIS due to  $T_1$  smearing can be minimized by use of composite saturation pulses to eliminate residual  $z$ -magnetization after each acquisition (Hubesch *et al* 1988, Matson *et al* 1988). Alternatively, each component experiment can be prefixed with a noise prepulse to randomize  $z$ -magnetization outside the desired VOI (Ordidge 1987). The resulting OSIRIS (outer volume suppressed image-related *in vivo* spectroscopy) method (Connelly *et al* 1988) is also less demanding on the ADC dynamic range. Yongbi *et al* (1995) implemented a similar approach for  $^1\text{H}$  ISIS using adiabatic pulses for outer volume signal suppression—although contamination still reached 45% with a small VOI. De Graaf *et al* (1995, 1996) built on this idea by implementing a modified ISIS sequence, OVS-ISIS, using BIR-4 pulses (Garwood and Ke 1991) that combine the effects of the noise pulses with adiabatic inversion to yield a single-shot version of ISIS. The most common approach, however, is to replace the  $90^\circ$  pulses with adiabatic half passage (AHP) pulses (Bendall and Pegg 1986, Ugurbil *et al* 1987, Segebarth *et al* 1988), the aim being to nutate magnetization completely into the transverse plane throughout the sample, regardless of  $\mathbf{B}_1$  inhomogeneity. However, the effectiveness of AHP pulse implementation in this regard has been shown to vary between different MR systems (Keevil *et al* 1995), and performance has been reported that is no better (Keevil and Newbold 2001, Burger *et al* 1992) or even poorer (Keevil *et al* 1992) than that obtained using conventional  $90^\circ$  pulses. It is likely that the adiabaticity condition (see section 2.1) is not being met in such cases.

Chemical shift offset is a problem in ISIS, as with nearly all techniques using static field gradients. Ordidge *et al* (1986) originally suggested alternation of the gradient direction between sets of ISIS experiments to overcome this, but then the size of the VOI, rather than its position, varies with chemical shift. In later work, Ordidge *et al* (1996) developed frequency offset corrected inversion (FOCI) pulses allowing adiabatic inversion with reduced power deposition so that chemical shift offset can be addressed through increased gradient strength. Payne and Leach (1997) have demonstrated a reduction in contamination (using the

measurement technique of Bovée *et al* (1995)) from around 15% to 4% when these pulses replace Silver–Hoult pulses in ISIS. Tannús and Garwood (1997) give a more comprehensive theory of gradient-modulated offset-independent adiabaticity (GOIA) pulses that satisfy the adiabaticity condition but are less sensitive to chemical shift offset. An interesting alternative solution has been proposed by Volk *et al* (1988). In the FRIVOL (FRrequency-Interval-selective VOlume Localization) sequence, two-dimensional ISIS is used to define a column, and a slice of this material is selected using special chemical shift selective RF and gradient pulses which refocus only the spectral line on resonance. The experiment can be repeated within the repetition time with each metabolite on resonance in turn. Since the object as a whole is never excited, the dynamic range problem is also reduced. However, some  $T_2$ -weighting is introduced by the use of an echo, and phase cycling is needed to overcome imperfections in the chemical shift selective pulse.

Müller *et al* (1988) have proposed extension of ISIS (and other techniques) to multiple slices or volumes offset along a single axis by addition of further inversion pulses offset in frequency and a more elaborate add/subtract scheme. A less time-consuming approach to the acquisition of ISIS spectra from an array of cubic elements, again using additional inversion pulses, has been described by Ordidge *et al* (1988). This method can be modified to allow division of an irregular volume into an array of cuboids of varying size. Alternatively, in conformal ISIS (C-ISIS) the shape of the VOI can be modified to a parallelepiped by using oblique gradients, or to a number of other polyhedral shapes, including concave volumes, by addition of further gradients and special composite pulses which function as logical operators (Sharp and Leach 1989a, 1992). Simultaneous multi-voxel acquisition is also possible (Sharp and Leach 1989b). Such volumes can be tailored more closely to irregular anatomical regions. The authors suggest extension to other conformal sequences such as C-ISIS/STEAM for proton spectroscopy.

ISIS can readily be combined with other localization techniques. Methods using a two-dimensional implementation to prepare a column of magnetization for interrogation using rotating frame MRS are described elsewhere in this review (see section 4.3). Two-dimensional ISIS has also been combined with DRESS in a technique known as CRISIS (Bottomley 1987) or CODEX (CODEd slice EXcitation) (Jung and Lutz 1988). This reduces the effect of patient motion along the axis of the DRESS slice, and also the complexity and ADC demands of ISIS, at the cost of some  $T_2$ -weighting (Jung *et al* 1992).

Reduced power deposition is achieved in an add/subtract method due to Tannús *et al* (1991) using GMAX (Gradient Modulated Adiabatic eXcitation) pulses (Johnson *et al* 1989). These pulses give slice selection in two acquisitions. In three dimensions eight experiments are still required, but this approach is less demanding on dynamic range and  $\mathbf{B}_1$  homogeneity.

ISIS owes its popularity for  $^{31}\text{P}$  studies, as compared to earlier techniques, to a combination of immunity to  $T_2$  decay, clean localization and clinically acceptable power deposition. There is potential for considerable background contamination, but this can be minimized by judicious choice of experimental cycle and VOI size.  $^1\text{H}$  studies form the vast majority of clinical spectroscopy work today, so use of ISIS is less widespread than in the past. It seems likely that any future developments in  $^{31}\text{P}$  localization techniques will centre on further reduction in  $T_E$  in PRESS and STEAM, combining excellent background suppression with ability to collect signals from species with short  $T_2$ .

### 5.7. Volume selection using multi-dimensional designer pulses and high-order gradients

The design of RF pulse and gradient waveforms to provide selective excitation that is geometrically tailored in two or three dimensions is a substantial field of research in its

own right. The principles of pulse design, and many of the applications, are beyond the scope of this review. The following brief discussion covers approaches that have been applied to spatial localization in MRS, but there is also a great deal of more general work on pulse design that may have implications in the field—for example, the recent work of Kobzar *et al* (2005) on ‘pattern pulses’. As well as spatially tailored excitation, pulse design encompasses ‘spectral–spatial’ pulses, which are selective in chemical shift as well as space and may have a role in water and lipid suppression or selective excitation of specific resonances.

Two-dimensional selective pulses for localized MRS were first described by Bottomley and Hardy (1987a, 1987b), who applied a 180° RF pulse and rotating gradient (generated by modulation of two orthogonal gradients) to invert a column of magnetization. This pulse was combined with DRESS (Bottomley *et al* 1984) in a volume selection technique known as PROGRESS (Point-resolved ROTating GRAdient Surface-coil Spectroscopy). Localization was relatively poor, with significant ‘ringing’ outside the desired VOI, but performance could be improved by numerical optimization using simulated annealing (Kirkpatrick *et al* 1983, Metropolis *et al* 1953), and Hardy *et al* (1988a, 1988b) presented results in which ringing was practically eliminated. However, these techniques are very demanding on gradient and RF hardware and probably not suitable for clinical application.

An alternative approach to the design of two-dimensional pulses has been pursued by Pauly *et al* (1989, 1990), who used analytical methods to design spiral  $k$ -space trajectories which, combined with suitable RF waveforms, produce self-refocused two-dimensional excitation pulses. These techniques can be extended to three-dimensional localization using a stacked spiral  $k$ -space trajectory (Pauly *et al* 1993). Morris *et al* (1991) took the RF waveforms developed by Pauly *et al* as a starting point for numerically optimized two- and three-dimensional pulses, and using more general RF waveforms Hardy and Cline (1989) were able to select discs, annuli, squares, circles and more elaborate shapes with only moderate ringing. Correction techniques to compensate for nonuniform sampling of  $k$ -space (Hardy *et al* 1990) allow extension to  $k$ -space trajectories other than a spiral. Such techniques have in the past been difficult to implement on conventional MR systems due to gradient amplitude and slew rate limitations (Spielman *et al* 1991). However, the gradient demands can be reduced by using ‘pinwheel’ pulses (Hardy and Bottomley 1991), which cover  $k$ -space in a number of shallow spirals. Takahashi and Peters (1995) have proposed an alternative approach in which the actual gradient waveform is measured and the RF waveform is modified to correct for gradient-related distortion. Applications of these techniques to MRS have been limited to date, but St Lawrence *et al* (1998) combined a two-dimensional pulse with PROPRES (see section 5.4.3) in an outer-volume saturation technique that minimizes contamination due to recovery of extraneous short- $T_1$  species. The two-dimensional pulse alone resulted in contamination of 37%, which reduced to <1% with the addition of PROPRES.

Serša and Macura (1996, 1997) have developed a technique known as CARVE (Completely Arbitrary Regional Volume Excitation), specifically intended for localized MRS, which uses a series of small flip-angle pulses interleaved with gradients to generate a  $k$ -space trajectory determined by the Fourier transform of the desired excitation volume. The flip angles and phases of the RF pulses and the gradient trajectory are optimized using simulated annealing. The complexity of the profile that may be excited is limited in practice by gradient hardware performance, but this can be addressed, and the technique extended to three-dimensional excitation, by dividing the required sequence into several portions that are executed separately and summing the results (Serša and Macura 1998). Sensitivity is improved if the flip angles are fixed and the desired profile achieved by weighting of the summed acquisitions (Serša and Macura 2000). This is an extremely promising method for conformal MRS.



**Figure 13.** (a) Array of proton NMR spectra, and (b) metabolite map showing the ratio of *N*-acetylaspartate to total creatine. Data acquired from the brain in a patient with left frontal anaplastic oligodendroglioma using two-dimensional spin-echo MRSI with PRESS volume selection and outer volume suppression (OVS).

Another approach to multi-dimensional excitation is the use of narrowband pulses in the presence of nonlinear magnetic field gradients to select circular or elliptical columns for subsequent interrogation using spectroscopic imaging—a technique known as SHOT (Selection with High-Order gradient) (Oh *et al* 1991). Despite promising results, the technique has not been pursued more generally because of the abnormal hardware requirements.

## 6. Magnetic resonance spectroscopic imaging

### 6.1. Introduction to MRSI

MR spectroscopic imaging (MRSI), otherwise known as chemical shift imaging (CSI), differs fundamentally from techniques discussed so far in this review. The purpose of these previous techniques is to restrict signal collection to a single region of interest, or voxel, within the sample. The ability offered by some techniques to collect data from several volumes either simultaneously or sequentially is an incidental, if sometimes very useful, feature.

MRSI, by contrast, employs slice selection and spatial encoding techniques drawn from MRI to collect spectra simultaneously from a one-, two- or three-dimensional array of voxels. Simultaneous spatial and spectral resolution allows multi-voxel MRS and creation of metabolite maps—images of the spatial distribution of individual metabolites (e.g., Luyten *et al* (1990)) (figure 13).

MRSI has a number of advantages relative to single-voxel techniques. It is possible to map metabolite levels within and around a lesion and in distant normal tissue simultaneously, rather than simply to collect a spectrum from a single location that must be chosen in advance, and these metabolite maps are intrinsically registered to structural MR images. This opens new vistas for MRS and provides biochemical data complementary to that available from techniques such as PET, and could do much to help overcome the reluctance of many in the radiological community to embrace MRS. Some of the problems encountered with single-voxel techniques using selective excitation are absent—for example, spatial offset due

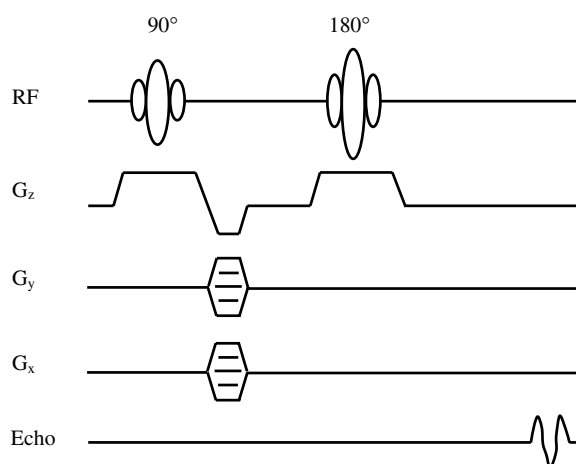


**Figure 14.** Typical two-dimensional spin-echo MRSI pulse sequence.

to chemical shift (Bottomley *et al* 1988). However, several new factors arise when considering the performance of MRSI, and these are discussed below.

MRSI may be regarded as a special case of MRI, just as much as a class of localized MRS, and detailed discussion soon leads to consideration of issues related to MRI pulse sequences and techniques that are beyond the scope of this review. The discussion of MRSI here will be largely restricted to spectroscopic aspects that allow comparison with single-voxel techniques. Similarly, issues related to the analysis and visualization of MRSI data sets are not discussed here: examples of the procedures adopted are described by Maudsley *et al* (1992).

### 6.2. Fourier techniques

Conventional MRSI emerged in the early 1980s, following the development of Fourier transform MRI (Brown *et al* 1982, Maudsley *et al* 1983, Haselgrove *et al* 1983, Pykett and Rosen 1983). Just as in MRI, an excitation pulse is applied to generate transverse magnetization. This magnetization precesses in the presence of one, two or three mutually orthogonal phase encoding gradients, so that phase angles develop which reflect position within the sample in one, two or three dimensions (see section 2.7.4) (figure 14). The phase encoding gradients are switched off, and signal is acquired as an FID or a spin echo. An important difference between MRSI and conventional MRI is that frequency encoding is generally not used, so that frequency differences within the acquired signal reflect only chemical shift. The process is repeated with various gradient amplitudes to provide a full set of phase-encoded signals, and Fourier transformation is carried out to yield an array of data resolved in frequency and in space. Two- and three-dimensional MRSI is preceded by selection of a slice or a thicker 'slab', respectively, to restrict the region of signal collection. One-dimensional MRSI is usually combined with two-dimensional static field gradient localization to facilitate spatial resolution within a selected column.

The MRSI signal may be collected as an FID or a spin echo. The disadvantage of FID acquisition is that phase evolution due to chemical shift is not refocused and causes distortion of the resulting spectra (Wang *et al* 1991). With sufficient SNR, this can be overcome by numerical post-processing to permit the production of high quality phosphorus metabolic images (Twieg *et al* 1989, Maudsley *et al* 1990). FID acquisition is sensitive to  $\mathbf{B}_0$

inhomogeneity favouring use of adiabatic excitation pulses (Brown *et al* 1989), and to eddy currents. Spin echo MRSI avoids these problems and is particularly suitable for proton MRS.  $T_2$  losses can be prohibitive for phosphorus studies, but this can be overcome with equipment capable of short echo times and effective eddy current compensation or shielding (Maudsley *et al* 1990).

Because MRSI uses only phase encoding, it is a time-consuming, low-resolution technique relative to conventional MRI. An  $n$ -dimensional study with a resolution of  $m$  pixels in each direction requires acquisition of at least  $m^n$  signals. If  $T_1$ -weighting is to be avoided, a repetition time  $T_R > 5T_1$  is needed (unless small flip angle excitation pulses are used). This limits the spatial resolution that is practically achievable. Also, the relatively low concentrations of metabolites of interest preclude high resolution on signal-to-noise grounds. MRS images therefore typically have only  $8 \times 8$  or  $16 \times 6$  voxels, resulting in poor sampling in  $k$ -space and a sinc-shaped point spread function (PSF) (or spatial response function, SRF) in the reconstructed image. The sensitivity profile of each voxel is degraded, so that the effective resolution of the image is considerably poorer than the nominal voxel size. There is signal loss from within the voxel, and PSF sidelobes lead to blurring and cross-contamination between voxels (known as Fourier bleed) (Wang *et al* 1991, Koch *et al* 1994). The poor PSF is the main limit on localization performance in MRSI. Performance parameters calculated from measured PSFs vary widely with hardware and sequence details (Bové *et al* 1998). Cross-contamination is increased in the presence of patient motion (Doyle *et al* 2000, Schwarz and Leach 2000). This can be minimized by signal averaging and by decreasing the number of phase encoding steps, which unfortunately coarsens sampling further and hence degrades the PSF.

The PSF can be improved by weighting the number of acquisitions made at each  $k$ -space point (Mareci and Brooker 1991, Pohmann and von Kienlin 2001), or by varying the repetition time (Kuhn *et al* 1996), excitation angle (Webb *et al* 1991), or density of sampling points (Greisler and von Kienlin 2003) through  $k$ -space. Hennig (1992) proposed the use of multi-slice selective pulses to provide discrete phase encoding, with a unique phase associated with each voxel on each repetition of the sequence. Alternatively, filtering and other post-processing techniques can be used to improve the PSF (Wang *et al* 1991, Koch *et al* 1994, Vikhoff-Baaz *et al* 2001, 2001b), but are generally less satisfactory than tailored data acquisition.

An important step in any MRS procedure is ‘shimming’—the process of optimizing the uniformity of the static magnetic field over the region from which signal is to be collected. MRSI requires the field to be shimmed over a whole slice, stack of slices or volume, which is difficult in the presence of significant susceptibility-related inhomogeneities—for example, at the edge of the brain. Poor shimming can impair water and lipid suppression, which are also prerequisites for successful MRSI, broaden spectral peaks and introduce image distortion. When MRSI is used in conjunction with single-voxel MRS (see below), susceptibility effects may also degrade the selected VOI. These effects can be minimized by careful placement of MRSI slices and VOIs (Vikhoff-Baaz *et al* 1999).

In MRSI of the brain, even in the absence of susceptibility problems, the PSF leads to Fourier bleed of intense lipid signals from the scalp into voxels within the brain. Various strategies have been proposed to tackle this, including novel sampling schemes to extend  $k$ -space coverage using fast imaging techniques or to allow lipid signals to be identified and eliminated in post-processing (Hu *et al* 1994, 1995, Haupt *et al* 1996, Metzger *et al* 1999, Ebel and Maudsley 2001). Panych *et al* (2005) have recently proposed novel excitation strategies using two-dimensional RF pulses to eliminate PSF sidelobes. More conventional inversion recovery lipid suppression techniques drawn from MRI may be used, but the details of these

are beyond the scope of this review (Ebel *et al* 2003). However, the problem is frequently addressed simply by selecting a large VOI using single-voxel localization and then performing MRSI within this volume (Luyten *et al* 1990, Spielman *et al* 1991). This can result in loss of useful cortical information (Tanaka *et al* 1991) and introduces chemical shift misregistration artefacts.

More recently outer volume saturation (OVS) techniques have been adopted for conformal suppression of superficial lipid signals. This is now a standard feature of MRSI on clinical MR scanners. Many of the techniques discussed in section 5.4, such as ROISTER (de Crespigny *et al* 1989), PROPRE (Singh *et al* 1990a) and BISTRO (Luo *et al* 2001), are capable of conformal suppression. For example, an approach to OVS based on PROPRE has been presented by Shungu and Glickson (1993, 1994). However, OVS as implemented on clinical MR systems usually consists simply of application of up to eight frequency selective excitation pulses with gradient dephasing at different orientations around the margin of the skull. Extension to three-dimensional suppression is also possible (Chen *et al* 1997).  $T_1$  recovery of the suppressed signals may be limited by flip angle optimization (Duyn *et al* 1992) or by repeated suppression (Posse *et al* 1995). Other pulse schemes with improved suppression characteristics have been proposed by Tran *et al* (2000) and Chu *et al* (2003).

Proton MRSI is more difficult outside the brain, since susceptibility variations are greater, but has found an important clinical role in prostate cancer (Kurhanewicz *et al* 1996). Here an important consideration is  $J$ -modulation of the citrate resonance (Cunningham *et al* 2005).

### 6.3. Projection reconstruction techniques

Projection reconstruction MRSI (Lauterbur *et al* 1975) is a surprisingly old technique. It predates the development of phase encoding and, in its original form employed only frequency encoding gradients. The basis is to collect FIDs with the gradient in each of a number of orientations and recover the image by filtered back-projection (Radon 1917). This approach has serious consequences for the quality of the acquired spectra, and in later work Lauterbur (1975) generated arrays of spectra by using slice selection rather than frequency encoding. Bendel *et al* (1980) and Hall and Sukumar (1982) restored weak frequency encoding gradients to reduce examination time at the cost of spatial resolution and line width. These problems were addressed to some extent in later work (Lauterbur *et al* 1984, Bernardo *et al* 1985, Haselgrove *et al* 1985), and the reduced examination time as compared to standard phase encoded MRSI was exploited by Lee and Lauterbur (1990) in a modification of the SLIM technique described in section 6.6. Combination with EPI-based techniques by Mansfield and co-workers is discussed below.

### 6.4. Rapid MRSI

Even modest resolution of  $16 \times 16$  voxels for a two-dimensional MRSI study requires an acquisition time in excess of 10 min. Three-dimensional studies may take several hours, which is prohibitive for clinical applications. There are a number of approaches, based on techniques developed in the context of MRI, to expedite data acquisition.

Modified  $k$ -space sampling schemes have been discussed previously in the context of PSF modification. A similar approach can be used to reduce acquisition time (Ehrhardt 1990, Maudsley *et al* 1994, Hugg *et al* 1996). Most commonly, a circularly or elliptically reduced scheme is adopted in which collection of high spatial frequency data (having both high  $k_x$  and high  $k_y$ ) is omitted, reducing experimental duration by as much as 40%. Other approaches derived from MRI, such as rectangular FOV techniques, can also be used (Golay *et al* 2002).

These schemes can adversely affect the PSF, but simultaneous  $k$ -space reduction and PSF improvement is possible (Ponder and Twieg 1994, Hetherington *et al* 1995).

An alternative approach to fast MRSI is to draw on the wealth of fast data acquisition techniques developed for MRI. The aim of these techniques is generally to cover  $k$ -space more rapidly without incurring heavy  $T_1$ -weighting by acquiring multiple signals following each excitation, either as a series of spin and/or gradient echoes or by collecting signals with a number of coils simultaneously. With appropriate modifications, many of these sequences are suitable for MRSI applications. A comparison of the properties and performance of many such techniques has been presented by Pohmann *et al* (1997), and will not be repeated here.

*6.4.1. Turbo spectroscopic imaging.* The fast or turbo spin echo technique, based on RARE (rapid acquisition with relaxation enhancement) (Hennig *et al* 1986), has become ubiquitous in MRI. In this sequence, a series of  $180^\circ$  refocusing pulses is applied so that a train of spin echoes is generated after each excitation. Each echo is separately phase encoded, so that  $k$ -space is covered in a reduced number of excitations. Each echo in the train has a different value of  $T_E$ , and  $T_2$ -weighting is dominated by the echo that contributes to the centre of  $k$ -space. In the spectroscopic version of this sequence (Duyn and Moonen 1993),  $k$ -space is divided into one circular and two or three annular regions, with two-dimensional phase encoding so arranged that one echo in each train contributes to each region (circular  $k$ -space reduction is intrinsic to the technique). The sequence is limited to three or four echoes because of  $T_2$  decay, and even then suffers from poor spectral resolution because of the short acquisition window. With this turbo spectroscopic imaging (TSI) technique, acquisition of  $32 \times 32$  voxels is possible in 11 min with an echo train length (ETL) of three (Liu *et al* 2001, Martin *et al* 2001) and 6 min with an ETL of four (Stengel *et al* 2004).

*6.4.2. Echo planar spectroscopic imaging.* In echo-planar imaging (EPI) (Mansfield 1977), a train of gradient echoes is collected very rapidly from a selected slice using an oscillating read-out gradient. Modified EPI sequences for MRSI have been proposed by a number of groups. The basis of all these techniques is the fact that chemical shift dephasing is not refocused in a gradient echo, so that the phase of magnetization evolves between echoes at a rate that depends on chemical shift. Phase encoding chemical shift in this way allows frequency encoding of each echo to be used for spatial localization in one dimension, as long as broadening of the spectral lines due to collection of the signal in the presence of a gradient can be overcome. Use of a periodic gradient waveform can eliminate line broadening, although the gradient switching frequency must exceed the desired spectral bandwidth (Macovski 1985), which is quite demanding on hardware.

Spectroscopic EPI, often known as echo planar shift mapping (EPSM) (Mansfield 1983, 1984), is capable in principle of single-shot imaging. This would require very rapid switching of two orthogonal gradients, providing fairly crude resolution in two spatial dimensions. A less demanding approach is to attempt only one-dimensional spatial localization during the echo train, with projection reconstruction or phase encoding used for the second dimension. The first such technique, projection–reconstruction echo planar (PREP) imaging, was proposed as early as 1983 (Mansfield 1983, 1984, Doyle and Mansfield 1987, Bowtell *et al* 1989). PREP uses a single oscillating gradient for one-dimensional localization and chemical shift encoding, with the gradient direction rotated over a series of acquisitions and projection reconstruction (see section 6.3) used to recover the image. PREP has been revived more recently, and Star-Lack (1999) has presented techniques for optimal gradient waveform design to maximize SNR. Projection reconstruction was replaced with conventional phase encoding of the second spatial dimension in later EPI-based methods due to Matsui *et al* (1985, 1986),

Guilfoyle *et al* (1989) and Webb *et al* (1989). As with conventional EPI, the gradient switching required by these sequences was beyond the capability of most clinical MR systems at the time. However, subsequent technological developments have allowed implementation of proton echo planar spectroscopic imaging (PEPSI) in two (Posse *et al* 1995) and three dimensions (Posse *et al* 1994), with total acquisition times of 64 s and a few minutes, respectively. The two-dimensional technique is fast enough to monitor physiological events in real time (Posse *et al* 1997). A similar approach has been reported by Adalsteinsson *et al* (1995). As well as increasing imaging speed, echo planar MRSI can be used to improve image resolution. Ebel and Maudsley (2003) have reported  $64 \times 48 \times 18$  voxel resolution in the head, exploiting the fact that reduced intravoxel dephasing when smaller voxels are selected offsets the loss of SNR. Greater speed is possible with the line scan echo planar MRSI (LSEPSI) technique (Oshio *et al* 2000) in which selective  $90^\circ$  and  $180^\circ$  pulses with mutually orthogonal gradients are used to select a column of spins for interrogation by an oscillating gradient, encoding the remaining spatial dimension and chemical shift information. Signals from columns covering an entire slice can be collected within 4 s without the need to wait for  $T_1$  recovery. The same group has presented line-scan turbo spin echo variants (Mulkern *et al* 1996, 2004) that, although slower, still image a slice in tens of seconds.

*6.4.3. Spiral spectroscopic imaging.* Apart from the conventional EPI sequence, other oscillating gradient techniques exist for rapid coverage of  $k$ -space and have been applied to MRSI. Application of oscillating orthogonal gradients during data collection can be used to cover  $k$ -space in a spiral trajectory, providing two-dimensional spatial encoding, whilst chemical shift information is also encoded in the phase of the acquired signal. The third spatial dimension is addressed using a conventional phase encoding gradient, giving a stacked spiral trajectory overall (Adalsteinsson *et al* 1998). These techniques are demanding in terms of reconstruction, because data must be regridded prior to Fourier transformation. Spiral acquisition has advantages in terms of PSF behaviour: the pitch of the  $k$ -space spirals can be varied throughout the trajectory to generate a sampling window that minimizes sidelobes (Adalsteinsson *et al* 1999), or a dual density approach can be adopted in which the centre of  $k$ -space is sampled densely and the pitch is increased to acquire data from the periphery and hence improve the PSF (Sarkar *et al* 2002). Because the stacked spiral trajectory repeatedly samples the centre of  $k$ -space, corrections can be applied for motion-induced phase variation (Kim *et al* 2004).

*6.4.4. Stochastic spectroscopic imaging.* Roos and Wong (1990) proposed an MRSI technique based on oscillating gradients in which conventional RF pulses are replaced by pulses with flip angles generated from a pseudo-random sequence. This technique, based on stochastic MRI methods developed by others (e.g., Blümich and Spiess (1986)), allows reduced power deposition without loss of sensitivity, reduced  $T_2$  dependence and better eddy current behaviour (Roos *et al* 1991). Signal is acquired after each excitation, and an estimate of spin distribution (in the spatial and chemical shift dimensions) is achieved by cross-correlation of this signal with a 'localization function' which is dependent on the gradient waveform and on a 'weighting function' selected by the user to minimize cross-contamination. Alternatively, if constant gradients are used and are incremented over a series of experiments, a backprojection method is produced which requires only multiplication in the frequency domain rather than cross-correlation in the time domain for image reconstruction (Janssen and Blümich 1992).

*6.4.5. MRSI using steady-state free precession.* Steady-state free precession (SSFP) denotes a class of pulse sequences that, although known for some years (Opelt *et al* 1986), have

only recently received widespread attention in MRI due to hardware improvements. In a generic SSFP sequence, low flip-angle RF pulses are applied repeatedly with  $T_R$  comparable to  $T_2$ , so that a steady state rapidly develops in which magnetization is recycled constantly between the longitudinal axis and the transverse plane. Each pulse generates an FID signal by tipping magnetization into the transverse plane, but also partially refocuses existing transverse magnetization into a spin echo-like signal. Both signals have complicated dependence on  $T_1$ ,  $T_2$  and a variety of pulse sequence factors, and sequences exist with a bewildering range of manufacturer-specific acronyms that use these two signals in different ways for imaging. Modified SSFP sequences using only phase encoding for spatial localization have now been applied for phosphorus (Speck *et al* 2002) and proton (Dreher *et al* 2003) MRSI. The several options for SSFP signal acquisition all present different challenges, for example in terms of  $T_1$ - and  $T_2$ -weighting, response to  $J$ -coupling and off-resonance effects. There is a trade-off between high SNR and speed, both favoured by short  $T_R$ , and spectral resolution, favoured by longer  $T_R$  to maximize phase dispersal. Thus the techniques are best suited to high-field MRS (3 T or more) as phase dispersal is faster.

*6.4.6. Echo time encoding.* Several authors have proposed alternative MRSI techniques whereby phase encoding of chemical shift is achieved prior to signal acquisition. In the original proposal of Sepponen *et al* (1984), the timing of the  $180^\circ$  pulse in a spin echo MRSI sequence is varied over a series of acquisitions with the echo time fixed so that the phase of the magnetization evolves under the influence of chemical shift for varying periods of time. Since chemical shift information is phase encoded during this interval, frequency encoding can be used for spatial localization, and there is a further time saving if chemical shift resolution can be sacrificed. Ford (1990) has proposed a similar method, known as GRAPES (GRAdient Amplitude Phase-Encoded Spectral) imaging, in which the echo time is varied instead. Norris and Dreher (1993) built on the method of Sepponen *et al* by encoding chemical shift information in an incremented evolution period between excitation and two-dimensional imaging—in this case using a RARE variant known as U-FLARE (Norris *et al* 1992). In the original implementation the  $90^\circ$ – $180^\circ$  pulse interval was fixed and the subsequent delay before the imaging module varied to achieve encoding, but in later work the position of the  $180^\circ$  pulse was varied within a fixed interval to improve performance, especially handling of  $J$ -modulation (Dreher and Leibfritz 1999). With prior knowledge about the resonances in the spectrum, the number of repetitions can be reduced to the minimum needed for chemical shift encoding, bringing a further time reduction (Ebel *et al* 2000). A modified version of the sequence was implemented for head imaging by Schäffter *et al* (1998). Imaging sequences other than U-FLARE have been used following spin preparation in very similar techniques. In the spectroscopic FLASH (SPLASH) method of Haase and Matthaei (1987), FLASH (Fast Low Angle SHot) (Haase *et al* 1986) is used, while Guimaraes *et al* (1999) used EPI, Dreher and Leibfritz (2000) a gradient and spin echo train hybrid known as GRASE (GRAdient And Spin Echo imaging) (Oshio and Feinberg 1991), and Dreher and Leibfritz (2002) a version of RARE (Hennig *et al* 1986). In the somewhat similar approach of Haase (1990), chemical shift information is introduced by allowing spins to precess in the interval between two  $90^\circ$  pulses of opposite sign prefixed to a snapshot FLASH sequence (Haase *et al* 1986). Twieg (1989) presented a hybrid method, with incrementation of the delay between excitation and an oscillating read-out gradient used to increase bandwidth to compensate for the hardware limitations of the time. Initially this was applied only to separation of fat and water images.

Another fast MRI technique that has now been applied to MRSI is BURST (Hennig and Hodapp 1993). In echo-time-encoded BURST imaging (EBI) (Jakob *et al* 1995), a train of low

flip-angle RF pulses is applied in the presence of a gradient to generate a number of transverse magnetization vectors which are refocused by a slice-selective refocusing pulse. The resulting train of spin echoes is read out in the presence of a frequency encoding gradient, generating as many individual echoes as there were RF pulses in the excitation train. Each of these echoes contains one-dimensional spatial information, and the chemical shift information evolves from echo to echo. Over a series of repetitions with different phase encoding gradients, the sequence provides echo-time encoding of chemical shift as well as two-dimensional spatial encoding. A modified technique allowing single-shot acquisition has been proposed by Jakob *et al* (1996). In this approach, SISSI (Single-Shot Spectroscopic Imaging) an oscillating read-out gradient produces a series of echo trains, and a phase encoding gradient is applied during the excitation pulse train. Each echo is frequency encoded, progression from echo to echo within a train provides spatial phase encoding, and progression from echo train to echo train provides phase encoding of chemical shift.

*6.4.7. Partially parallel spectroscopic imaging.* Recently, partially parallel imaging techniques such as SENSE (SENSitivity Encoding) (Pruessmann *et al* 1999) have been introduced in MRI. These techniques use the predetermined sensitivity profiles of an array of receive coils to ‘unwrap’ a severely aliased image, allowing dramatic reduction in  $k$ -space coverage and hence increased imaging speed without loss of spatial resolution. Partially parallel acquisition has now been introduced for MRSI (Dydak *et al* 2001), with a SENSE acceleration factor of 2 along each in-plane axis giving a four-fold reduction in scan duration. Spectral as well as spatial resolution is preserved, although the unfolding of the aliased data can leave residual aliased PSFs. Current developments in multiple channel spectrometers and multiple receiver coil technology will allow much higher acceleration factors in the near future. For even faster imaging, SENSE-SI can readily be combined with other approaches to fast MRSI, such as TSI (Dydak *et al* 2003).

### *6.5. Hadamard techniques*

Hadamard spectroscopic imaging (HSI) is an alternative to Fourier methods of spatial encoding. As in Fourier MRSI, magnetization is encoded and signal derived from the subject is transformed to yield a set of localized signals. The process of spatial encoding is more elaborate than in Fourier MRSI, but Hadamard transformation is less mathematically demanding and less prone to cross-contamination. In the one-dimensional case, magnetization in each of  $n$  ‘slices’ of the sample is tipped through a nutation angle of  $\pm\alpha$  (depending on the method,  $\alpha = 90^\circ$  or  $180^\circ$ ) according to the sign of the element in the corresponding column of a given row of an  $n$ th-order Hadamard matrix. This is usually achieved using compound, multifrequency RF pulses and gradients. A total of  $n$  separate experiments are performed, corresponding to the  $n$  rows of the matrix. The array of signals collected is multiplied by the inverse matrix to yield a diagonalized matrix containing  $n$  signals originating from the chosen slices. Extension to higher dimensions requires ‘nested’ acquisitions just as in Fourier imaging. For  $n$  by  $m$  resolution in two dimensions,  $n$  experiments corresponding to the  $n$  rows of one Hadamard matrix must be performed for each of  $m$  encoding steps, corresponding to the  $m$  rows of another Hadamard matrix, in the second dimension. The choice of  $\alpha$  and the number of spatial dimensions determine whether transverse or longitudinal magnetization is modulated to achieve spatial encoding. Early HSI techniques used longitudinal modulation ( $\alpha = 180^\circ$ ) (Bolinger and Leigh 1988), which is in essence a generalization of multi-voxel ISIS (Ordidge *et al* 1988) (see section 5.6) and suffers from many of the same drawbacks. Transverse modulation ( $\alpha = 90^\circ$ ) (Goelman *et al* 1990) is an improvement in this respect, and offers the additional advantage that the composite pulses are easier to design. Adiabatic

pulses can improve  $B_1$ -insensitivity and definition of the volume elements (Goelman and Leigh 1991a, de Graaf and Nicolay 1996), but it can be shown that, due to the properties of Hadamard matrices, the localization performance of HSI sequences is insensitive to pulse imperfections which result in partial inversion (Goelman and Leigh 1993). Since selective excitation is used for encoding, HSI is unusual among MRSI methods in that localization is affected by chemical shift offset, which can be overcome using generalized matrices with off resonance terms (Goelman and Leigh 1991b). HSI may also be combined with conventional MRSI to reduce acquisition time and improve SNR (Dreher and Leibfritz 1994, Gonen *et al* 1995, 1997). When a surface coil is used, it is beneficial in terms of localization quality and PSF-related contamination to use HSI along the axis of the coil, where  $B_1$  inhomogeneity is greatest, and conventional Fourier methods for the other two dimensions (Goelman 1999). For brain MRS using a volume coil, PRESS and one-dimensional HSI can be used to prepare a stack of slices for two-dimensional MRSI (Gonen *et al* 1998).

An alternative HSI technique has been proposed by Sharp and Leach (1989b) as a development of C-ISIS. This method is less susceptible to contamination due to  $T_1$  relaxation of extraneous signal.

#### 6.6. Volume selection by phase encoding

The techniques described here do not meet our previous definition of MRSI, in that they aim to select a single voxel, or a small number of discrete voxels, rather than to map signal throughout a slice or volume. However, they are placed here as they achieve this using phase encoding, and hence stand somewhere between conventional single-voxel techniques and spectroscopic imaging. From another perspective they may be regarded as closely related to Fourier series windowing (see section 4.3), with static field gradients replacing the  $B_1$  gradients used in those techniques. For an overview that emphasizes the close relationship between both types of FSW technique, conventional MRSI and techniques such as SLIM and SLOOP (see below), the reader is referred to Hodgkinson and Hore (1995).

Fourier series windowing uses weighted addition of signals collected using different phase encoding steps to synthesize a spatial localization window. The conventional version, based on  $B_1$  gradients, is limited to one-dimensional localization because of the practicalities of RF coil design and construction. However, the same concept can be extended to phase encoding using static field gradients, permitting two- or three-dimensional localization to better defined VOIs. For example, Hendrich *et al* (1994b) demonstrated selection of circular VOIs, with potential for extension to cylinders, spheres and ellipsoids in three dimensions. Incorporation of anatomical prior knowledge facilitates a class of techniques that approach the ideal of localized spectroscopy: the collection of data exclusively from one or more regions of tissue of arbitrary shape.

Hu *et al* (1988) have shown mathematically and experimentally that spectra from  $n$  discrete homogeneous regions of arbitrary shape comprising an imaging volume can be reconstructed from a minimum of  $n$  differently phase encoded NMR signals in a Fourier MRSI technique with appropriate mathematical processing. The SLIM (Spatial Localization by IMaging) technique requires prior knowledge about each of the regions, which is derived from MR images. SLIM can generate spectra from a sample containing a small number of homogeneous regions much more rapidly than conventional MRSI, and the spectra will be more truly representative of the regions of interest within the sample since the localized volumes can be tailored in shape and since, at least ideally, cross-contamination is greatly reduced as compared to conventional MRSI methods. The performance of SLIM has been modelled and discussed extensively by Liang and Lauterbur (1993).

The assumption of homogeneous composition is fundamental to SLIM. Significant cross-contamination can occur if it is not satisfied. Liang and Lauterbur (1991) have used a generalized series approach (GSLIM) rather than being restricted to Fourier series and have thus greatly reduced cross-contamination and extended the utility of the technique to situations in which one or more compartments are inhomogeneous. The series could be modified further to incorporate other *a priori* constraints. von Kienlin and Mejia (1991) adopt a different approach, SLOOP (Spectral LOcalization with Optimal Pointspread function), in which the phase encoding gradients are numerically optimized to minimize cross-contamination and maximize sensitivity within the regions of interest. Extension to three dimensions and incorporation of additional prior knowledge allows successful quantitative MRS of anatomical regions in the heart with high SNR and excellent contamination behaviour, despite high concentrations of metabolites in the chest wall (Löffler *et al* 1998, Meininger *et al* 1999). For further details, the reader is referred to a review by von Kienlin *et al* (2001). A more unusual development is integration of SLOOP with nonlinear phase encoding gradients, allowing these too to be optimized to the sample geometry (Pohmann *et al* 1999). A variety of alternative approaches to optimal *k*-space sampling for tailored acquisition have subsequently been proposed, but none have yet been implemented practically (e.g., Gao and Reeves 2000, 2001). Tsao (2001) has shown that the alternative finite support extrapolation approach pursued by Plevritis and Macovski (1995a, 1995b) is a weak special case of generalized series model such as GSLIM.

In a similar approach, Hodgkinson and Hore (1995) used an extended version of static field FSW to localize on compartments of arbitrary shape, blurred to facilitate localization in a practical number of steps. An iterative approach is used to find the minimum number of acquisitions required to localize to this blurred compartment with a level of localization quality chosen by the user. Thus there is a trade-off between localization quality and experimental efficiency. Simulations suggest that the rigorous SLIM approach and the more empirical extended FSW give essentially similar results, with the latter offering a more practical solution in the absence of a small number of homogeneous compartments.

The phase-encoded selection technique (PEST) of Sharp and Leach (1994) is unusual in that the localized volume is encoded into longitudinal magnetization prior to a single read-out, rather than requiring summation of a number of acquired signals. The technique utilizes the following sequence:

$$G_i \{90^\circ[x'] / \sqrt{-t\phi} - 180^\circ[y'] - t\phi - 90^\circ[-x'] - \text{spoil}\}_n - 90^\circ[x'] - Acq \quad (31)$$

where  $t_\phi$  is the duration of the phase encoding gradient. The preparation episode is repeated  $n$  times, each with a different gradient amplitude, and encoded magnetization is rephased and returned to the  $z$ -axis after each encoding step. Transverse magnetization is eliminated by a spoiler gradient. Appropriate choice of  $n$  and the phase encoding gradient amplitudes results in spatial modulation of  $z$ -magnetization such that a window with an approximately sinc<sup>2</sup> profile is selected and can be read out. The strength of this technique is immunity to chemical shift offset, since none of the pulses are spatially selective. However, localization quality is clearly poor compared to other techniques considered in this section.

## 7. Conclusions

The wide variety of spatially localization techniques available for use in MRS is a tribute to the ingenuity of researchers over the past 25 years. There is no single 'best' technique: the optimal method in a particular setting depends on numerous factors, including the anatomical

area of interest, the nature of any pathology that may be present, the properties of the nucleus to be studied, the length of time available for the examination, and the experience of the investigator. For most users a fundamental limitation will be the limited range of techniques implemented on commercial MR systems, but even this affords a great deal of flexibility.

The earliest approach to localization was the use of a simple surface coil. This spawned a host of methods based on surface coils and RF pulses alone, which have now been almost entirely superseded—although depth pulse methods are finding a new role in carbon-13 MRS. The relatively poor localization performance and technical complexity that characterizes these techniques made them less attractive for widespread use once static field gradient techniques became available. This is not to say that excellent results cannot be achieved with careful optimization in skilled and experienced hands.

Techniques based on static field gradients that can be implemented using volume coils with relatively homogeneous  $B_1$  fields offer improved sensitivity, signal uniformity and anatomical access. Early examples such as VSE, SPARS and DIGGER, which attempted to eliminate magnetization outside the VOI, developed from previous field focusing and topical NMR methods. They were revolutionary in their time, and have a legacy in the form of the OVS methods often used today in combination with MRSI and other localization techniques. However, the requirement to eliminate magnetization throughout the sample outside a relatively small VOI limits flexibility, is technically demanding, and often entails power deposition problems. The other main categories of static field technique—volume-selected echoes and post-acquisition signal combination—include sequences that remain in almost ubiquitous use for proton and phosphorus MRS, respectively. A common feature that contributes to the success of these approaches is the fact that pulse clusters affect only magnetization within the three intersecting slices that define the VOI. In the case of PRESS and STEAM, these slices are the only source of background contamination, which can be almost entirely eliminated with effective spoiling, while with ISIS they are often the dominant source because of  $T_1$  smearing. However, PRESS, STEAM and ISIS are by no means panaceas for MRS. Like all static field gradient techniques, they bring with them problems such as chemical shift misregistration and relaxation time weighting. They must be applied thoughtfully and with due regard to known sources of contamination and signal loss or modulation, such as complicated  $J$ -coupling effects in the echo-based sequences. Empirical assessment of localization performance under the conditions of use is important in this context, but is often overlooked.

Just as static field gradient techniques displaced earlier surface coil techniques, so, it might be argued, MRSI is now becoming dominant. The ability to collect data from an array of voxels is attractive in many situations, but MRSI is prone to Fourier bleed (and hence is less well suited to quantitative studies), and usually requires combination with single-voxel localization and OVS techniques to tackle lipid contamination. Single-voxel techniques generally offer better performance when a focal region or lesion is to be studied. However, emerging approaches to fast MRSI, building on pulse sequences and  $k$ -space trajectories developed in the context of MRI, are beginning to address issues of speed and resolution. Partially parallel imaging, and the multi-channel hardware developing to accommodate it, is likely to be an important factor in this process. Thus, while MRI may be regarded as the progeny of NMR, it seems likely that the future of MRS will be guided largely by developments in MRI methodology.

### Acknowledgments

The work by the author and colleagues described in the review was supported by the European Union (COMAC-BME II.1.3), Guy's and St Thomas' NHS Foundation Trust and the Guy's

and St Thomas' Charity. Thanks are due to Dr Geoff Charles-Edwards for assistance with figures 4 and 12.

## References

- Abduljalil A M, Rath D P, Hui Z, Aletras A H, McCartney W C and Robitaille P M L 1996 Spatial localization with modified Fourier series windows: applications to transmural  $^{13}\text{C}$  nuclear magnetic resonance analysis of the *in vivo* myocardium *Investig. Radiol.* **31** 611–8
- Ackerman J J H, Grove T H, Wong G H, Gadian D G and Radda G K 1980 Mapping of metabolites in whole animals by  $^{31}\text{P}$  NMR using surface coils *Nature* **283** 167–70
- Adalsteinsson E, Irrazabal P, Spielman D M and Macovski A 1995 Three-dimensional spectroscopic imaging with time-varying gradients *Magn. Reson. Med.* **33** 461–6
- Adalsteinsson E, Irrazabal P, Topp S, Meyer C, Macovski A and Spielman D M 1998 Volumetric spectroscopic imaging with spiral-based  $k$ -space trajectories *Magn. Reson. Med.* **39** 889–98
- Adalsteinsson E, Star-Lack J, Meyer C H and Spielman D M 1999 Reduced spatial side lobes in chemical-shift imaging *Magn. Reson. Med.* **42** 314–23
- Andrew E R 2000 Magnetic resonance imaging: a historical overview *Methods in Biomedical Magnetic Resonance Imaging and Spectroscopy* ed I R Young (Chichester: Wiley)
- Aue W P, Müller S, Cross T A and Seelig J 1984 Volume-selective excitation: a novel approach to topical NMR *J. Magn. Reson.* **56** 350–4
- Baum J, Tycko R and Pines A 1985 Broadband and adiabatic inversion of a two-level system by phase-modulated pulses *Phys. Rev. A* **32** 3435–47
- Bendall M R 1983 Portable NMR sample localization methods using inhomogeneous RF irradiation coils *Chem. Phys. Lett.* **99** 310–5
- Bendall M R 1984 Elimination of high-flux signals near surface coils and field gradient sample localisation using depth pulses *J. Magn. Reson.* **59** 406–29
- Bendall M R and Gordon R E 1983 Depth and refocusing pulses designed for multiphase NMR with surface coils *J. Magn. Reson.* **53** 365–85
- Bendall M R, McKendry J M, Cresshull I D and Ordidge R J 1984 Active detune switch for complete sensitive-volume localization in *in vivo* spectroscopy using multiple r.f. coils and depth pulses *J. Magn. Reson.* **60** 473–8
- Bendall M R and Pegg D T 1984 DEPT at depth: polarization transfer and sample localisation combined using surface coils *J. Magn. Reson.* **57** 337–43
- Bendall M R and Pegg D T 1985a Theoretical description of depth pulse sequences, on and off resonance, including improvements and extensions thereof *Magn. Reson. Med.* **2** 91–113
- Bendall M R and Pegg D T 1985b Sensitive-volume localization for *in vivo* NMR using heteronuclear spin-echo pulse sequences *Magn. Reson. Med.* **2** 298–306
- Bendall M R and Pegg D T 1986 Uniform sample excitation with surface coils for *in vivo* spectroscopy by adiabatic rapid half passage *J. Magn. Reson.* **67** 376–81
- Bendel P, Lai C-M and Lauterbur P C 1980 P-31 spectroscopic zeugmatography of phosphorus metabolites *J. Magn. Reson.* **38** 343–56
- Bernardo M L, Lauterbur P C and Hedges L K 1985 Experimental example of NMR spectroscopic imaging by projection reconstruction involving an intrinsic frequency dimension *J. Magn. Reson.* **61** 168–74
- Blackledge M J, Styles P and Radda G K 1987 Rotating-frame depth selection and its application to the study of human organs *J. Magn. Reson.* **74** 246–58
- Bleaney B I and Bleaney B 1976 *Electricity and Magnetism* (Oxford: Oxford University Press)
- Bloch F, Hanson W and Packard M E 1946 Nuclear induction *Phys. Rev.* **69** 127
- Blümich B and Spiess H W 1986 NMR imaging with incommensurate sampling and gradient modulation rates *J. Magn. Reson.* **66** 66–73
- Bolinger L and Leigh J S 1988 Hadamard spectroscopic imaging (HSI) for multivolume localization *J. Magn. Reson.* **80** 162–7
- Bottomley P A 1982 Localised NMR spectroscopy by the sensitive point method *J. Magn. Reson.* **50** 335–8
- Bottomley P A 1984 Selective volume method for performing localized NMR spectroscopy *US Patent* 4480 228
- Bottomley P A 1987 Spatial localization in NMR spectroscopy *in vivo* *Ann. NY Acad. Sci.* **508** 333–48
- Bottomley P A, Charles H C, Roemer P B, Flamig D, Engeseth H, Edelstein W A and Mueller O M 1988 Human *in vivo* phosphate metabolite imaging with  $^{31}\text{P}$  NMR *Magn. Reson. Med.* **7** 319–36
- Bottomley P A, Foster T B and Darrow R D 1984 Depth-resolved surface-coil spectroscopy (DRESS) for *in vivo*  $^1\text{H}$ ,  $^{31}\text{P}$  and  $^{13}\text{C}$  NMR *J. Magn. Reson.* **59** 338–42

- Bottomley P A and Hardy C J 1987a PROGRESS in efficient three-dimensional spatially localised *in vivo*  $^{31}\text{P}$  NMR spectroscopy using multidimensional spatially selective ( $\rho$ ) pulses *J. Magn. Reson.* **74** 550–6
- Bottomley P A and Hardy C J 1987b Two-dimensional spatially selective spin inversion and spin-echo refocusing with a single magnetic resonance pulse *J. Appl. Phys.* **62** 4284–90
- Bottomley P A, Smith L S, Leue W M and Charles C 1985 Slice interleaved depth-resolved surface-coil spectroscopy (SLIT DRESS) for rapid P-31 NMR *in vivo* *J. Magn. Reson.* **64** 347–51
- Bovée W M M J *et al* 1998 Absolute metabolite quantification by *in vivo* NMR spectroscopy: IV. Multicentre trial on MRSI localisation tests *Magn. Reson. Imaging* **16** 1113–25
- Bovée W M M J, Keevil S F, Leach M O and Podo F 1995 Quality assessment in *in vivo* NMR spectroscopy: II. A protocol for quality assessment *Magn. Reson. Imaging* **13** 123–9
- Bowtell R, Cawley M G and Mansfield P 1989 Proton chemical-shift mapping using PREP *J. Magn. Reson.* **82** 634–9
- Briand J and Hall L D 1988 VOISINER, a new method for spatially resolved NMR spectroscopy *J. Magn. Reson.* **80** 559–62
- Briand J and Hall L D 1991 Spatially localized NMR with the VOISINER sequence *J. Magn. Reson.* **94** 234–57
- Brown T R, Buchthal S D, Murphy-Boesch J, Nelson S J and Taylor J S 1989 A multislice sequence for  $^{31}\text{P}$  *in vivo* spectroscopy: 1D chemical-shift imaging with an adiabatic half-passage pulse *J. Magn. Reson.* **82** 629–33
- Brown T R, Kincaid B M and Ugurbil K 1982 NMR chemical shift imaging in three dimensions *Proc. Natl. Acad. Sci. USA* **79** 3523–6
- Burger C, Buchli R, McKinnon G, Meier D and Boesiger P 1992 The impact of the ISIS experiment order on spatial contamination *Magn. Reson. Med.* **26** 218–30
- Burtscher I M, Johansson E, Holtås S and Ståhlberg F 1999 Quality assessment of localization technique performance in small volume *in vivo*  $^1\text{H}$  MR spectroscopy *Magn. Reson. Imaging* **17** 1511–9
- Canet D, Boudot D, Belmajdoub A, Retournard A and Brondeau J 1988 Accurate spatial localization by a novel pulse sequence using an RF field gradient and a DANTE-like pulse train *J. Magn. Reson.* **79** 168–75
- Chen C-N and Hoult D I 1989 *Biomedical Magnetic Resonance Technology* (Bristol: Adam Hilger)
- Chen Y J, Rachamadugu S and Fernandez E J 1997 Three dimensional outer volume suppression for short echo time *in vivo*  $^1\text{H}$  spectroscopic imaging in rat brain *Magn. Reson. Imaging* **15** 839–45
- Chew W M, Chang L-H, Flamig D P and James T L 1987 The SWIFT method for *in vivo* localized excitation (SMILE) *J. Magn. Reson.* **75** 523–8
- Choi I-Y, Tkáč I and Gruetter R 2000 Single-shot, three-dimensional 'non-echo' localization method for *in vivo* NMR spectroscopy *Magn. Reson. Med.* **44** 387–94
- Chu A, Alger J R, Moore G J and Posse 2003 Proton echo-planar spectroscopic imaging with highly effective outer volume suppression using combined presaturation and spatially selective echo dephasing *Magn. Reson. Med.* **49** 817–21
- Connelly A, Counsell C, Lohman J A B and Ordidge R J 1988 Outer volume suppressed image related *in vivo* spectroscopy (OSIRIS), a high-sensitivity localization technique *J. Magn. Reson.* **78** 519–25
- Cox S J and Styles P 1980 Towards biochemical imaging *J. Magn. Reson.* **40** 209–12
- Crowley M G and Ackerman J J H 1985 Enhanced surface-coil spatial localization with an inhomogeneous surface gradient *J. Magn. Reson.* **65** 522–5
- Cunningham C H, Vigneron D B, Marjanska M, Chen A P, Xu D, Hurd R E, Kurhanewicz J, Garwood M and Pauly J M 2005 Sequence design for magnetic resonance spectroscopic imaging of prostate cancer at 3T *Magn. Reson. Med.* **53** 1033–9
- Damadian R, Minkoff M, Goldsmith M, Stanford M and Koutcher J 1976 Field focusing nuclear magnetic resonance (FONAR): visualisation of a tumor in a live animal *Science* **194** 1430–2
- de Crespigny A J S, Carpenter T A and Hall L D 1989 Region-of-interest selection by outer-volume saturation *J. Magn. Reson.* **85** 595–603
- de Graaf R A 1998 *In Vivo NMR Spectroscopy: Principles and Techniques* (Chichester: Wiley)
- de Graaf R A, Luo Y, Terpstra M, Merkle H and Garwood M 1995 A new localization method using an adiabatic pulse, BIR-4 *J. Magn. Reson. B* **106** 245–52
- de Graaf R A, Luo Y, Garwood M and Nicolay K 1996  $B_1$ -insensitive single-shot localization and water suppression *J. Magn. Reson. B* **113** 35–45
- de Graaf R A and Nicolay 1996 Multislice imaging with adiabatic pulses using transverse Hadamard encoding *J. Magn. Reson. B.* **113** 97–101
- Doddrell D M, Brooks W M, Bursing J M, Field J, Irving M G and Baddeley H 1986a Spatial and chemical-shift-encoded excitation: SPACE, a new technique for volume-selected NMR spectroscopy *J. Magn. Reson.* **68** 367–72

- Doddrell D M, Bulsing J M, Galloway G J, Brooks W M, Field J, Irving M and Baddeley H 1986b Discrete isolation from gradient-governed elimination of resonances: DIGGER, a new technique for *in vivo* volume-selected NMR spectroscopy *J. Magn. Reson.* **70** 319–26
- Doddrell D M, Field J, Brereton I M, Galloway G J, Brooks W M and Irving M G 1987 Application of surface coil reception to record volume-selected high-resolution proton *in vivo* spectra using a combined DIGGER-SPACE pulse sequence *J. Magn. Reson.* **73** 159–67
- Doddrell D M, Galloway G J, Brooks W M, Bulsing J M, Field J C, Irving M G and Baddeley H 1986c The utilization of two frequency-shifted sinc pulses for performing volume-selected *in vivo* NMR spectroscopy *Magn. Reson. Med.* **3** 970–5
- Doyle M and Mansfield P 1987 Chemical shift imaging: a hybrid approach *Magn. Reson. Med.* **5** 255–61
- Doyle V L, Howe F A and Griffiths J R 2000 The effects of respiratory motion on CSI localized MRS *Phys. Med. Biol.* **45** 2093–104
- Dreher W, Geppert C, Althaus M and Leibfritz D 2003 Fast proton spectroscopic imaging using steady-state free precession methods *Magn. Reson. Med.* **50** 453–60
- Dreher W and Leibfritz D 1994 Double-echo multislice proton spectroscopic imaging using Hadamard slice encoding *Magn. Reson. Med.* **31** 596–600
- Dreher W and Leibfritz D 1999 Improved proton spectroscopic U-FLARE imaging for the detection of coupled resonances in the rat brain *in vivo* *Magn. Reson. Imaging* **17** 611–21
- Dreher W and Leibfritz D 2000 A new method for fast proton spectroscopic imaging: spectroscopic GRASE *Magn. Reson. Med.* **44** 668–72
- Dreher W and Leibfritz D 2002 Fast proton spectroscopic imaging with high signal-to-noise ratio: spectroscopic RARE *Magn. Reson. Med.* **47** 523–8
- Duyn J H, Matson G B, Maudsley A A and Weiner M W 1992 3D phase encoding spectroscopic imaging of human brain *Magn. Reson. Imaging* **10** 315–9
- Duyn J H and Moonen C T W 1993 Fast proton spectroscopic imaging of human brain using multiple spin echoes *Magn. Reson. Med.* **30** 409–14
- Dydak U, Pruessmann K P, Weiger M, Tsao J, Meier D and Boesiger P 2003 Parallel spectroscopic imaging with spin-echo trains *Magn. Reson. Med.* **50** 196–200
- Dydak U, Weiger M, Pruessmann K P, Meier D and Boesiger P 2001 Sensitivity-encoded spectroscopic imaging *Magn. Reson. Med.* **46** 713–22
- Ebel A, Dreher W and Leibfritz D 2000 A fast variant of  $^1\text{H}$  spectroscopic U-FLARE imaging using adjusted chemical shift phase encoding *J. Magn. Reson.* **142** 241–53
- Ebel A, Govindaraju V and Maudsley A A 2003 Comparison of inversion recovery preparation schemes for lipid suppression in  $^1\text{H}$  MRSI of human brain *Magn. Reson. Med.* **49** 903–8
- Ebel A and Maudsley A A 2001 Comparison of methods for reduction of lipid contamination for *in vivo* proton MR spectroscopic imaging of the brain *Magn. Reson. Med.* **46** 706–12
- Ebel A and Maudsley A A 2003 Improved spectral quality for 3D spectroscopic imaging using a high spatial resolution acquisition strategy *Magn. Reson. Imaging* **21** 113–20
- Ehrhardt J C 1990 MR data acquisition and reconstruction using efficient sampling schemes *IEEE Trans. Med. Imaging* **9** 305–9
- Emsley L and Bodenhausen G 1990 Volume-selective NMR spectroscopy with self-refocusing pulses *J. Magn. Reson.* **87** 1–17
- Engelstad B L, White D L, Moseley M E and Stark D D 1990 Localization of P-31 MR signal with use of superparamagnetic iron oxide particles *Radiology* **176** 467–72
- Ernst T and Chang L 1996 Elimination of artifacts in short echo time  $^1\text{H}$  MR spectroscopy of the frontal lobe *Magn. Reson. Med.* **36** 462–8
- Ernst T and Hennig J 1991a Coupling effects in volume selective  $^1\text{H}$  spectroscopy of major brain metabolites *Magn. Reson. Med.* **21** 82–96
- Ernst T and Hennig J 1991b Double-volume spectroscopy with interleaved acquisitions using tilted gradients *Magn. Reson. Med.* **20** 27–35
- Evelhoch J L, Crowley M G and Ackerman J J H 1984 Signal-to-noise optimisation and observed volume localisation with circular surface coils *J. Magn. Reson.* **56** 110–24
- Felblinger J, Kreis R and Boesch C 1998 Effects of physiologic motion of the human brain upon quantitative  $^1\text{H}$ -MRS: analysis and correction by retrogating *NMR Biomed.* **11** 107–14
- Ford J J 1990 Gradient-amplitude phase-encoded spectral (GRAPES) imaging: a novel approach to spin-echo chemical-shift imaging *J. Magn. Reson.* **87** 346–51
- Frahm J, Merboldt K-D and Hänicke W 1987 Localized proton spectroscopy using stimulated echoes *J. Magn. Reson.* **72** 502–8

- Friedrich J and Freeman R 1988 Spatial localisation using a 'straddle coil' *J. Magn. Reson.* **77** 101–18
- Galloway G J, Brereton I M, Brooks W M, Field J, Irving M, Baddeley H and Doddrell D D 1987a A comparison of some gradient-encoded volume-selection techniques for *in vivo* NMR spectroscopy *Magn. Reson. Med.* **4** 393–8
- Galloway G J, Brooks W M, Bulsing J M, Brereton I M, Field J, Irving M, Baddeley H and Doddrell D M 1987b Improvements and extensions to the DIGGER technique for performing spatially selective excitation *J. Magn. Reson.* **73** 360–8
- Gao Y and Reeves S J 2000 Optimal *k*-space sampling in MRSI for images with a limited region of support *IEEE Trans. Med. Imaging* **19** 1168–78
- Gao Y and Reeves S J 2001 Fast *k*-space sample selection in MRSI with a limited region of support *IEEE Trans. Med. Imaging* **20** 868–76
- Garwood M and de la Barre L 2001 The return of the frequency sweep: designing adiabatic pulses for contemporary NMR *J. Magn. Reson.* **153** 155–77
- Garwood M and Ke Y 1991 Symmetric pulses to induce arbitrary flip angles with compensation for RF inhomogeneity and resonance offsets *J. Magn. Reson.* **94** 511–25
- Garwood M, Robitaille P-M and Ugurbil K 1987 Fourier series windows on and off resonance using multiple coils and longitudinal modulation *J. Magn. Reson.* **75** 244–60
- Garwood M, Schleich T, Ross B D, Matson G B and Winters W D 1985 A modified rotating frame experiment based on a Fourier series window function: application to *in vivo* spatially localised NMR spectroscopy *J. Magn. Reson.* **65** 239–51
- Garwood M, Ugurbil K, Schleich T, Petelin M, Sublett E, From A H L and Bache R J 1986 *In vivo* spatially localized surface-coil NMR spectroscopy utilizing a Fourier series window function and two surface coils *J. Magn. Reson.* **69** 576–81
- Geppert C, Dreher W and Leibfritz D 2003 PRESS-based proton single-voxel spectroscopy and spectroscopic imaging with very short echo times using asymmetric RF pulses *MAGMA* **16** 144–8
- Goelman G 1999 Hadamard encoding with surface coils for high SNR MR spectroscopy *Magn. Reson. Imaging* **17** 777–81
- Goelman G and Leigh J S 1991a  $B_1$ -insensitive Hadamard spectroscopic imaging technique *J. Magn. Reson.* **91** 93–101
- Goelman G and Leigh J S 1991b Corrections for chemical shift localization errors in the HSI technique *Proc. Soc. Magn. Reson. Med.* (Berkeley, CA: SMRM) p 455
- Goelman G and Leigh J S 1993 Hadamard spectroscopic imaging technique insensitive to pulse imperfections *J. Magn. Reson. A* **105** 78–81
- Goelman G, Subramanian V H and Leigh J S 1990 Transverse Hadamard spectroscopic imaging technique *J. Magn. Reson.* **89** 437–54
- Golay X, Gillen J, van Zijl P C M and Barker P B 2002 Scan time reduction in proton magnetic resonance spectroscopic imaging of the human brain *Magn. Reson. Med.* **47** 384–7
- Gonen O, Arias Mendoza F and Goelman G 1997 3D localized *in vivo*  $^1\text{H}$  spectroscopy of human brain by using a hybrid of 1D-Hadamard with 2D chemical shift imaging *Magn. Reson. Med.* **37** 644–50
- Gonen O, Hu J, Stoyanova R, Leigh J S, Goelman G and Brown T R 1995 Hybrid three dimensional (1D-Hadamard, 2D-chemical shift imaging) phosphorus localized spectroscopy of phantom and human brain *Magn. Reson. Med.* **33** 300–8
- Gonen O, Murdoch J B, Stoyanova R and Goelman G 1998 3D multivoxel proton spectroscopy of human brain using a hybrid of 8th order Hadamard encoding with 2D chemical shift imaging *Magn. Reson. Med.* **39** 34–40
- Gordon R E, Hanley P E and Shaw D 1982 Topical magnetic resonance *Prog. NMR Spectrosc.* **15** 1–47
- Gordon R E, Hanley P E, Shaw D, Gadian D G, Radda G K, Styles P, Bore B J and Chan L 1980 Localization of metabolites in animals using P-31 topical magnetic resonance *Nature* **287** 367–8
- Granot J 1986 Selected volume excitation using stimulated echoes (VEST): applications to spatially localized spectroscopy and imaging *J. Magn. Reson.* **70** 488–92
- Granot J, Ben Mair J, Arrive L, Menu Y, Martin N and Nahum H 1990 Volume-localized  $^{31}\text{P}$  spectroscopy via combined selective presaturation and selective excitation *J. Magn. Reson.* **89** 139–45
- Greisler A and von Kienlin M 2003 Efficient *k*-space sampling by density-weighted phase-encoding *Magn. Reson. Med.* **50** 1266–75
- Guilfoyle D N, Blamire A, Chapman B, Ordidge R J and Mansfield P 1989 PEEP—a rapid chemical-shift imaging method *Magn. Reson. Med.* **10** 282–7
- Guimaraes A R, Baker J R, Jenkins B G, Lee P L, Weisskoff R M, Rosen B R and González 1999 Echoplanar chemical shift imaging *Magn. Reson. Med.* **41** 877–82
- Gyngell M L, Frahm J, Merboldt K D, Hänicke W and Bruhn H 1988 Motion rephasing in gradient-localized spectroscopy *J. Magn. Reson.* **77** 596–8

- Haase A 1986 Localization of unaffected spins in NMR imaging and spectroscopy (LOCUS spectroscopy) *Magn. Reson. Med.* **3** 963–9
- Haase A 1990 Snapshot FLASH MRI: applications to  $T_1$ ,  $T_2$  and chemical shift imaging *Magn. Reson. Med.* **13** 77–89
- Haase A, Frahm J, Matthaei W, Hänicke W and Merboldt K-D 1986 FLASH imaging: rapid NMR imaging, using low flip-angle pulses *J. Magn. Reson.* **67** 258–66
- Haase A, Hänicke W and Frahm J 1984 The influence of experimental parameters in surface coil NMR *J. Magn. Reson.* **56** 401–12
- Haase A and Matthaei D 1987 Spectroscopic FLASH NMR imaging (SPLASH imaging) *J. Magn. Reson.* **71** 550–3
- Hafner H-P, Radii E and Seelig J 1990 Two-volume acquisition in image guided proton spectroscopy *Magn. Reson. Med.* **15** 135–41
- Hahn E L 1950 Spin echoes *Phys. Rev.* **80** 580–94
- Hall L D and Sukumar S 1982 Chemical microscopy using a high resolution NMR spectrometer: a combination of tomography/spectroscopy using either H-1 or C-13 *J. Magn. Reson.* **50** 161–4
- Hardy C J and Bottomley P A 1991  $^{31}\text{P}$  spectroscopic localization using pinwheel NMR excitation pulses *Magn. Reson. Med.* **17** 315–27
- Hardy C J, Bottomley P A, O'Donnell M and Roemer P 1988a Optimisation of two-dimensional spatially selective NMR pulses by simulated annealing *J. Magn. Reson.* **77** 233–50
- Hardy C J, Bottomley P A and Roemer P 1988b Off-axis spatial localization with frequency modulated nuclear magnetic resonance rotating ( $\rho$ ) pulses *J. Appl. Phys.* **63** 4741–3
- Hardy C J and Cline H E 1989 Spatial localization in two dimensions using NMR designer pulses *J. Magn. Reson.* **82** 647–54
- Hardy C J, Cline H E and Bottomley P A 1990 Correcting for nonuniform  $k$ -space sampling in two-dimensional NMR selective excitation *J. Magn. Reson.* **87** 639–45
- Haselgrove J, Gilbert K and Leigh J S 1985 Chemical-shift imaging using filtered back-projection algorithms *Magn. Reson. Med.* **2** 195–202
- Haselgrove J C, Subramanian V H, Leigh J S, Gyulai L and Chance B 1983 *In-vivo* one-dimensional imaging of phosphorus metabolites by phosphorus-31 nuclear magnetic resonance *Science* **220** 1170–3
- Haupt C I, Schuff N, Weiner M W and Maudsley A A 1996 Removal of lipid artifacts in  $^1\text{H}$  spectroscopic imaging by data extrapolation *Magn. Reson. Med.* **35** 678–87
- Haxo R S, Lawry T J, Karczmar G S, Schliech T, Weiner M W and Matson G B 1989 An optimized, transposed selective RF pulse for the SPARS experiment *Proc. Soc. Magn. Reson. Med.* (Berkeley, CA: SMRM) p 865
- Hendrich K, Merkle H, Weisdorf S, Vine W, Garwood M and Ugurbil K 1991 Phase-modulated rotating frame spectroscopic localization using an adiabatic plane-rotation pulse and a single surface coil *J. Magn. Reson.* **92** 258–75
- Hendrich K, Hu X P, Menon R S, Merkle H, Camarata P, Heros R and Ugurbil K 1994b Spectroscopic imaging of circular voxels with a 2-dimensional Fourier-series window technique *J. Magn. Reson. B.* **105** 225–32
- Hendrich K, Xu Y, Kim S G and Ugurbil K 1994a Surface coil cardiac tagging and  $^{31}\text{P}$  spectroscopic localization with  $B_1$  insensitive adiabatic pulses *Magn. Reson. Med.* **31** 541–5
- Hennig J 1992 Chemical shift imaging with phase encoding RF-pulses *Magn. Reson. Med.* **25** 289–98
- Hennig J, Boesch C, Gruetter R and Martin E 1987 Homogeneity spoil spectroscopy as a tool of spectrum localization for *in vivo* spectroscopy *J. Magn. Reson.* **75** 179–83
- Hennig J and Hodapp M 1993 BURST imaging *MAGMA* **1** 39–48
- Hennig J, Naureth A and Friedburg H 1986 RARE imaging: a fast method for clinical MR *Magn. Reson. Med.* **3** 823–33
- Hetherington H P, Luney D J E, Vaughan J T, Pan J W, Ponder S L, Tschendel O, Twieg D B and Pohost G M 1995 3D  $^{31}\text{P}$  spectroscopic imaging of the human brain at 4.1 T *Magn. Reson. Med.* **33** 427–31
- Himmelreich U and Dobson G P 2000 Detection and quantification of free cytosolic inorganic phosphate and other phosphorus metabolites in the beating mouse heart muscle *in situ NMR Biomed.* **13** 467–73
- Hodgkinson P and Hore P J 1995 Optimizing spatially localized NMR *J. Magn. Reson. B* **106** 261–9
- Hoult D I 1979 Rotating frame zeugmatography *J. Magn. Reson.* **33** 183–7
- Hoult D I, Busby S J, Gadian D G, Radda G K, Richards R E and Seeley P J 1974 Observation of tissue metabolites using  $^{31}\text{P}$  nuclear magnetic resonance *Nature* **252** 285–7
- Hsu A T, Hunter W W, Schmalbrock P and Marshall A G 1987 Stored waveform inverse Fourier transform (SWIFT) excitation for water-suppressed whole-body slice-selected proton chemical shift spectra at 1.5 tesla *J. Magn. Reson.* **72** 75–88
- Hu X, Levin D N, Lauterbur P C and Spraggins T 1988 SLIM: spectral localization by imaging *Magn. Reson. Med.* **8** 314–22

- Hu X, Patel M, Chen W and Uğurbil K 1995 Reduction of truncation artifacts in chemical-shift imaging by extended sampling using variable repetition time *J. Magn. Reson. B.* **106** 292–6
- Hu X, Patel M and Uğurbil K 1994 A new strategy for spectroscopic imaging *J. Magn. Reson. B.* **103** 30–8
- Hubesch B, Sappey-Marinié D, Roth K, Sanuki E, Hodes J E, Matson G B and Weiner M W 1988 Improved ISIS for studies of human brain and brain tumours *Proc. Soc. Magn. Reson. Med.* (Berkeley, CA: SMRM) p 348
- Hugg J W, Maudsley A A, Weiner M W and Matson G B 1996 Comparison of *k*-space sampling schemes for multidimensional MR spectroscopic imaging *Magn. Reson. Med.* **36** 469–73
- Jackson E F, Narayana P A and Kudrle W A 1988 A comparison of spatially resolved spectroscopy and stimulated echo acquisition mode sequences for volume-localized spectroscopy *J. Magn. Reson.* **80** 23–38
- Jackson J A and Langham W H 1968 Whole-body NMR spectrometer *Rev. Sci. Instrum.* **39** 510–3
- Jakob P M, Décorps M, Ziegler A and Doran S 1995 Echo-time encoded BURST imaging (EBI)—a novel technique for spectroscopic imaging *Magn. Reson. Med.* **33** 573–8
- Jakob P M, Kober M, Kober F, Pohmann R and Haase A 1996 Single-shot spectroscopic imaging (SISSI) using a PEEP/BURST hybrid *J. Magn. Reson. B* **110** 278–83
- Janssen J and Blümich B 1992 Stochastic spectroscopic imaging *J. Magn. Reson.* **99** 525–32
- Jehenson P and Bloch G 1991 Elimination of surface signals by a surface-spoiling magnetic field gradient: theoretical optimization and application to human *in vivo* NMR spectroscopy *J. Magn. Reson.* **94** 59–72
- Johnson A J, Garwood M and Ugurbil K 1989 Slice selection with gradient-modulated adiabatic excitation despite the presence of large  $B_1$  inhomogeneities *J. Magn. Reson.* **81** 653–60
- Jung W-I, Küper K, Schick F, Bunse M, Pfeffer M, Pfeffer K, Dietze G and Lutz O 1992 Localized phosphorus NMR spectroscopy: a comparison of the FID, DRESS, CRISIS/CODEX and STEAM methods *in vitro* and *in vivo* using a surface coil *Magn. Reson. Imaging* **10** 655–62
- Jung W-I and Lutz O 1988 Volume selective NMR spectroscopy by coded slice excitation (CODEX) *Z. Naturforsch.* **43a** 909–13
- Kanamori K and Ross B D 1999 Localized N-15 NMR spectroscopy of rat brain by ISIS *Magn. Reson. Med.* **41** 456–63
- Karczmar G S, Matson G B and Weiner M W 1986 A single acquisition localisation technique *Magn. Reson. Med.* **3** 341–5
- Katz-Brull R and Lenkinski R E 2004 Frame-by-frame PRESS  $^1\text{H}$ -MRS of the brain at 3T: the effects of physiological motion *Magn. Reson. Med.* **51** 184–7
- Keevil S F, Porter D A and Smith M A 1990 A method for characterising localisation techniques in volume selected nuclear magnetic resonance spectroscopy *Phys. Med. Biol.* **35** 821–34
- Keevil S F, Porter D A and Smith M A 1992 Experimental characterisation of the ISIS technique for volume selected NMR spectroscopy *NMR Biomed.* **5** 200–8
- Keevil S F *et al* 1995 Quality assessment in *in vivo* NMR spectroscopy: IV. A multicentre trial of test objects and protocols for performance assessment in clinical NMR spectroscopy *Magn. Reson. Imaging* **13** 139–57
- Keevil S F and Newbold M C 2001 The performance of volume selection sequences for *in vivo* NMR spectroscopy: implications for quantitative MRS *Magn. Reson. Imaging* **19** 1217–26
- Kim D-H, Adalsteinsson E and Spielman D M 2004 Spiral readout gradients for the reduction of motion artifacts in chemical shift imaging *Magn. Reson. Med.* **51** 458–63
- Kim H, Thompson R B, Hanstock C C and Allen P S 2005 Variability of metabolite yield using STEAM or PRESS sequences *in vivo* at 3.0 T, illustrated with *myo*-inositol *Magn. Reson. Med.* **53** 760–9
- Kimmich R and Hoepfel D 1987 Volume-selective multipulse spin-echo spectroscopy *J. Magn. Reson.* **72** 379–84
- Kimmich R, Schnur G, Hoepfel D and Ratzel D 1987 Volume-selective multi-pulse spin-echo spectroscopy and selective suppression of spectral lines *Phys. Med. Biol.* **32** 1335–43
- Kimmich R, Rommel R and Knüttel A 1989 Theoretical treatment of volume-selective NMR spectroscopy (VOSY) applied to coupled spin systems *J. Magn. Reson.* **81** 333–8
- Kinchesh P and Ordidge R J 2005 Spin-echo MRS in humans at high field: LASER localization using FOCI pulses *J. Magn. Reson.* **175** 30–43
- Kirkpatrick S, Gelatt C D and Vecchi M P 1983 Optimisation by simulated annealing *Science* **220** 671–80
- Kobzar K, Luy B, Khaneja N and Glaser S J 2005 Pattern pulses: design of arbitrary excitation pulses as a function of pulse amplitude and offset *J. Magn. Reson.* **173** 229–35
- Koch T, Brix G and Lorenz W J 1994 Theoretical description, measurement and correction of localization errors in  $^{31}\text{P}$  chemical-shift imaging *J. Magn. Reson. B.* **104** 199–211
- Kuhn B, Dreher W, Norris D G and Leibfritz 1996 Fast proton spectroscopic imaging employing *k*-space weighting achieved by variable repetition times *Magn. Reson. Med.* **35** 457–64

- Kurhanewicz J, Vigneron D B, Hricak H, Narayan P, Carroll P and Nelson S J 1996 Three-dimensional H-1 MR spectroscopic imaging of the *in situ* human prostate with high (0.24–0.7-cm<sup>3</sup>) spatial resolution *Radiology* **198** 795–805
- Lauterbur P C 1973 Image formation by induced local interactions: examples employing nuclear magnetic resonance *Nature* **243** 190
- Lauterbur P C, Kramer D M, House W V and Chen C-N 1975 Zeugmatographic high resolution nuclear magnetic resonance spectroscopy: images of chemical inhomogeneity within macroscopic objects *J. Am. Chem. Soc.* **97** 6866–8
- Lauterbur P C, Levin D N and Marr R D 1984 Theory and simulation of NMR spectroscopic imaging and field plotting by projection reconstruction involving an intrinsic frequency dimension *J. Magn. Reson.* **59** 536–41
- Lawry T J, Karczmar G S, Weiner M W and Matson G B 1989 Computer simulation of MRS localization techniques: an analysis of ISIS *Magn. Reson. Med.* **9** 299–314
- Leach M O, Collins D J, Keevil S F, Rowland I, Smith M A, Henriksen O, Bovée W M M J and Podo F 1995 Quality assessment in *in vivo* NMR spectroscopy: III. Clinical test objects: design, construction and solutions *Magn. Reson. Imaging* **13** 131–7
- Lee H and Lauterbur P C 1990 Frequency-encoded SLIM *Proc. Soc. Magn. Reson. Med.* (Berkeley, CA: SMRM) p 1086
- Levitt M H 1982 Symmetrical composite pulse sequences for NMR population inversion: I. Compensation of radiofrequency field inhomogeneity *J. Magn. Reson.* **48** 234–64
- Liang Z-P and Lauterbur P C 1991 A generalized series approach to MR spectroscopic imaging *IEEE Trans. Med. Imaging* **10** 132–7
- Liang Z-P and Lauterbur P C 1993 A theoretical analysis of the SLIM technique *J. Magn. Reson. B* **102** 54–60
- Liu H, Hall W A, Martin A J and Truwit C L 2001 An efficient chemical shift imaging scheme for magnetic resonance-guided neurosurgery *J. Magn. Reson. Imaging* **14** 1–7
- Liu H Y and Zhang J Y 1999 An efficient MR phosphorus spectroscopic localization technique for studying ischaemic heart *J. Magn. Reson. Imaging* **10** 892–8
- Ljungberg M, Starck G, Forssell-Aronsson E, Vikhoff-Baaz B, Alpsten M and Ekholm S 1995 Signal profile measurements for evaluation of the volume-selection performance of ISIS *NMR Biomed.* **8** 271–7
- Ljungberg M, Starck G, Vikhoff-Baaz B, Alpsten M, Ekholm S and Forssell-Aronsson E 2000 Extended ISIS sequences insensitive to T<sub>1</sub> smearing *Magn. Reson. Med.* **44** 546–55
- Ljungberg M, Starck G, Vikhoff-Baaz B, Alpsten M, Ekholm S and Forssell-Aronsson E 2002 The magnitude of signal errors introduced by ISIS in quantitative <sup>31</sup>P MRS *MAGMA* **14** 30–8
- Ljungberg M, Starck G, Vikhoff-Baaz B, Forssell-Aronsson E, Alpsten M and Ekholm S 1998 Signal profile measurements of single- and double-volume acquisitions with image-selected *in vivo* spectroscopy for <sup>31</sup>P magnetic resonance spectroscopy *Magn. Reson. Imaging* **16** 829–37
- Löffler R, Sauter R, Kolem H, Haase A and von Kienlin M 1998 Localized spectroscopy from anatomically matched compartments: improved sensitivity and localization for cardiac <sup>31</sup>P MRS in human *J. Magn. Reson.* **134** 287–99
- Longo R and Vidimari R 1994 *In vivo* localised <sup>1</sup>H NMR spectroscopy: an experimental characterization of the PRESS technique *Phys. Med. Biol.* **39** 207–15
- Luo Y, de Graaf R A, de la Barre L, Tannus A and Garwood M 2001 BISTRO: an outer-volume suppression method that tolerates RF field inhomogeneity *Magn. Reson. Med.* **45** 1095–102
- Luyten P R, Groen J P, Vermeulen J W A H and den Hollander J A 1989 Experimental approaches to image localised human <sup>31</sup>P NMR spectroscopy *Magn. Reson. Med.* **11** 1–21
- Luyten P R, Marien A J H, Heindel W, van Gerwen P H J, Herholz K, den Hollander J A, Friedman G and Heiss W-D 1990 Metabolic imaging of patients with intracranial tumors: H-1 MR spectroscopic imaging and PET *Radiology* **176** 791–9
- Luyten P R, Marien A J, Sijtsma B and den Hollander J A 1986 Solvent-suppressed spatially resolved spectroscopy: an approach to high-resolution NMR on a whole body MR system *J. Magn. Reson.* **67** 148–55
- Macovski A 1985 Volumetric NMR imaging with time-varying gradients *Magn. Reson. Med.* **2** 29–40
- Mansfield P 1977 Multi-planar image formation using NMR spin-echoes *J. Phys. C: Solid State Phys.* **10** L55–L58
- Mansfield P 1983 Spatial mapping of the chemical shift in NMR *J. Phys. D: Appl. Phys.* **16** L235–L8
- Mansfield P 1984 Spatial mapping of the chemical shift in NMR *Magn. Reson. Med.* **1** 370–86
- Mansfield P and Grannell P K 1973 NMR diffraction in solids *J. Phys. C: Solid State Phys.* **6** L422–6
- Mao J, Mareci T H and Andrew 1988 Experimental study of optimal selective 180° radiofrequency pulses *J. Magn. Reson.* **79** 1–10
- Mareci T H and Brooker H R 1991 Essential considerations for spectral localization using indirect gradient encoding of spatial information *J. Magn. Reson.* **92** 229–46

- Marshall I and Wild J M 1997 Calculations and experimental studies of the lineshape of the lactate doublet in PRESS-localized  $^1\text{H}$  MRS *Magn. Reson. Med.* **38** 415–9
- Marshman M F, Brereton I M, Rose S E, O'Connor A J and Doddrell M 1992 Application of self-refocusing band-selective RF pulses for spectroscopic localization *Magn. Reson. Med.* **25** 248–59
- Martin A, Liu H, Hall W A and Truwit C L 2001 Preliminary assessment of turbo spectroscopic imaging for targeting in brain biopsy *Am. J. Neuroradiol.* **22** 959–68
- Matson G B, Meyerhoff D J, Lawry T J, Lara R S, Duijijn J, Deicken R F and Weiner M W 1993 Use of computer simulations for quantitation of  $^{31}\text{P}$  ISIS MRS results *NMR Biomed.* **6** 215–24
- Matson G B, Twieg D B, Karczmar G S, Lawry T J, Gober J R, Valenza M, Boska M D and Weiner M W 1988 Applications of image-guided surface coil P-31 MR spectroscopy to human liver, heart and kidney *Radiology* **169** 541–7
- Matsui S, Sekihara K and Kohno H 1985 High-speed spatially resolved high-resolution NMR spectroscopy *J. Am. Chem. Soc.* **107** 2817–8
- Matsui S, Sekihara K and Kohno H 1986 Spatially resolved NMR spectroscopy using phase-modulated spin-echo trains *J. Magn. Reson.* **67** 476–90
- Maudsley A A, Govindaraju V, Young K, Aygula Z K, Pattany P M, Soher B J and Matson G B 2005 Numerical simulation of PRESS localized MR spectroscopy *J. Magn. Reson.* **173** 54–63
- Maudsley A A, Hilal S K, Perman W H and Simon H E 1983 Spatially resolved high resolution spectroscopy by 'four-dimensional' NMR *J. Magn. Reson.* **51** 147–52
- Maudsley A A, Lin E and Weiner M W 1992 Spectroscopic imaging display and analysis *Magn. Reson. Imaging* **10** 471–85
- Maudsley A A, Matson G B, Hugg J W and Weiner M W 1994 Reduced phase encoding in spectroscopic imaging *Magn. Reson. Med.* **31** 645–51
- Maudsley A A, Twieg D B, Sappey-Mariniere D, Hubsch B, Hugg J W, Matson G B and Weiner M W 1990 Spin echo  $^{31}\text{P}$  spectroscopic imaging in the human brain *Magn. Reson. Med.* **14** 415–22
- Meininger M, Landschütz W, Beer M, Seyfarth T, Horn V, Pabst T, Haase A, Hahn D, Neubauer S and von Kienlin M 1999 Concentrations of human cardiac phosphorus metabolites determined by SLOOP  $^{31}\text{P}$  NMR spectroscopy *Magn. Reson. Med.* **41** 657–63
- Metropolis N, Rosenbluth A W, Rosenbluth M N, Teller A H and Teller E 1953 Equation of state calculations by fast computing machines *J. Chem. Phys.* **21** 1087–92
- Metz K R, Boehmer J P, Bowers J L and Moore J R 1994 Rapid rotating-frame imaging using an RF pulse-train (RIPT) *J. Magn. Reson. B.* **103** 152–61
- Metzger G, Sarkar S, Zhang X D, Heberlein K, Patel M and Hu X P 1999 A hybrid technique for spectroscopic imaging with reduced truncation artifact *Magn. Reson. Imaging* **17** 435–43
- Michael D and Schleich T 1991 Effect of differential saturation on the spatial localization performance of depth pulses *Magn. Reson. Med.* **18** 294–308
- Mlynárik V, Gruber S, Starčuk Z, Starčuk Z and Moser E 2000 Very short echo time proton MR spectroscopy of human brain with a standard transmit/receive surface coil *Magn. Reson. Med.* **44** 964–7
- Moon R B and Richards J H 1973 Determination of intracellular pH by  $^{31}\text{P}$  magnetic resonance *J. Biol. Chem.* **248** 7276–8
- Moonen C T W, Sobering G, van Zijl P C M, Gillen J, von Kienlin M and Bizzi A 1992 Proton spectroscopic imaging of the human brain *J. Magn. Reson.* **98** 556–75
- Moonen C T W, von Keinlin M, van Zijl P C M, Cohen J, Gillen J, Daly P and Wolf G 1989 Comparison of single-shot localization methods (STEAM and PRESS) for *in vivo* proton NMR spectroscopy *NMR Biomed.* **2** 201–8
- Morris P G, McIntyre D J O, Rourke D E and Ngo J T 1991 The design of practical selective pulses for magnetic resonance imaging and spectroscopy using SPINCALC *Magn. Reson. Med.* **17** 33–40
- Mulkern R V, Chen N-K, Oshio K, Panych L P, Rybicki F J and Gambarota G 2004 Fast spectroscopic imaging strategies for potential applications in fMRI *Magn. Reson. Imaging* **22** 1395–405
- Mulkern R V, Meng J, Oshio K and Tzika A A 1996 Line scan imaging of brain metabolites with CPMG sequences *J. Magn. Reson. Imaging* **6** 399–405
- Müller S, Aue W P and Seelig J 1985a NMR imaging and volume-selective spectroscopy with a single surface coil *J. Magn. Reson.* **63** 530–43
- Müller S, Aue W P and Seelig J 1985b Practical aspects of volume selective excitation (VSE): compensation sequences *J. Magn. Reson.* **65** 332–8
- Müller S, Sauter R, Weber H and Seelig J 1988 Multivolume selective spectroscopy *J. Magn. Reson.* **76** 155–61
- Narayana P A, Fotedar L K, Jackson E F, Bohan T P, Butler I J and Wolinsky J S 1989 Regional *in vivo* proton magnetic resonance spectroscopy of brain *J. Magn. Reson.* **83** 44–52

- Narayana P A, Jackson E F, Hazle J D, Fotedar L K, Kulkarni M V and Flamig D P 1988a *In vivo* localised proton spectroscopic studies of human gastrocnemius muscle *Magn. Reson. Med.* **8** 151–9
- Narayana P A, Jensen D J, Jackson E F and Brey W W 1988b Practical problems and solutions in spatially resolved spectroscopy *J. Magn. Reson.* **79** 11–20
- Norris D G, Börnert P, Reese T and Leibfritz 1992 On the application of ultra-fast RARE experiments *Magn. Reson. Med.* **27** 142–64
- Norris D G and Dreher W 1993 Fast proton spectroscopic imaging using the sliced *k*-space method *Magn. Reson. Med.* **30** 641–5
- Norris D G, Lüdemann H and Leibfritz D 1991 An analysis of the effects of short  $T_2$  values on the hyperbolic-secant pulse *J. Magn. Reson.* **92** 94–101
- Odeblad E, Bhar B N and Lindström G 1956 Proton magnetic resonance of human red blood cells in heavy-water exchange experiments *Arch. Biochem. Biophys.* **63** 221–5
- Oh C H, Hilal S K, Cho Z H and Mun I K 1990 New spatial localization method using pulsed high-order field gradients (SHOT: Selection with High-Order gradientT) *Magn. Reson. Med.* **18** 63–70
- Oppelt A, Graumann R, Barfuß H, Fischer H, Hartl W and Schajor W 1986 FISP—eine neue schnelle pulssequenz für die kernspintomographie *Electromedica* **54** 15–8
- Ordidge R J 1987 Random noise selective excitation pulses *Magn. Reson. Med.* **5** 93–8
- Ordidge R J, Bendall M R, Gordon R E and Connelly A 1985 Volume selection for *in vivo* biological spectroscopy *Magnetic Resonance in Biology and Medicine* ed G Govil, C L Khetrpal and A Saran (New Delhi: Tata McGraw-Hill)
- Ordidge R J, Bowley R M and McHale G 1988 A general approach to selection of multiple cubic volume elements using the ISIS technique *Magn. Reson. Med.* **8** 323–31
- Ordidge R J, Connelly A and Lohman J A B 1986 Image-selected *in vivo* spectroscopy (ISIS): a new technique for spatially selective NMR spectroscopy *J. Magn. Reson.* **66** 283–94
- Ordidge R J, Wylezinska M, Hugg J W, Butterworth E and Franconi F 1996 Frequency offset corrected inversion (FOCI) pulses for use in localized spectroscopy *Magn. Reson. Med.* **36** 562–6
- Oshio K and Feinberg D A 1991 GRASE (gradient- and spin-echo) imaging: a novel fast MRI technique *Magn. Reson. Med.* **20** 344–9
- Oshio K, Kyriakos W and Mulkern R V 2000 Line scan echo planar spectroscopic imaging *Magn. Reson. Med.* **44** 521–4
- Pan J W, Hetherington H P, Hamm J R, Rothman D L and Schulman R G 1989 Volume localization with a single surface coil *J. Magn. Reson.* **81** 608–16
- Panych L P, Zhao L and Mulkern R V 2005 PSF-choice: a novel MRI method for shaping point-spread functions in phase-encoding dimensions *Magn. Reson. Med.* **54** 159–68
- Pauly J, Hu B S, Wang S J, Nishimura D G and Macovski A 1993 A three-dimensional spin-echo or inversion pulse *Magn. Reson. Med.* **29** 2–6
- Pauly J, Nishimura D and Macovski A 1989 A *k*-space analysis of small-tip-angle excitation *J. Magn. Reson.* **81** 43–56
- Pauly J, Nishimura D and Macovski A 1990 A linear class of large-tip-angle selective excitation pulses *J. Magn. Reson.* **82** 571–87
- Payne G S and Leach M O 1997 Implementation and evaluation of frequency offset corrected inversion (FOCI) pulses on a clinical MR system *Magn. Reson. Med.* **38** 828–33
- Pekar J, Leigh J S and Chance B 1985 Harmonically analysed sensitivity profile—a novel approach to depth pulses for surface coils *J. Magn. Reson.* **64** 115–9
- Plevritis S K and Macovski A 1995a MRS imaging using anatomically based *k*-space sampling and extrapolation *Magn. Reson. Med.* **34** 686–93
- Plevritis S K and Macovski A 1995b Spectral extrapolation of spatially bounded images *IEEE Trans. Med. Imaging* **14** 487–97
- Pohmann R, Rommel E and von Kienlin M 1999 Beyond *k*-space: spectral localization using higher order gradients *J. Magn. Reson.* **141** 197–206
- Pohmann R and von Kienlin M 2001 Accurate phosphorus metabolite images of the human heart by 3D acquisition-weighted CSI *Magn. Reson. Med.* **45** 817–26
- Pohmann R, von Kienlin M and Haase A 1997 Theoretical evaluation and comparison of fast chemical shift imaging methods *J. Magn. Reson.* **129** 145–60
- Ponder S L and Twieg D B 1994 A novel sampling method for 31P spectroscopic imaging with improved sensitivity, resolution and sidelobe suppression *J. Magn. Reson. B* **104** 85–8
- Posse S, Dager S R, Richards T L, Yuan C, Ogg R, Artru A A, Müller-Gärtner H-W and Hayes C 1997 *In vivo* measurement of regional brain metabolic response to hyperventilation using magnetic resonance: proton echo planar spectroscopic imaging (PEPSI) *Magn. Reson. Med.* **37** 858–65

- Posse S, DeCarli C S and LeBihan D 1994 3D echo-planar MR spectroscopic imaging at short echo times in human brain *Radiology* **192** 733–8
- Posse S, Tedeschi G, Risinger R, Ogg R and LeBihan D 1995 High speed  $^1\text{H}$  spectroscopic imaging in human brain by echo-planar spatial-spectral encoding *Magn. Reson. Med.* **33** 34–40
- Pruessmann K P, Weiger M, Scheidegger M B and Boesiger P 1999 SENSE: sensitivity encoding for fast MRI *Magn. Reson. Med.* **42** 952–62
- Purcell E M, Torrey H C and Pound R V 1946 Resonance absorption by nuclear magnetic moments in a solid *Phys. Rev.* **69** 37–8
- Pykett I L and Rosen B R 1983 Nuclear magnetic resonance: *in vivo* proton chemical shift imaging *Radiology* **149** 197–201
- Radda G K, Bore P J and Rajagopalan B 1983 Clinical aspects of  $^{31}\text{P}$  NMR spectroscopy *Br. Med. Bull.* **40** 155–9
- Radon J 1917 Über die Bestimmung von Funktionen durch ihre Integralwerte längs gewisser Mannigfaltigkeiten *Ber. Verh. Sächs. Gesell. Wiss., Lpg* **69** 262–77
- Robitaille P-M, Merkle H, Sublett E, Hendrich K, Lew B, Path G, From A H L, Bache R J, Garwood M and Ugurbil K 1989 Spectroscopic imaging and spatial localisation using adiabatic pulses and applications to detect transmural metabolite distributions in the canine heart *Magn. Reson. Med.* **10** 14–37
- Romer T, Gewisse B, Stiller D, Plotz M, Lawaczek R and Wolf K-J 1989 MRS of liver tumours: volume selection with the aid of magnetite particles *Proc. Soc. Magn. Reson. Med.* (Berkeley, CA: SMRM) p 408
- Rommel E and Kimmich R 1989a Slice excitation and localised NMR spectroscopy on the basis of spin locking *J. Magn. Reson.* **83** 299–308
- Rommel E and Kimmich R 1989b  $T_{1\rho}$  dispersion imaging and volume-selective  $T_{1\rho}$  dispersion weighted NMR spectroscopy *Magn. Reson. Med.* **12** 390–9
- Roos M S and Wong S T S 1990 Spatial localization in stochastic NMR imaging with oscillating gradients *J. Magn. Reson.* **87** 554–66
- Roos M S, Wong S T S and Frederick B de B 1991 Fast spectroscopic imaging with a rotating oscillating gradient. *Proc. Soc. Magn. Reson. Med.* (Berkeley, CA: SMRM) p 187
- Ryner L N, Ke Y and Thomas M A 1998 Flip angle effects in STEAM and PRESS—optimized versus sinc RF pulses *J. Magn. Reson.* **131** 118–25
- Sauter R, Mueller S and Weber H 1987 Localization in *in vivo*  $^{31}\text{P}$  NMR spectroscopy by combining surface coils and slice-selective saturation *J. Magn. Reson.* **75** 167–73
- Schwarz A J and Leach M O 2000 Implications of respiratory motion for the quantification of 2D MR spectroscopic imaging in the abdomen *Phys. Med. Biol.* **45** 2105–16
- Scott K N, Brooker H R, Fitzsimmons J R, Bennett H F and Mick R C 1982 Spatial localisation of P-31 nuclear magnetic resonance signal by the sensitive point method *J. Magn. Reson.* **50** 339–44
- Seeger U, Klose U, Seitz D, Nägele T, Lutz O and Grodd W 1998 Proton spectroscopy of human brain with very short echo time using high gradient amplitudes *Magn. Reson. Imaging* **16** 55–62
- Segebarth C M, Balériaux D F, de Beer R, van Ormondt D, Mariën A, Luyten P R and den Hollander J 1989  $^1\text{H}$  image-guided localized  $^{31}\text{P}$  NMR spectroscopy of the human brain: quantitative analysis of  $^{31}\text{P}$  spectra measured on volunteers and on intracranial tumor patients *Magn. Reson. Med.* **11** 349–66
- Segebarth C, Grivinec A, Luyten P R and den Hollander J A 1988  $^1\text{H}$  image-guided localized  $^{31}\text{P}$  spectroscopy of the human liver *Magn. Reson. Med. Biol.* **1** 7–16
- Segebarth C, Luyten P R and den Hollander J A 1987 Improved depth-selective single surface-coil  $^{31}\text{P}$  NMR spectroscopy using a combination of  $B_1$  and  $B_0$  selection techniques *J. Magn. Reson.* **75** 345–51
- Sepponen R E, Sipponen J T and Tanttu J I 1984 A method for chemical shift imaging: demonstration of bone marrow involvement with proton chemical shift imaging *J. Comput. Assist. Tomogr.* **8** 585–7
- Serša I and Macura S 1996 Excitation of arbitrary shapes in nuclear magnetic resonance by a random walk in discrete  $k$  space *J. Magn. Reson. B* **111** 186–8
- Serša I and Macura S 1997 Excitation of arbitrary shapes by gradient optimized random walk in discrete  $k$ -space *Magn. Reson. Med.* **37** 920–31
- Serša I and Macura S 1998 Excitation of complicated shapes in three dimensions *J. Magn. Reson.* **135** 466–77
- Serša I and Macura S 2000 Volume selective detection by weighted averaging of constant tip angle scans *J. Magn. Reson.* **143** 208–12
- Shäffter T, Börmert P, Leussler C, Carlsen I C and Leibfritz D 1998 Fast  $^1\text{H}$  spectroscopic imaging using a multi-element head-coil array *Magn. Reson. Med.* **40** 185–93
- Shaka A J and Freeman R 1985a Spatially selective pulse sequences: elimination of harmonic responses *J. Magn. Reson.* **62** 340–5
- Shaka A J and Freeman R 1985b A composite  $180^\circ$  pulse for spatial localization *J. Magn. Reson.* **63** 596–600
- Shaka A J and Freeman R 1985c 'Prepulses' for spatial localization *J. Magn. Reson.* **64** 145–50

- Shaka A J, Keeler J, Smith M B and Freeman R 1985 Spatial localisation of NMR signals in an inhomogeneous radiofrequency field *J. Magn. Reson.* **61** 175–80
- Sharp J C and Leach M O 1989a Conformal NMR spectroscopy: accurate localisation to noncuboidal volumes with optimum SNR *Magn. Reson. Med.* **11** 376–88
- Sharp J C and Leach M O 1989b Conformal localisation: applications to multi-volume MRS and MRI. *Proc. Soc. Magn. Reson. Med.* (Berkeley, CA: SMRM) p 640
- Sharp J C and Leach M O 1992 Rapid localisation of concave volumes by conformal NMR spectroscopy *Magn. Reson. Med.* **23** 386–93
- Sharp J C and Leach M O 1994 Phase-encoded selection technique (PEST) for slice selection without resonant-frequency-offset errors *J. Magn. Reson. B* **103** 168–74
- Sharp J C, Leach M O and Collins D J 1992 A single-shot shimming sequence using low-power RF noise pulses for localized *in vivo* NMR spectroscopy *Phys. Med. Biol.* **37** 281–7
- Shaw T M, Elskens R H and Kunsman C H 1952 Proton magnetic resonance absorption and water content of biological materials *Phys. Rev.* **85** 708
- Shaw T M and Palmer K J 1951 Nuclear magnetic resonance absorption in proteins *Phys. Rev.* **83** 213
- Shungu D C and Glickson J D 1993 Sensitivity and localisation enhancement in multinuclear *in vivo* NMR spectroscopy by outer volume presaturation *Magn. Reson. Med.* **30** 661–71
- Shungu D C and Glickson J D 1994 Band-selective spin echoes for *in vivo* localized  $^1\text{H}$  NMR spectroscopy *Magn. Reson. Med.* **32** 277–84
- Silver M S, Joseph R I and Hoult D I 1984 Highly selective  $\pi/2$  and  $\pi$  pulse generation *J. Magn. Reson.* **59** 347–51
- Silver M S, Joseph R I and Hoult D I 1985 Selective spin inversion in nuclear magnetic resonance and coherent optics through an exact solution of the Bloch–Riccati equations *Phys. Rev. A* **31** 2753–5
- Singh S and Brody W R 1993 Projection presaturation: III. Accurate selective excitation or presaturation of the regions of tailored shape in the presence of short- $T_1$  species *J. Magn. Reson. B* **101** 52–62
- Singh S, Rutt B K and Henkelman R M 1990a Projection presaturation: a fast and accurate technique for multidimensional spatial localization *J. Magn. Reson.* **87** 567–83
- Singh S, Rutt B K and Napel S 1990b Projection presaturation: II. Single-shot localization of multiple regions of interest *J. Magn. Reson.* **90** 313–29
- Slotboom J, Mehlkopf A F and Bovée W M M J 1991 A single-shot localization pulse sequence suited for coils with inhomogeneous RF fields using adiabatic slice-selective RF pulses *J. Magn. Reson.* **95** 396–404
- Slotboom J, Mehlkopf A F and Bovée W M M J 1994 The effects of frequency-selective RF pulses on  $J$ -coupled spin- $\frac{1}{2}$  systems *J. Magn. Reson. A* **108** 38–50
- Speck O, Scheffler K and Hennig J 2002 Fast  $^{31}\text{P}$  chemical shift imaging using SSFP methods *Magn. Reson. Med.* **48** 633–9
- Spielman D, Pauly J, Macovski A and Enzmann D 1991 Spectroscopic imaging with multidimensional pulses for excitation: SIMPLE *Magn. Reson. Med.* **19** 67–84
- St Lawrence K, Lee T-Y and Henkelman M 1998 Spatial localization combining projection presaturation with a two-dimensional excitation pulse *Magn. Reson. Med.* **40** 944–7
- Starck G, Lundin R, Forssell-Aronsson E, Arvidsson M, Alpsten M and Ekholm S 1995 Evaluation of volume-selection methods in *in vivo* MRS: design of a new test phantom *Acta Radiol.* **36** 317–22
- Star-Lack J 1999 Optimal gradient waveform design for projection imaging and projection reconstruction echoplanar spectroscopic imaging *Magn. Reson. Med.* **41** 664–75
- Stengel A, Neumann-Haefelin T, Singer O C, Neumann-Haefelin C, Zanella F E, Lanfermann H and Pilatus U 2004 Multiple spin-echo spectroscopic imaging for rapid quantitative assessment of *N*-acetylaspartate and lactate in acute stroke *Magn. Reson. Med.* **52** 228–38
- Straubinger K, Schick F and Lutz O 1995 Relaxation of AB spin systems in stimulated-echo spectroscopy *J. Magn. Reson. B.* **109** 251–8
- Styles P, Scott C A and Radda G K 1985 A method for localizing high-resolution NMR spectra from human subjects *Magn. Reson. Med.* **2** 402–9
- Takahashi A and Peters T 1995 Compensation of multi-dimensional selective excitation pulses using measured  $k$ -space trajectories *Magn. Reson. Med.* **34** 446–56
- Tanaka C, Umeda M, Higuchi T, Naruse S, Horikawa Y, Ebisu T, Nishikawa H and Ueda S 1991 Non-volume selected spectroscopic imaging in the brain and cerebral disorders *Proc. Soc. Magn. Reson. Med.* (Berkeley, CA: SMRM) p 1060
- Tannús A and Garwood M 1997 Adiabatic pulses *NMR Biomed.* **10** 423–34
- Tannús A, Garwood M, Panepucci H and Bonagamba T J 1991 Localized proton spectroscopy with 3D-GMAX. *Proc. Soc. Magn. Reson. Med.* (Berkeley, CA: SMRM) p 1060

- Theberge J, Menon R S, Williamson P C and Drost D J 2005 Implementation issues of multivoxel STEAM-localized  $^1\text{H}$  spectroscopy *Magn. Reson. Med.* **53** 713–8
- Thiel T, Czisch M, Elbel G K and Hennig J 2002 Phase coherent averaging in magnetic resonance spectroscopy using interleaved navigator scans: compensation of motion artifacts and magnetic field instabilities *Magn. Reson. Med.* **47** 1977–82
- Thompson R B and Allen P S 1999 Sources of variability in the response of coupled spins to the PRESS sequence and their potential impact on metabolite quantification *Magn. Reson. Med.* **41** 1162–9
- Thompson R B and Allen P S 2001 Response of metabolites with coupled spins to the STEAM sequence *Magn. Reson. Med.* **45** 955–65
- Thulborn K R and Ackerman J J H 1983 Absolute molar concentrations by NMR in inhomogeneous  $B_1$ : a scheme for analysis of *in vivo* metabolites *J. Magn. Reson.* **55** 357–71
- Tkáč I, Starčuk Z, Choi I-Y and Gruetter R 1999 *In vivo*  $^1\text{H}$  NMR spectroscopy of rat brain at 1 ms echo time *Magn. Reson. Med.* **41** 649–56
- Trabesinger A H, Meier D, Dydak U, Lamerichs R and Boesiger P 2005 Optimizing PRESS localized citrate detection at 3 tesla *Magn. Reson. Med.* **54** 51–8
- Tran T-K C, Vigneron D B, Sailasuta N, Tropp J, Le Roux P, Kurhanewicz J, Nelson S and Hurd R 2000 Very selective suppression pulses for finite-MRSI studies of brain and prostate cancer *Magn. Reson. Med.* **43** 23–33
- Tsao J 2001 Extension of finite-support extrapolation using the generalized series model for MR spectroscopic imaging *IEEE Trans. Med. Imaging* **20** 1178–83
- Twieg D B 1989 Multiple-output chemical-shift imaging (MOCSI)—a practical technique for rapid spectroscopic imaging *Magn. Reson. Med.* **12** 64–73
- Twieg D B, Meyerhoff D J, Hubesch B, Roth K, Sappey-Marinié D, Boska M D, Gober J R, Schaefer S and Weiner M W 1989 Phosphorus-31 magnetic resonance spectroscopy in humans by spectroscopic imaging: localized spectroscopy and metabolite imaging *Magn. Reson. Med.* **12** 291–305
- Tycko R and Pines A 1984 Spatial localization of NMR signals by narrowband inversion *J. Magn. Reson.* **60** 156–60
- Tyszka J M and Silverman J M 1996 Navigated single-voxel short-echo-time proton spectroscopy of moving objects *J. Magn. Reson. B* **112** 302–6
- Tyszka J M and Silverman J M 1998 Navigated single-voxel proton spectroscopy of the human liver *Magn. Reson. Med.* **39** 1–5
- Ugurbil K, Garwood M and Bendall M R 1987 Amplitude- and frequency-modulated pulses to achieve  $90^\circ$  plane rotations with inhomogeneous  $B_1$  fields *J. Magn. Reson.* **72** 177–85
- Vikhoff-Baaz B, Ljungberg M, Starck G, Forssell-Aronsson E, Jönsson L, Alpstein M and Ekholm S 2001 Performance of 2D  $^1\text{H}$  spectroscopic imaging of the brain: some practical considerations regarding the measurement procedure *Magn. Reson. Imaging* **17** 919–31
- Vikhoff-Baaz B, Starck G, Ljungberg M, Lagerstrand K, Forssell-Aronsson E and Ekholm S 2001 Effects of  $k$ -space filtering and image interpolation on image fidelity in  $^1\text{H}$  MRSI *Magn. Reson. Imaging* **19** 1227–34
- Volk A, Tiffon B, Mispelter J and Lhoste J-M 1988 High-resolution localised spectroscopy at 4.7 tesla by frequency-interval-selective volume localisation (FRIVOL) *J. Magn. Reson.* **76** 386–92
- von Kienlin M, Beer M, Greiser A, Hahn D, Harre K, Köstler H, Landschütz W, Pabst T, Sandstede J and Neubauer S 2001 Advances in human cardiac  $^{31}\text{P}$ -MR spectroscopy: SLOOP and clinical applications *J. Magn. Reson. Imaging* **13** 521–7
- von Kienlin M and Mejia R 1991 Spectral localization with optimal pointspread function *J. Magn. Reson.* **94** 268–87
- von Kienlin M, Remy C, Benabid A L and Decorps M 1988 Symmetric pulses for spatially resolved spectroscopy *J. Magn. Reson.* **79** 382–8
- Wang Z, Bolinger L, Subramanian V H and Leigh J S 1991 Errors of Fourier chemical-shift imaging and their corrections *J. Magn. Reson.* **92** 64–72
- Webb A G, Briggs R W and Mareci T H 1991 Volume-localised spectroscopy using selective Fourier transform with windowing by variable-tip-angle excitation *J. Magn. Reson.* **94** 174–9
- Webb P, Spielman D and Macovski A 1989 A fast spectroscopic imaging method using a blipped phase encode gradient *Magn. Reson. Med.* **12** 306–15
- Wilman A H and Allen P S 1993 An analytical and experimental evaluation of STEAM versus PRESS for the observation of the lactate doublet *J. Magn. Reson. B* **101** 102–5
- Yablonskiy D A, Neil J J, Raichle M E and Ackerman J J H 1998 Homonuclear  $J$  coupling effects in volume localized NMR spectroscopy: pitfalls and solutions *Magn. Reson. Med.* **39** 169–78
- Yongbi N M, Payne G S, Collins D J and Leach M O 1995 Quantification of signal selection efficiency, extra volume suppression and contamination for ISIS, STEAM and PRESS localized  $^1\text{H}$  NMR spectroscopy using an EEC localization test object *Phys. Med. Biol.* **40** 1293–303

- Zhang W and van Hecke P 1990 Water suppression in single-scan and multi-scan localized proton spectroscopy *Magn. Reson. Med. Biol.* **4** 165–9
- Zhao X L, Prost R W, Li Z and Li S J 2005 Reduction of artifacts by optimization of the sensitivity map in sensitivity-encoded spectroscopic imaging *Magn. Reson. Med.* **53** 30–4
- Zhong K and Ernst T 2004 Localized *in vivo* human  $^1\text{H}$  MRS at very short echo times *Magn. Reson. Med.* **52** 898–901
- Zhu J M and Smith I C P 1999 Stimulated anti-echo selection in spatially localized NMR spectroscopy *J. Magn. Reson.* **136** 1–5